COVER PAGE

AD_____

Award Number: W81XWH-11-1-0525

TITLE: Identification of the Gene for Scleroderma in the Tsk/2 Mouse Strain: Implications for Human Scleroderma Pathogenesis and Subset Distinctions

PRINCIPAL INVESTIGATOR: Elizabeth P. Blankenhorn, Ph. D / Michael L. Whitfield, Ph.D

CONTRACTING ORGANIZATION: The Trustees of Dartmouth College

REPORT DATE: July 2014

TYPE OF REPORT: Annual

PREPARED FOR: U.S. Army Medical Research and Materiel Command
Fort Detrick, Maryland 21702-5012

REPORT DOCUMENTATION PAGE	Form Approved OMB No. 0704-0188

1. REPORT DATE July2014	2. REPORT TYPE	3. DATES COVERED
	Annual	1 Jul 2013 - 30 Jun 2014

4. TITLE AND SUBTITLE
Identification of the Gene for Scleroderma in the Tsk/2 Mouse Strain: Implications for Human Scleroderma Pathogenesis and Subset Distinctions

5a. CONTRACT NUMBER

5b. GRANT NUMBER
W81XWH-11-1-0525

5c. PROGRAM ELEMENT NUMBER

6. AUTHOR(S)
Elizabeth P. Blankenhorn, PhD
Carol Artlett, PhD
Michael Whitfield, PhD
E-Mail: eblanken@drexelmed.edu

5d. PROJECT NUMBER

5e. TASK NUMBER

5f. WORK UNIT NUMBER

7. PERFORMING ORGANIZATION NAME(S) AND ADDRESS(ES)
Drexel University College of Medicine, Philadelphia, PA, 19129
D

8. PERFORMING ORGANIZATION

9. SPONSORING / MONITORING AGENCY NAME(S) AND ADDRESS(ES)
U.S. Army Medical Research and Materiel Command
Fort Detrick, Maryland 21702-5012

10. SPONSOR/MONITOR'S ACRONYM(S)

11. SPONSOR/MONITOR'S REPORT NUMBER(S)

12. DISTRIBUTION / AVAILABILITY STATEMENT
Approved for Public Release; Distribution Unlimited

13. SUPPLEMENTARY NOTES

14. ABSTRACT

This project is focused on an animal model of the human disease, systemic sclerosis (SSc), called Tsk2/+. The SSc-like traits in Tsk2/+ heterozygotes are highly penetrant. With their readily apparent skin fibrosis resulting from ECM anomalies, Tsk2/+ mice have signs that resemble human SSc features, making it useful as a pre-clinical model. In this report, we show a clear time dependence on the gene expression in the skin of the Tsk2/+ mice. We have pinpointed a mutation in *Col3a1* that is the Tsk2 gene, and have confirmed the sequence difference between Tsk2/+ and the parent strain, 101/H. We present results on the expression of TGFβ mRNA from cells cultured from Tsk2/+ and WT littermates that suggest a mechanism for the up-regulation of TGFβ seen in the mutant strain. We show that elastin content in the skin, known to be controlled by TGFβ and possibly up-regulated in SSc, is the earliest indicator of tight-skin in the tissue. Finally, we show that Tsk2/+ mice, and mouse fibroblasts transfected with Col3a1 from Tsk2/+, share a substantial fibrotic gene expression program compared to WT mice or transfectants, indicating that expression of the *Col3a1*^{Tsk2} gene alone accounts for the trait in Tsk2/+ mice.

15. SUBJECT TERMS Animal model, systemic sclerosis, scleroderma, Tsk2/+, fibrosis, gene, genetics, TGFβ

16. SECURITY CLASSIFICATION OF:			17. LIMITATION OF ABSTRACT	18. # OF PAGES	19a. NAME OF RESPONSIBLE PERSON
					USAMRMC
a. REPORT	b. ABSTRACT	c. THIS PAGE			19b. TELEPHONE NUMBER *(include area code)*
U	U	U	UU	110	

Table of Contents

1. INTRODUCTION

Scleroderma and systemic sclerosis (SSc) is a heterogenous disease of fibrosis and inflammation, concomitant with significant autoimmunity. SSc often presents with skin manifestations and Raynaud's phenomenon; the extent and location of fibrotic lesions in people with SSc contributes to the diagnoses of disease subtypes and prognosis. Several preclinical animal models for SSc exist. Tsk2/+ mice were discovered more than two decades ago when progeny of a 101/H male in an ENU mutagenesis experiment were noted with very tight skin. *Tsk2* is homozygous lethal, similar to the *Tsk1* mouse model of SSc which results from duplication of the fibrillin gene. Tsk1 has been one of the most commonly used models for SSc and therefore has been extensively characterized. The SSc-like traits in Tsk2/+ heterozygotes are highly penetrant. In addition to a readily apparent skin fibrosis resulting from ECM anomalies, Tsk2/+ mice show more autoimmune and inflammatory features than Tsk1/+, and their longer lifespan and immune features that closely resemble human SSc features are ideal for use as a pre-clinical model. The Tsk2 mutation has been bred onto a homogeneous inbred (C57Bl/6, or B6) background in Dr. Blankenhorn's laboratory. B6.Tsk2/+ mice have many features of the human disease, including tight skin, dysregulated extracellular matrix deposition, and significant autoimmunity. We have found that Tsk2-mediated autoimmune and fibrotic signs develop *progressively* with age and manifest differently in females than males, a phenomenon also observed in human SSc. These SSc phenotypes in B6.Tsk2 mice are all likely due to a single genetic mutation, which we have now unidentified. We proposed to identify the *Tsk2* gene and understand its mechanism of action as outlined in our statement of work. This mouse affords a unique opportunity to examine the pathways leading to the multiple clinical parameters of fibrotic disease from birth onward, and we describe our studies from the second year of the grant below. This work was accomplished by researchers at Drexel University College of Medicine and Dartmouth Geisel School of Medicine under the partnering PI option.

2. KEYWORDS:

Scleroderma and systemic sclerosis (SSc); animal models; mice; Tsk2/+ mice; genetic mapping; fibroproliferative subset; TGFβ; TWEAK/FN14 signaling; genetic mutation; *Col3a1;* COL3A1; genomic DNA sequencing; RNA-Seq; microarray; *in vitro culture;* transfection; plasmid; skin and lung fibrosis.

3. ACCOMPLISHMENTS

Milestones were assigned to this proposal, with tasks to be accomplished by each investigator. The overall **summary** of our progress relative to these tasks is given below, followed by a complete discussion of our work the past three years.

Milestone 1 Identify Tsk2/+ gene - **This is now DONE.**

Task 1 was for the Blankenhorn laboratory to collect DNA for sequencing (Months 1-6), which we have done. In year 1, we collected the Tsk2/+ and 101/H (parental strain) DNAs for sequencing on the 454.

Task 2 (Months 6-12) was to select anchor sequences for Nimblegen chip design, so that chromosome 1 DNA in the Tsk2/+ interval could be sequenced. This was done in year 1 by our subcontractors at ASRI, Dr. Fen Hu and Dr. Garth Ehrlich.

Task 3 (Month 6-12): Dr. Hu and her colleagues have hybridized the mouse genomic DNA to the chips and collected Tsk2/+ interval DNA, meeting this target. They have sequenced both Tsk2/+ and 101/H interval DNA.

Task 4: We assembled all the sequence data in years 1 and 2, and have aligned the sequences to compare and report all observed polymorphisms. At Drexel, we completed amplification and re-sequencing of the target gene this year (year 2, on schedule), Blankenhorn lab.

Milestone 2 Determination of mechanism of action of Tsk2/+ gene: two hypotheses on this are discussed.

Task 1 (Months 18-32): At Drexel, we were to breed Tsk2/+ mice to a knockout mouse with a deficiency in the newly-identified *Tsk2* gene, to determine if either Tsk2 or wild-type allele can complement the genetic deficiency. Last year, we reported that *Col3A1* is the gene underlying *Tsk2,* and so the Blankenhorn laboratory purchased and bred three Col3A1 KO/WT heterozygous male mice to Tsk2/+ dams in July 2012 (month 12). **This is now DONE.**

Task 2 (Months 1-36). Correlate the known actions of the Tsk2 gene at Drexel with gene expression data at Dartmouth (Aim 2) and with the presence of proliferating cells (Aim 3). In this Task, largely accomplished at Dartmouth with the microarray studies (months 4-12), we are establishing the timeline for the gene signatures in male and female Tsk2/+ mice. We will then examine the corresponding Tsk2/KO mice for these phenotypes to detect alterations in the TGFβ1-driven proliferative, fibrotic signature of the Tsk2/+ gene when it is absent. This year, we have added a task to the project: we have found that mouse skin samples for gene expression studies need to be stratified for hair cycle. This has delayed some of our gene signature analyses until year 2 and 3, as the earlier samples sent to Dartmouth were not all in the same stage of the hair cycle, which dramatically alters the landscape of the skin. **This is now DONE.**

Also part of Milestone 2 was the aim to make fibroblast cultures from the mice. Originally planned for the appropriate conditional TGFβR animals so that alterations to TGFβ1 signaling taking place early in mouse post-natal development can be monitored, we have found this to be a good approach for the analyses of all the genotypes. **This is now DONE.**

Another component of Milestone 2: Based on Dr. Whitfield's preliminary results with whole genome profiling, and on Dr. Blankenhorn's with selected TGFβ1-dependent target gene expression, we expect that TGFβ1 is a necessary component in the disease pathway. Therefore, we are ordering the TGFβR conditional KO mice and the transgenic mice bearing *cre* recombinase under the control of a collagen promoter. We should have them in hand this fall. When bred to Tsk2/+ mice, these constructs will help us to fully understand the timeline of the TGFβ signature. At Drexel, we will breed Tsk2/+ mice to TGFβR conditionally deficient mice (by breeding the Tsk2/+ mutation onto a floxed TGFβR2 KO and then breed the resulting mice to B6.Col-Cre animals) to determine the interaction between TGFβ1 and *Tsk2*. Approximately equal numbers of wild-type (WT) and Tsk2/+ mutant progeny with the dominant TGFβR conditionally deficient trait will be born and used (Months 24-36). We will then correlate the known actions of the *Tsk2* gene AT DREXEL with gene expression data AT DARTMOUTH in Aim 2 and with the presence of proliferating cells in Aim 3, by examining the corresponding Tsk2/KO mice for these phenotypes to detect alterations in the TGFβ1-driven proliferative, fibrotic signature of the Tsk2/+ gene when it is absent. Months 18-36, Blankenhorn laboratory; months 12-18 in the Whitfield laboratory. **We have chosen a different KO to study, based on preliminary results from Year 3.**

Milestone 3 Determine the timing of TGFβ activation in the Tsk2/+ mice, and differences between males and females. Dr. Blankenhorn will send mouse tissues to Dr. Whitfield, who will do the RNA work. **This is now DONE.**

Task 1 (Months 1-36): The Blankenhorn laboratory will breed sufficient numbers of mice to collect skin at postnatal Day 0, day 7, day 14, day 21 as well as 1 month and 4 months. These mice are used by all three investigators, and whenever possible, each individual mouse was studied for the relevant traits in each laboratory, so that histology and RNA transcript analysis will occur on the same animal. We have met our targets in year 1. In Year 2, this task was accomplished, and in year 3, we will add samples where stratification by hair cycle has been done. **This is now DONE.**

Task 2 (Months 4-12) Prepare RNA from skin at Drexel and hybridize DNA microarrays at Dartmouth. Data will be analyzed, processed and stored. In practice, we found it better to send whole skin samples to Dartmouth and prepare the RNA there. **This is now DONE.**

Task 3 (Months 12-36): At Dartmouth perform data analysis for expression of TGFβ as well as other gene signatures, both profibrotic (IL13 and IL4) and those that may not be expected (genome-wide). **This is now DONE.**

Task 4 (12-24 months, if necessary): If the microarray study is unclear, we had proposed a small number of RNASeq runs to validate the gene expression data. This was unnecessary for these goals.

Task 5 (dependent timing): Immunohistochemistry will be performed for the validation of TGFβ signatures found in the microarrays. This will be performed by the Artlett and Blankenhorn laboratories. This study relies on the completion of Aim 2 (Milestones 2 and 3), for which we need microarray data from all ages. This is still ongoing, but **some of the results from this Task 5 have been published**.

Milestone 4 Characterize how well the Tsk2/+ mouse approximates human SSc at different time points. These tasks are on time, and to be conducted largely in year 3.

Task 1: At Dartmouth, map mouse genes to human orthologs, integrate mouse and human data using Distance Weighted Discrimination to remove systematic biases, and cluster mouse and human data (months 12-36). **This is now DONE.**

Task 2: At Dartmouth, Analyze data-driven groupings, pathways, computational validation and data interpretation (months 12-36). Data analysis for expression of proliferative signatures will give us a way to understand the subset of SSc patients that exhibit diffuse clinical symptoms with signs of cell proliferation. This is a special investigation of proliferative signatures by the Whitfield group to capitalize on their extensive experience with cell cycle and proliferative motifs in gene expression. It was scheduled for months 8-24, and **is now DONE**.

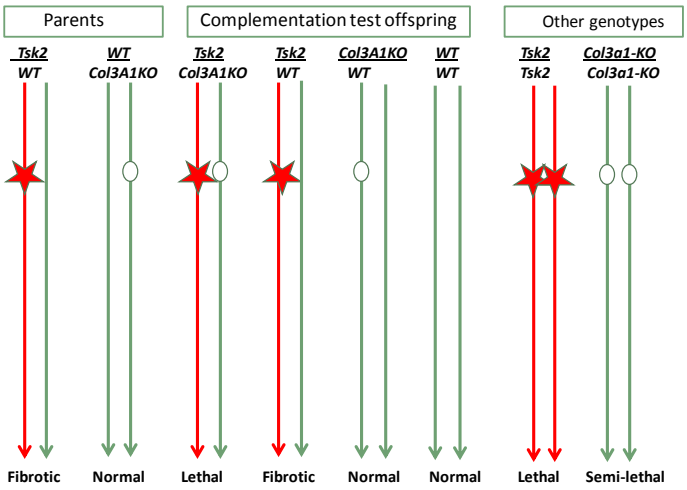

Figure 1. Complementation testing proves Tsk2 is C33S: Red lines indicate the mutated chromosome from Tsk2/+ mice and green lines indicate a normal chromosome 1. Ovals:Col3a1 knocked out in BALB/c mice; red star shows the Tsk2 mutation. Outcomes associated with each genotype are indicated below.

Milestone 5

Task 1: We will perform confirmation qRT-PCR on select genes based on Aim 2 in the Blankenhorn and Whitfield laboratories. We had scheduled this for months 4-24; this work is ongoing due to the confounding hair cycle. We modified this task to extend to year three as well, to ensure full study of interesting gene expression patterns over mouse developmental ages. In the Drexel laboratories, we plan experimentation on the mechanotension of the ECM when it contains Tsk2/+ collagen in comparison to ECM containing WT collagen, after the identification of the Tsk2/+ candidate gene by Aim 1. We have started this; one issue is how slowly the mouse fibroblasts grow. A final goal within this milestone is to characterize the disorder to understand how the *Tsk2* mutation acts to elicit it. **These goals are included in our hypothesis about the mechanism of action of *Col3a1*^{Tsk2} (see below)**

Milestone 6 Cross-breed Tsk2/+ mice to Wsh mast cell knockout mice (at Drexel). This Milestone was ***deleted*** and supplanted by other work, as described in the Year 1 Progress report.

PRELIMINARY RESULTS BY MILESTONE

Milestone 1 : The nucleotide sequence of the Tsk2/+ region was accomplished in year 1 and 2, and the initial report of the sequencing capture and early resequencing at Drexel was made in the year 1 progress report. This work is in our submitted manuscript,

We confirmed the global sequencing result at Drexel and also evaluated the remaining SNPS by phototyping[1, 2]. Of these, only the Col3A1 non-synonymous coding SNP was validated; two intronic SNPs in the GULP1 gene also distinguish Tsk2/+ from all other strains for which chr 1 genotyping is available. The Col3a1 SNP results in a Cys to Ser change in the PIIINP (N-terminal) cleavage product of the Col3a1.

Milestone 2: Breeding to Col3A1 KO:

We began the breeding necessary for the genetic complementation test of *Col3a1* by breeding the Tsk2/+ line to BALB.Col3A1KO mice (heterozygotes as well). Results were collected in year 2. **This study provided the definitive evidence that *Col3a1* is the gene mutated in Tsk2/+ mice**. We hypothesized that combining the Tsk2 mutation with a Col3a1- allele would not generate a viable genotype, and the Tsk2/*Col3a1*KO mice would die in utero. There are four possible genotypes in the cross: (1)Tsk2/+; (2)Tsk2/*Col3A1*KO; (3)Col3A1KO/*Col3A1*KO; and (4)*Col3A1*KO/+. Our analysis of the litters confirmed this prediction: we found no Tsk2/Col3a1- mice among the neonates (i.e., this genotype is nonviable), out of 33 offspring born in this cross (Figure 1; Table 1). This implies that the C33S mutation in *Col3a1* is the causative mutation, because the Tsk2-bearing chromosome has no functional *Col3a1* gene. While the compound heterozygotes couldn't survive without a functional allele of *Col3a1* (and C33S is the only mutation within *Col3a1* in the Tsk2/+ mice), there were a few Col3A1KO/Col3A1KO homozygotes born. These mice did not thrive and were sacrificed to provide neonatal skin fibroblast cultures.

Parents	Tsk2/+ Tight skin	+/+ Normal skin	Tsk2/Tsk2 (lethal)
Tsk2/+ x Tsk2/+	22	21	0
	$Col3a1^{+}$/ $Col3a1^{-}$ Normal skin	$Col3a1^{+}$/ $Col3a1^{+}$ Normal skin	$Col3a1^{-}$/ $Col3a1^{-}$ (Moribund)
$Col3a1^{-/+}$ x $Col3a1^{-/+}$	16	13	3
	WT/$Col3a1^{+}$ Normal skin	Tsk2/$Col3a1^{+}$ Tight skin	WT/$Col3a1^{-}$ Normal skin	Tsk2/$Col3a1^{-}$
Tsk2/+ x $Col3a1^{-/+}$	12	10	11	0

Table 1: Offspring born of Tsk2 and Col3a1-KO mice. The breeding scheme for maintaining the two mutant lines is shown in the first two rows, with the phenotypes in the pups heading each column. The complementation test of (Tsk2/+ x Col3a1-/+) is shown in the bottom panel.

Milestone 2 also had the aim to make fibroblast cultures from the mice.

Fibroblast cultures were established in Blankenhorn and Artlett lab in months 8-24. Western blots of collagen expression were compared to hydroxyproline and Sirius red measurements. A very small but consistent and significant average difference is seen between WT and Tsk2/+ fibroblasts collected at day 1 (Figure 2), but by day 28 and older, this difference is difficult to repeat. Ascorbic acid supplementation did not reveal any further differences. One note – we have not observed proliferation differences in Tsk2/= vs. WT fibroblasts in vitro.

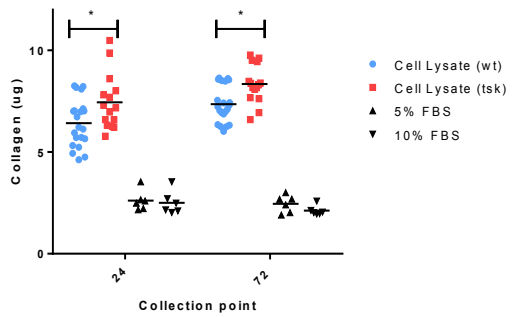

Source of Variation	P value summary	Significant?
Interaction	ns	No
Genotype	***	Yes
Hrs	***	Yes

Figure 2. Collagen synthesis in vitro, stratified by Tsk2/+ genotype.

In year 3, we developed a new method using the Col3a1-KO fibroblasts, to prove that Tsk2 is Col3a1(C->S). Although the complementation test proved definitively that lethality is due to *Col3a1*^{Tsk2} in the compound heterozygote, this experiment did not prove that fibrosis was also due to the *Col3a1*^{Tsk2} allele. Because the compound heterozygous animals do not survive to accumulate fibrotic levels of ECM, a direct *in vivo* test is impossible, so we performed an '*in vitro* complementation' test, wherein we transfected mutant or wild-type *Col3a1* cDNA into *Col3a1*-KO fibroblasts, harvested from a *Col3a1*-KO/KO homozygote at birth. Using the production of COL1A1 as a measure of fibrosis (shown to be expressed at high levels in Tsk2/+ skin and used as a marker of fibrosis [3, 4]), we assessed both protein and mRNA levels in fibroblasts that received DNA from a plasmid containing a single allele of a single *Col3a1* gene. In three independent experiments, COL1A1 protein was significantly elevated after 48 hours of transfection with *Col3a1*^{Tsk2} relative to transfection with *Col3a1*^{WT} (**Fig. 3**); mRNA for *Col1a1* was likewise increased in cells transfected with mutant *Col3a1*^{Tsk2} cDNA. Transfection efficiencies were equal in each of the experiments (**Fig. 3**).

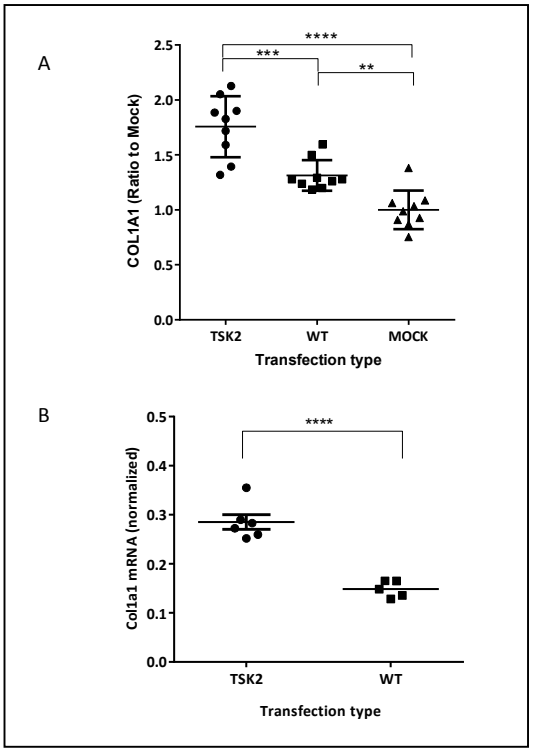

Figure 3. Mouse Col3a1-KO fibroblasts transfected with a plasmid bearing the mutant Col3a1Tsk2 express 34% more COL1A1 protein than Col3a1WT transfectants. Near-confluent dishes of COL3A1-deficient fibroblasts were transfected (three dishes each) with either of the two plasmids for 3 h, glycerol shocked, then washed and incubated for 48 hours. Three independent experiments were performed.

(A) Culture supernatants were collected and assayed by Western blot for COL1A1 secretion. Comparisons by one-way ANOVA show that cells that received Col3a1Tsk2 produced significantly more COL1A1 than cells transfected with Col3a1WT ($p<0.001$) or mock transfectants ($p<0.0001$); cells receiving wild-type Col3a1 also produced more COL1A1 than the mock ($p<0.01$). The mean ratio of COL1A1 in Col3a1Tsk2 -transfected cells to that in the mock transfections is 1.757; mean ratio of COL1A1 in Col3a1WT -transfected cells to mock is 1.313.

(B) Col1a1 mRNA (normalized to housekeeping gene expression) is also more highly expressed in COL3A1-deficient fibroblasts after transfection with Col3a1TSK than with Col3a1WT ($p<0.0001$). Cell lysates from two of the experiments were collected to determine that plasmids were transfected with equal efficiency, not shown).

Milestone 3 and 5: RNA gene expression profiling.

We reported (in our Year 1 Progress Report) the initiation of the planned RNA gene expression profiling by DNA microarray at Dartmouth. To accomplish this milestone we analyzed skin from both wt and Tsk2/+ mice at 4, 8, 12, and 20 weeks of age for both males and females.

We analyzed 4 independent skin samples each for WT and Tsk2/+ mice at each time point for both male (24 microarrays) and female mice (24 microarrays). Each of these was analyzed separately. We found a clear time dependence of the gene expression in Tsk2/+ that also varied by gender. Analysis of the female mice at 4, 8, 12 and 20 weeks of age identified specific gene expression signatures at each time point and it was very clear that some time points had very significant changes in gene expression (4 and 12 weeks), whereas other time points (8 and 20 weeks) show many fewer significant genes with higher False Discovery Rates (FDRs). A similar finding was observed for males except the largest changes were observed at 8 weeks and the fewest changes observed at 4 and 12 weeks, suggesting that the gene expression changes in male Tsk2/+ mice are changing at a different rate, or at different developmental time points, than occurs in female mice (**Figure 4)**.

Based on data from Dr. Blankenhorn's laboratory, the hypothesis was developed that hair cycle varied between Tsk2/+ and WT as well as between males and females. In addition, this process appears somewhat

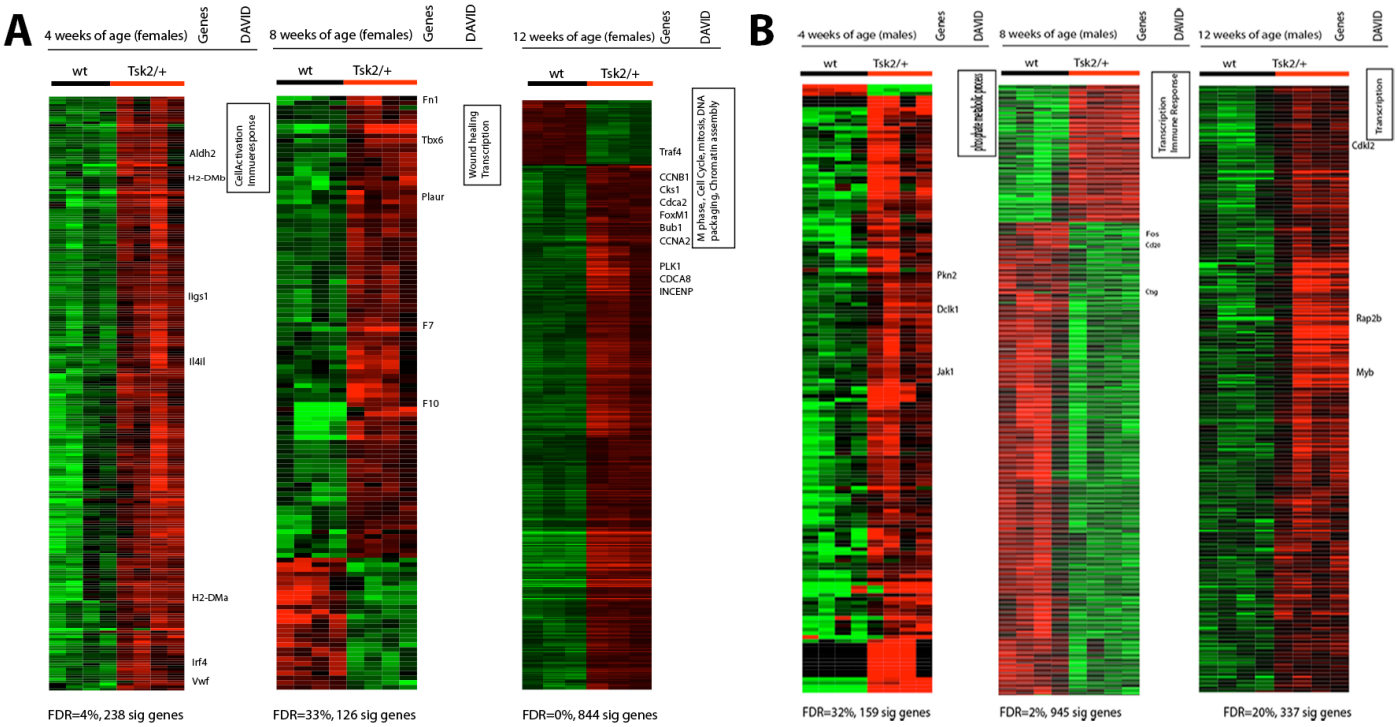

Figure 4. Genes differentially expressed between Tsk2/+ and WT differ by time point and gender. Four-week and 12-week female Tsk2/+ mice (panel A), as well as 8-week male Tsk2/+ mice (panel B) show significantly more differentially genes at a low false discovery rate (FDR). We used Significance Analysis of Microarrays (SAM) to compare WT and Tsk2/+ mice at different time points for each gender. A. 238 significant genes at 4% FDR were identified in 4-week old females, whereas, only 126 significant genes were obtained at 8-week time point (FDR=33%). However, 12-week old females showed the most significant differential gene expression with 844 significant genes (0.1% FDR). B. For males the most significant difference was observed in 8 week old animals. The 8-week old male Tsk2/+ mice showed 945 significant genes (FDR=2). 4-week and 12-week male Tsk2/+ mice showed significant differential gene expression but at very high FDR. Very similar results were seen with confirming RT-PCR of selected transcripts (data not shown) in male and female mice of different ages.

---

stochastic, occurring in different animals of the same genotype and gender at different times. We therefore have recently revisited the above analysis controlling for hair cycle stage for each sample and only using those samples that are at the same stae. We repeated the gene expression analysis and show that by eliminating those samples from mice in anagen, we increased the number of genes we are able to select, and correspondingly reduced our overall FDR due to decrease sample variation (Figure 5). The number of genes that can be selected at a given FDR is shown for each gender and age group of mice in Figure 5.

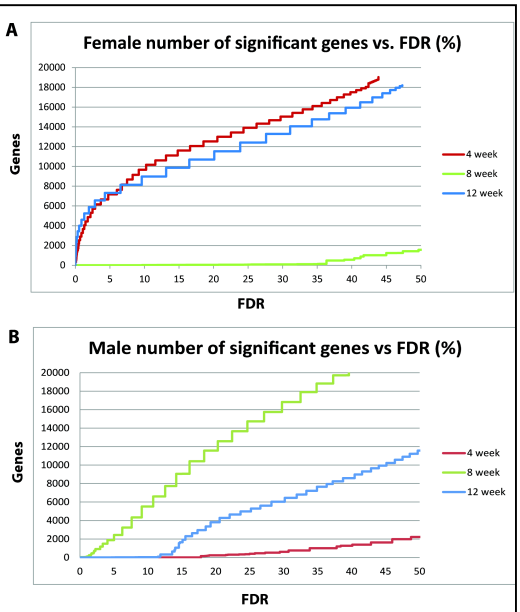

Figure 5. Number of differentially expressed genes by FDR. A. Females at each age were analyzed for genes differentially expressed between WT and Tsk2/+. The most significant changes are observed at 4 and 8 weeks. B. Males show a different distribution with the largest changes occurring at 8 and 12 weeks, and relatively few changes occurring at 4 weeks.

A TGFβ-responsive gene signature is activated in Tsk2/+

Using samples from 4-week old female mice that show the most significant change in gene expression when we compare WT and tsk2/+ mice (Figure 6), we asked if there was change in the expression of TGFβ-regulated genes in these mice. Our analysis of

the Gene Ontology (GO) annotations shows that the majority of genes up-regulated in Tsk2/+ mouse skin at 4 weeks of age map to the GO Biological processes of Cell adhesion and Cell morphogenesis (DAVID, Benjamini-corrected $p < 0.05$). Genes that show increased expression include *Col6a1, Col6a2, Col5a1, Sparc* and *Thy1*. Many of these genes are known targets of the profibrotic cytokine TGFβ.

In order to formally identify the TGFβ responsive genes in an unbiased fashion, we used a unique 674-gene TGFbeta signature that we previously developed from human dermal fibroblasts [5]. Those human genes were then mapped to 526 mouse gene orthologs using the Mouse Genome Informatics (MGI) Mouse/Human Orthology Phenotype Annotations table (The Jackson Laboratory, Bar Harbor, Maine). Out of those 526 orthologs, 459 genes were annotated on the Agilent 4X44K Mouse Whole Genome Microarray. We then removed those genes that were likely to be affected by the hair growth cycle, or background noise, and in the end used 134 genes as our final, mouse TGFβ-responsive gene signature. These 134 genes represent the core TGFβ signature and includes the well-characterized TGFβ target genes.

Enrichment of the TGFβ responsive gene signature was analyzed in skin samples from 4-week old female mice that show the largest changes in gene expression (see above) and in samples that have been controlled for anagen (e.g. any sample that was in anagen was removed and only samples not in active hair cycle growth were considered). We then calculated enrichment of the TGFβ gene signature in each mouse sample by calculating the Pearson correlation coefficients between the centroid and the gene expression for each 4-week female mouse skin biopsy. These data are shown in Figure 6 and clearly show enrichment for TGFβ-responsive gene expression in Tsk2/+ female mice at 4 weeks of age. Overall, our results clearly show enrichment of the TGFβ-responsive gene signature in Tsk2/+ mice but not in WT mice, and this is dependent on age and hair cycle. We have collected skin samples to study even younger mice (2 weeks of age), in which we have seen a signature difference in males in preliminary analyses (Fig 6, next page)

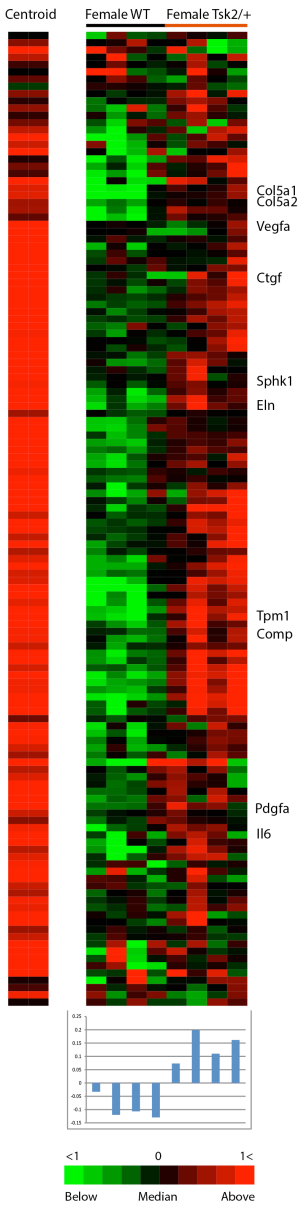

Figure 6. A TGFβ- responsive gene expression signature is activated in 4-week old female Tsk2/+ mice not in WT. A TGFβ responsive gene signature centroid was generated from TGFβ-treated human primary fibroblast [5]. The centroid representing the average of the TGFβ responsive genes is shown to the left of the heat map. Pearson correlations between the centroid and each array were calculated and are plotted directly beneath each microarray analyzing WT or Tsk2/+ mice from 4-week old female mice. Several known Tgfβ target genes are highlighted.

Milestone 4. Characterize how well the Tsk2/+ mouse approximates human SSc at different time points.

These tasks were conducted largely in year 3. We have used a genome-wide interspecies comparative analysis of mouse models and SSc patients, to determine which animal models of SSc best reflect the disease on a molecular level, providing models for study and pre-clinical testing[6]. Using gene expression as a readily quantifiable phenotype in skin, we have shown that three SSc models (Tsk2/+, the sclGVHD model, and bleomycin-induced fibrosis) are similar to their respective human subsets, not simply by gross morphology approximations but by robust molecular measures[6]. This is a significant contribution to the SSc field as it provides new, urgently needed insight into the genome-wide molecular changes that are common to mouse models **and** human SSc patients. It pinpoints which animal model should be used for developing specific therapeutics targeted at each of the different molecular intrinsic subsets of SSc, which are the **inflammatory, fibroproliferative,**

normal-like and limited subsets[7-10]. We found that skin of young Tsk2/+ mice share gene expression features with the ***fibroproliferative*** SSc subset, which represents 30 – 40% of the diffuse SSc (dSSc) patients. These features include enrichment of a TGFβ-responsive signature (**Fig. 6**) and a signature characteristic of proliferating cells. Other models examined include the sclGVHD model[11], the bleomycin-induced (Bleo) fibrosis model and the TβRIIΔk-fib model (unpublished); these mimic the *inflammatory* subset of SSc patients[6].

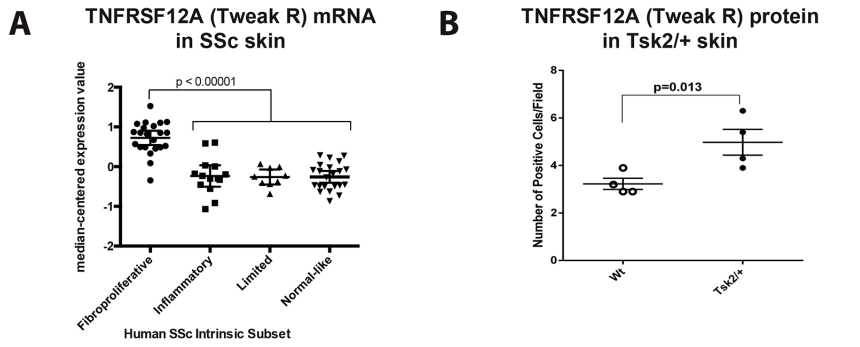

Figure 7. Tweak R (TNFRSF12A) is highly differentially expressed in both the fibroproliferative SSc patients and the Tsk2/+ mouse model. (A) SSc patients in the fibroproliferative subset express significant more tnfrsf12a (Tweak-R) than normal controls or patients in the inflammatory, proliferative or normal-like subsets (p < 0.00001). (B) Tsk2/+ mice expressed 1.6-fold more TNFRSF12A (TWEAK-R) than wild type littermates (p=0.013). Four-week-old female mice were scored for the number of TWEAK-R (Fn14)+ cells per field of view (400X magnification). Significance was calculated with a paired t-test using at least 8 fields of view per mouse and 4 mice per genotype.

Given the observation that the production of a major indicator of fibrosis, COL1A1, is increased by the transfection of the *Col3a1*^{Tsk2} gene, we assessed the impact of the mutant gene genome-wide. RNA from the *Col3a1*^{Tsk2} and *Col3a1*^{WT} transfected *Col3a1*-KO fibroblasts and from four week-old Tsk2/+ and WT littermate skin was analyzed by cDNA microarray. Differentially expressed pathways between the two transfections was determined by Gene Set Enrichment Analysis (GSEA). Transfection of *Col3a1*^{Tsk2} results in significant enrichment of genes associated with fibrotic Gene Ontology (GO) terms including *basement membrane*, *extracellular matrix*, *integrin binding*, and *transmembrane receptor protein kinase activity* (Figure 3D; GSEA FDR < 5%). The biological processes observed in the skin of four 4-week old female Tsk2/+ mice relative to WT littermates also shows increases in genes associated with GO terms *extracellular matrix*, *integrin binding* and *basal lamina* (ZL, CB, KBL, CA, EPB, MLW, manuscript *in preparation*).

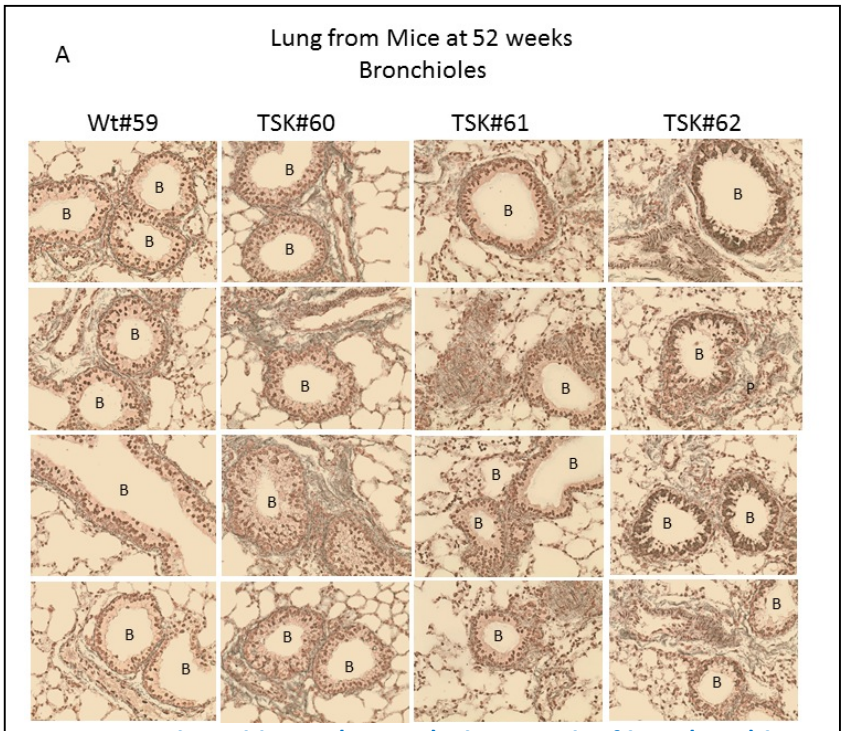

Figure 8. In the wild-type (WT#59), the reticular fibers (gray) line the bronchioles (B) tightly and are well delineated. In TSK2/+ (Tsk2#60, Tsk2#61, and Tsk2#62), the reticular fibers appear to be disorganized around the base of the bronchioles and there is more COL3A1 in the surrounding adventitia.

The genes that significantly contributed to the GSEA pathway enrichment in the transfected fibroblasts were extracted from microarray data of the transfections, as well as from female Tsk2/+ and WT skin at 4 weeks of age (Figure 3E-F), and were elevated both in the fibroblasts transfected with *Col3a1*^{Tsk2} and in Tsk2/+ mouse skin. These include those genes typically associated with fibrosis including CTGF, THY1, FBN1, the collagens, laminins, TGFB1, TGFBR1, ADAMTS family genes and MMP11. In addition, there was up-regulation in *Col3a1*^{Tsk2}-transfected fibroblasts

and Tsk2/+ skin RNA of the VEGF-Receptors *FLT1* and *FLT4*, as well as genes associated with PDGF signaling (PDGFRB and PDGFRL). These data indicate that expression of the *Col3a1*^{Tsk2} gene alone can induce a fibrotic gene expression program.

Milestone 4, new data

Of interest, there is a new pathway in fibrosis that we discovered in this study. To confirm the molecular similarities between the patients in the *fibroproliferative* subset and Tsk2/+ mice we analyzed the expression of the TGFβ-regulated gene tumor necrosis factor receptor superfamily, member 12a (*tnfrsf12a*; also designated *Tweak-R*, *fibroblast growth factor-inducible-14*). *Tweak-R* is highly expressed in the *fibroproliferative* subset and was among a set of genes highly correlated to worse skin disease. Gene expression differences there were confirmed by qRT-PCR [7]. *Tweak-R* mRNA levels were also found increased in the fibroproliferative subsets of Milano *et al.* (**Figure 7a**; $p < 0.00001$). We performed IHC on sections of skin taken from Tsk2/+ and their wild-type littermates to detect the levels of TWEAK-R. The *Tweak-R* gene is induced by TGFβ [12] and there is an ~1.5-fold increase in numbers of TWEAK-R positive cells at in skin of 4-week-old female Tsk2/+ mice compared to their littermates (Figure 7B; $p = 0.013$). Taken together with the findings of enrichment of TGFβ-signaling in *fibroproliferative* skin biopsies [13], it seems that Tsk2/+ skin at one month reflects the biology of this subset of SSc.

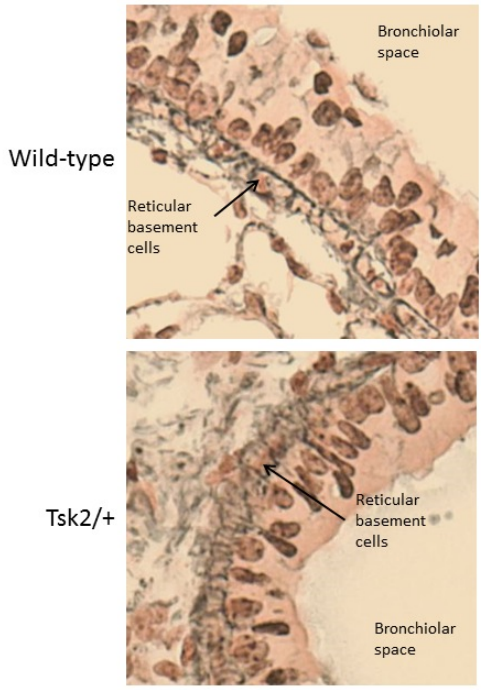

Figure 9. Reticular fibers are disorganized surrounding reticular basement cells in Tsk2/+ mice.

Milestone 5 : Reticular fibers staining of lung tissue

We further pursued the finding of abnormal reticular fibers (type III collagen) in the tissues and investigated lung in Tsk2/+ and wild-type littermate mice. We found that Tsk2/+ mice in addition to having abnormal reticular fibers in the skin (2012 report) we also demonstrate reticular fiber abnormalities in the lung of Tsk2/+ mice at 52 weeks of age (**Figures 8-11).** We are currently investigating earlier time points to determine whether this observation holds true in younger animals. **Figure 8** gives an overview of the overall pathological differences that we observed between Tsk2/+ and their wild-type littermates. These differences are described in more detail in **Figures 9, 10 and 11**. We note that all aspects of the lung tissue in the Tsk2/+ mouse show an overt increase in reticular fibers.

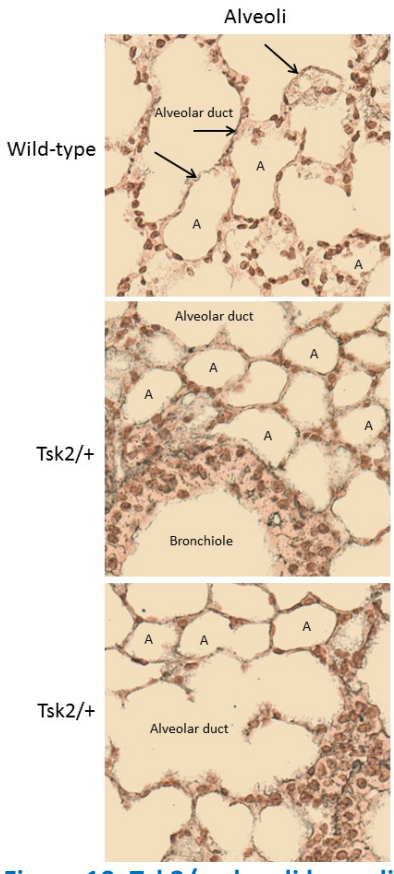

Figure 10. Tsk2/+ alveoli have diffuse and disorganized reticular fibers (gray stain), whereas there was well defined collagen in the wild-type mouse (arrows).

On closer examination of the reticular fibers surrounding the bronchioles, we observed that in the wild-type lung there was a single layer of reticular basement cells surrounded by reticular fibers that was densely stained (arrow). However in the Tsk2/+ mouse the even though the bronchioles were surrounded by a single layer of reticular basement cells (arrow), the reticular fibers were diffuse and not well defined (**Figure 8**). We noted additional lung abnormalities in the Tsk2/+ mouse. We observed that there were

increased reticular fibers surrounding the alveoli. Alveoli are normally supported by a fine network of fibers (arrows in wild-type image) however in the Tsk2/+ mouse, there was increased staining for type III collagen and we also noted that this was also disorganized and not well delineated as that observed in the wild-type mouse at the same age (**Figure 9)**.

Finally we note that the smooth muscle in the lung had heavy staining in the Tsk2/+ mouse and that there were thickened areas of stain between the columnar epithelial cells (**Figure 10**).

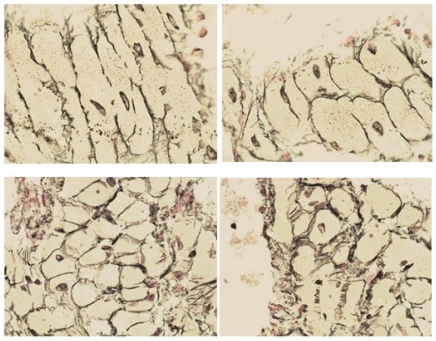

Figure 11. Tsk2/+ mice demonstrate increased reticular fibers surrounding epithelial cells of the lung. Note the increased deposition of stain between the cells in the Tsk2/+ lung.

Previously it has been reported that Tsk2/+ mice had an emphysema type pathology in the lung; however we did not observe this phenotype. We found that the lung parenchyma overall was normal with the exception of the increased reticular fiber staining as shown above.

Based on our finding that there is a mutation in the PIIINP region of the *Col3α1* gene, and that it has been reported that the PIIINP fragment is involved in fibrillogenesis of type I collagen, we speculated that we would not be able to extract protein from the skin of these mice as easily as from the wild-type mice using 1M NaCl or 0.5M acetic acid. Indeed, we found that less protein was extracted with 1M NaCl from the Tsk2/+ skin but the amount of extracted protein with 0.5M acetic acid was not significantly different. Acid extractable protein was found to be 0.33 mg/ml in the wild-type vs 0.32 mg/ml in Tsk2, p=0.47; whereas for salt extracted protein there was 0.86 mg/ml from the wild-type vs. 0.68 mg/ml from Tsk2, p=0.045. We are extending these findings to additional animals and want to determine why there is less extractable protein in Tsk skin. Our goal now is to establish how this mutation alters collagen fibrillogenesis leading to thickened skin and altered reticular fiber pathology.

We submitted a grant application to the Scleroderma Research Foundation on this extensive study of the lung phenotypes in Tsk2/+ mice, which had not been appreciated prior to our study, but it was not funded.

We began the investigation altered protein synthesis of specific genes in the skin of the Tsk2/+ mouse as determined by the increased gene expression that was identified in collaboration with Dr. Michael Whitfield at Dartmouth. This is the subject of a grant application to the NIH (reviewed, Oct 2014).

CONCLUSION:

A non-synonymous mutation in COL3A1 is the causative mutation in Tsk2/+. This mutation results in a time-dependent activation of numerous gene expression pathways, including TGFβ-1 and TWEAK/FN14 signaling, that varies by gender and age. The mechanism by which the COL3A1 mutation causes these changes is yet unknown but we have developed a new hypothesis that the N-terminal propeptide, where the mutation lies, cannot effectively bind TGFβ-1, something we will be examining carefully in future studies.

KEY RESEARCH ACCOMPLISHMENTS Summary (Jul 1, 2011-June 30, 2014)

- We completed the nucleotide sequencing of the mouse Tsk2/+ interval. A number of single nucleotide polymorphisms were found and verified by SNP allele-specific PCR analysis [1] for these previously unsequenced strains (101/H, the parental strain; and B6.tsk2, the B6 congenic strain bearing mutated 101/H DNA on chromosome 1 that contains the Tsk2/+ mutation).
- *Col3A1* is the Tsk2 gene. This SNP is the only one in the interval that shows a coding mutation; it also is interesting that it often shows an expression difference, unlike any of the other genes with non-coding SNPs.

- The mutation lies in the PIIINP fragment of COL3A1^{TSK2}. This peptide is cleaved off the pro-col3a1 pro-protein, and circulates in the body, and is also active locally. We have formed a new hypothesis that the PIIINP^{Tsk2} form cannot bind TGFβ or a related protein, bone morphogenetic protein-2 (BMP-2) as well as PIIINP^{WT} and that this leads to fibrosis and tight skin in mice. This proposition has considerable support from studies of PINP and PIINP[14, 15], and we have recently submitted a grant application to the Scleroderma Foundation to study this intriguing hypothesis. If proven true, for example, it would mean that the excess circulating PIIINP in SSc patients and other fibrotic disorders is functional and is part of a regulatory mechanism to control fibrosis.
- The genetic complementation test of *Col3a1* (mice bred from the Tsk2/+ line to BALB.Col3A1KO mice) was unequivocal and proved *Col3A1* is the *Tsk2* gene
- We proved that the excess deposition of collagen matrix does not occur until well after the Tsk2/+ tight skin phenotype is evident. However, other TGFβ-target genes are elevated as early as two weeks of age.
- Deletion of the NLRP3 inflammasome, or the fibulin-5 gene (Fbln5-KO) had no effect on tight skin or fibrosis, even though the former had a small effect on wound healing, and the latter reduced elastic fibers in the skin. Both these results have been published (see appendix).
- We have prepared a large number of fibroblast cell lines in preparation for *in vitro* studies of the Tsk2 trait under selective conditions.
- Microarray profiling of Tsk2/+ mice at 4, 8, 12 and 20 weeks have now been performed for both male and female mice totaling > 48 samples (we have previously only reported results at two time points for a single gender that totaled 8 samples). We have identified genes that are differentially regulated at each time point. Our prior data was suggestive of increased TGFβ signaling but did not show this directly using an experimentally derived TGFβ gene signature. We have now demonstrated that this is indeed the case. Tsk2/+ mice have a TGFβ1 signature that is seen in a global assessment of mRNA from skin in a carefully controlled study using littermates (Tsk2/+ and WT) at timed stages and stratified by sex. Controlling for hair cycle dramatically improves our ability to detect differently expressed genes and we are now mining these carefully controlled data for differentially expressed pathways.
- We have identified increased activity of members of a new pathway (TWEAK/FN14) in human SSc patients (of the fibroproliferative subset), in Tsk2 mice, and in fibroblasts transfected with *Col3a1*^{Tsk2} cf. *Col3a1*^{WT}. This led us to order FN14-KO mice from Dr. Linda Burkly (Biogen Idec) to breed to Tsk2/+ dams, eventually to create the Tsk2 mutation on a FN14 background. We are excited by this finding, which could be translated into a new therapeutic target for scleroderma.

The next reporting period:

As this is the final report, "Nothing to Report."

4. IMPACT

What was the impact on the development of the principal discipline(s) of the project?

There were several surprises from our three years of work on fibrosis and scleroderma in the model mouse, Tsk2/+: one is that a single amino acid change in the N-terminal propeptide of COL3A1 (PIIINP) can cause such a profound change in gene expression, dermal health status, tightness of skin, inhibition of wound healing, and fibrosis. Given this, we have had to revise our hypothesis of the function of this PIIINP fragment that we now believe is not a benign cleavage product but instead a key modulator of skin (and perhaps lung [16]) health. This has led us to further hypothesize that the circulating PIIINP that is elevated in patients with fibrotic disease [17, 18] is not simply a benign biomarker of unfavorable outcomes, but rather may be

produced as a consequence of excess COL3A1 production, and that it has a separate function as a compensatory factor, acting to inhibit TGFβ signaling and shut down ECM deposition. The Tsk2 mutation likely inactivates this function, allowing TGFβ production and fibrosis. This notion is highly novel, as there are no publications on the role of PIIINP in scleroderma or any other fibrotic disease.

What was the impact on other disciplines?

Recently, general scientific opinion articles have suggested that animal models and studies therein are dispensable; that the mouse does not model human disease sufficiently well to deserve much effort to study it. In the specific case of Tsk2/+, some reviewers have said that because the mutation in *Col3a1*^{Tsk2} has never been observed in human patients (nor has it been searched for), the Tsk2/+ model is irrelevant. In fact, what we found is that Tsk2/+ mice model the fibroproliferative subset of SSc patients at the level of expressed genes and pathways, including TWEAK/FN14 (aka TWEAK-R). Thus, Tsk2/+ is the *only* animal model that resembles this subset of patients, making it particularly important for SSc research. Our careful dissection of this mouse model of SSc at the levels of gene expression, protein expression, tissue injury and whole body traits has given us more information on its relevance to a particularly difficult-to-treat subset of SSc patients, a link that we argue would be true for other disciplines as well.

What was the impact on technology transfer?

We have submitted a proposal to NIH to explore the possibilities of inhibiting TWEAK-R in animal models of SSc, with an eye toward doing so in human subjects. We are planning a submission of an SBIR-like grant this fall to the Scleroderma Research Foundation that will, we hope, involve Biogen Idec, a company with extensive experience, reagents and interest in this signaling pathway.

What was the impact on society beyond science and technology?

Scleroderma is an incurable disease that often has a very poor prognosis. If our results are confirmed and found to translate to the human disease, we could propose at least two ways to ameliorate the tightness of skin of these patients, especially for the fibroproliferative intrinsic molecular subset of patients: manipulation of TWEAK/FN14 and exploration of the potential therapeutic role of PIIINP.

5. CHANGES/PROBLEMS

None to report.

6. PRODUCTS:

REPORTABLE OUTCOMES (July 1, 2011 to June 30, 2014)

Oral Presentations: (Chronological Order)

Fall/11- Michael L. Whitfield, PhD. “Capturing the heterogeneity in systemic sclerosis with high-throughput gene expression profiling” Drexel University Department of Immunology and Microbiology Seminar Series.

3/12 Kristen Long Ph.D. “The Tsk2/+ animal model of Scleroderma”, PhD thesis defense.

6/12 Michael L. Whitfield, PhD. “Capturing the heterogeneity in systemic sclerosis with high-throughput gene expression profiling”. Synergy Translation Research Program, Geisel School of Medicine at Dartmouth. Lebanon, NH

6/12 Michael Whitfield, PhD. “Intrinsic Gene Expression Subsets of Systemic Sclerosis Are Stable in Serial Skin Biopsies and Show Differential Therapeutic Response” Division of Rheumatology, Brigham and Women’s Hospital, Harvard Medical School, Boston MA.

6/12 Michael Whitfield, PhD. “Capturing the heterogeneity in systemic sclerosis with high-throughput gene expression profiling” Scleroderma NIAMS Center of Research Translation Advisory Committee and Investigators Meeting, Boston University School of Medicine, Boston MA

8/12 Elizabeth Blankenhorn, " Genetic control of fibrosis in the Tsk2 Model of Scleroderma". Whitfield Laboratory Annual Retreat. New Hampshire, August 2012

9/12 Chelsea Burgwin, year 3 graduate student supported by DOD. "Mapping the Mutation in the Tight Skin 2 model of systemic sclerosis and Development of an *in vitro* Model." Molecular Cell Biology and Genetics Seminar Series, Drexel University College of Medicine ,September 2012.

10/12 Michael Whitfield, PhD. “Subsetting systemic sclerosis by high-throughput gene expression”. Scleroderma SCOT clinical trial investigators meeting (NIH sponsored), Potomac MD

11/12 Michael Whitfield, PhD. “NIAMS p30 Microarray Core for Scleroderma”, P30 Investigators and Users National presentation. Boston, MA

3/13 Michael Whitfield, PhD. “Integrative Genomics in Systemic Sclerosis”, Stanford Epithelial Biology Program. Stanford, CA

3/13 Michael Whitfield, PhD. “Plasticity and interconnectivity of the SSc intrinsic Subsets” Scleroderma Research Foundation Workshop, San Francisco, CA

4/13 Michael L. Whitfield, PhD "P50 Core: A focus on Next Generation Generation sequencing methods in SSc-PAH". Scleroderma NIAMS Center of Research Translation Advisory Committee and Investigators Meeting, Boston University School of Medicine, Boston MA.

3/13 Zhenghui Li (Whitfield Lab). “Identifying Genetic Variation in the Tsk2/+ Model of Systemic Sclerosis” Molecular and Cellular Biology Program, Research in Progress.

5/13 Michael L. Whitfield, PhD "Personalized Medicine and Disease Pathogenesis in Systemic Sclerosis by Integrative Genomics" Geisel School of Medicine, Department of Micro-Immuno Annual Retreat.

6/13 Zhenghui Li (Whitfield lab), "RNA-seq and miR-seq analysis of SSc skin across intrinsic gene expression subsets shows differential expression of non-coding RNAs regulating SSc gene expression" FGED Meeting, Seattle WA.

6/13 Michael L. Whitfield, PhD "P30 SSc Microarray and Bioinformatics Core: Services to the national SSc community". Boston MA.

8/13 Elizabeth Blankenhorn PhD, Plenary talk, “The genetic basis for Tsk2/+ fibrosis” 13th International Workshop on Scleroderma Research, Boston, Massachusetts, August 2013.

8/13 Zhenghui Li(Whitfield lab), “RNA-Seq and miRNA-seq analysis of SSc skin across intrinsic gene expression subsets…” 13th International Workshop on Scleroderma Research, Boston, Massachusetts, August 2013.

1/14 Chelsea Burgwin, year 4 graduate student supported by DOD. “Tsk2/+ Wound Healing and *in vitro* Model” Molecular Cell Biology and Genetics Seminar Series, Drexel University College of Medicine, September 2012.

3/14 Chelsea Burgwin, year 4 graduate student supported by DOD. “Tsk2/+ Wound Healing and *in vitro* Model” University of Pennsylvania’s Cell Mechanics Journal Club and Presentation Series, March 2014.

6/14 Chelsea Burgwin, year 4 graduate student supported by DOD. “Signaling in Skin and Fibroblasts from Tsk2/+ Mice: Elucidating the Mechanism in the Tsk2/+ Mouse Model of Scleroderma” 2014 International Symposium on Molecular Medicine and Infectious Disease, Drexel University, June 2014.

6/14 Elizabeth Blankenhorn PhD, “Genetics of scleroderma in animal models” 2014 International Symposium on Molecular Medicine and Infectious Disease, Drexel University (June 2014).

6/14 Kristen Long PhD, “The role of elastin in wound healing and tight skin trait in Tsk2 mice”2014 International Symposium on Molecular Medicine and Infectious Disease, Drexel University (June 2014).

6/14 Michael L. Whitfield PhD, “Intrinsic molecular subsets of scleroderma”2014 International Symposium on Molecular Medicine and Infectious Disease, Drexel University (June 2014).

6/14 Carol Artlett PhD, “Role of the Inflammasome and miRNA in fibrosis” 2014 International Symposium on Molecular Medicine and Infectious Disease, Drexel University (June 2014).

Abstracts and Presentations: (Chronological Order)

1. Long, K.B., C.M. Burgwin, C.M. Artlett and E.P. Blankenhorn. “Elastin and collagen anomalies in pre-fibrotic skin in the Tsk2/+ mouse, a model for Scleroderma.” 20th Annual Infection and Immunity Forum, Eastern PA Branch of ASM, Drexel University College of Medicine, Philadelphia, Pennsylvania, June 2011.

2. Long, K.B., C.M. Burgwin, C.M. Artlett and E.P. Blankenhorn. “Examination of prefibrotic and fibrotic disease in Tsk2/+ mice shows early ECM changes are attributable to elastin dysregulation.” 12th International Workshop on Scleroderma Research, Cambridge, UK, July 2011.

3. Long*, K.B., C.M. Burgwin, C.M. Artlett and E.P. Blankenhorn. “Examination of prefibrotic and fibrotic disease in Tsk2/+ mice shows early ECM changes are attributable to elastin dysregulation.” Drexel University College of Medicine, Discovery Day Research Symposium, Philadelphia, Pennsylvania, October 2011. *Outstanding Platform Presentation award winner

4. John, A.K., K.B. Long, L. Cort and E.P. Blankenhorn. “Fibroblast investigations suggest that increased collagen production is cell-autonomous in the Tsk2/+ mouse model of scleroderma.” Drexel University College of Medicine, Discovery Day Research Symposium, Philadelphia, Pennsylvania, October 2011.

5. C.M. Burgwin, K.B. Long, Zhenghui Li*, C.M. Artlett, M. Whitfield*, and E.P. Blankenhorn. “Mapping of the Mutation in the Tight Skin 2 model of systemic sclerosis” Department of Microbiology and Immunology, Drexel Univ. College of Medicine, Philadelphia, PA. *Dartmouth Medical School, Hanover, NH, Institute for Molecular Medicine and Infectious Disease International Symposium, Philadelphia, PA, June 2012

6. Zhenghui L. "Identifying Genetic Variations in the Tsk2 Model of Scleroderma". Dartmouth MCB Program Annual Retreat. Whitefield, New Hampshire, August 2012

7. Burgwin, C.M., K.B. Long, Z. Li., C.M. Artlett, M.L. Whitfield and E.P. Blankenhorn. “Complementation Experiment Examining the Role Collagen3α1 plays in Disease Development of the Tight Skin 2 Mouse Model of Systemic Sclerosis” Discovery Day, Drexel University College of Medicine, Philadelphia, Pennsylvania, October 2012.

8. Zhenghui Li, Eleni Marmarelis, Qu Kun, Lionel Brooks, Gavin D. Grant, Patricia A. Pioli, Howard Chang, Robert Lafyatis, and Michael L. Whitfield. "RNA-seq and miR-seq analysis of SSc skin across intrinsic gene expression subsets shows differential expression of non-coding RNAs regulating SSc gene expression". Functional Genomics Data Society 15th Annual Meeting, Seattle, Washington, June 2013

9. Zhenghui Li, Kristen Long, Carol Artlett, Elizabeth Blankenhorn and Michael L. Whitfield. "Identifying Genetic Variations in the Tsk2 Model of Scleroderma". Dartmouth MCB Program Annual Retreat. Whitefield, New Hampshire, August 2013

10. Burgwin, C.M., K.B. Long, Zhenghui Li, M. Whitfield, C.M. Artlett, E.P Blankenhorn “TGF-β’s and Elastin’s Roles in Disease Progression in the Tsk2/+ Mouse Model of Systemic Sclerosis.”

a. 13th International Workshop on Scleroderma Research, Boston, Massachusetts, August 2013. *Won Drexel GSA Travel Award

b. Discovery Day, Drexel University College of Medicine, Philadelphia, Pennsylvania, October 2013. *Poster won Honorable Mention.

11. Burgwin, C.M., S. Sassi-Gaha, K.B. Long, Zhenghui Li, M. Whitfield, C.M. Artlett, E.P Blankenhorn "Elucidating the Mechanism of Fibrosis in the Tight skin 2 (Tsk2/+) Mouse Model of Scleroderma" 2014 International Symposium on Molecular Medicine and Infectious Disease, Drexel University, Philadelphia, Pennsylvania, June 2014.

12. Zhenghui Li, Kristen Long, Carol Artlett, Elizabeth Blankenhorn and Michael L. Whitfield. "Identifying Genetic Variations in the Tsk2 Model of Scleroderma". Dartmouth MCB Program Annual Retreat. Whitefield, New Hampshire, August 2014.

Manuscripts:

1. Long, K.B., Li, Z.., Burgwin, C., Choe, S.G., Martyanov, V., Sassi-Gaha, S., Earl, J., Eutsey, R., Ahmed, A., Ehrlich, G.D., Artlett, C.M., Whitfield, M.L., and Blankenhorn, E. P. The Tsk2/+ fibrotic phenotype is due to a gain-of-function mutation in the PIIINP segment of the Col3a1 gene. *Journal of Investigative Dermatology*, 2014 (in press)
2. Long, K.B., Artlett, C.M., and Blankenhorn E. P. Tight Skin 2 Mice exhibit a novel time line of events leading to increased extracellular matrix deposition and dermal fibrosis, *Matrix Biology*, doi: 10.1016/j.matbio.2014.05.002. PMID: 24820199, 2014
3. Long*, K.B., Burgwin*, C.M., Huneke, R., Artlett, C.M., and Blankenhorn, E. P. The wound healing deficit in Tsk2/+ is due to excess elastin. Advances in Wound Care, *in press,* 2014. PMID: 25207200. *Equal contributions. Invited submission, and Dr. Blankenhorn was a guest editor of this journal issue.
4. Sargent, J.L., Zhenghui Li, A.O. Aliprantis, M. Greenblatt, R. Lemaire, M.H. Wu, J. Wei, A. Harris, K. Long, C.M. Burgwin, C.M. Artlett, E.P. Blankenhorn, R. Lafyatis, J. Varga, S. H. Clark, M.L. Whitfield. "Interspecies Comparative Genomics Identifies Optimal Murine Models of Scleroderma Subsets" Submitted.
5. Zhenghui Li, Kristen B. Long, Chelsea Burgwin, Carol M. Artlett and Elizabeth P. Blankenhorn, Michael L. Whitfield. The Tsk2/+ mouse model of Systemic Sclerosis shows variable age and gender dependent gene expression in skin. Manuscript *in preparation*.

Degrees obtained that are supported by this award

Chelsea M. Burgwin is working on her PhD thesis, expected defense in Spring, 2015. Her work is directly supported by this grant.

Zhenghui Li is working toward his PhD thesis with an expected completion date in 2015. His work is directly supported by this grant.

Kristen Long successfully defended her PhD thesis, entitled "Examination of a model of systemic sclerosis, the Tight Skin 2 mouse: before, during and after fibrotic disease" in April, 2012. She was awarded her PhD by Drexel University College of Medicine in May 2012. Her work was directly supported by this grant.

Development of cell lines, tissue or serum repositories

We have developed a large number of Tsk2/+ and WT littermate fibroblast cell lines from mice of various ages and both sexes.

7. PARTICIPANTS & OTHER COLLABORATING ORGANIZATIONS

There were no changes to the personnel at Drexel and no new changes in the laboratory of the partnering PI,

Dr. Michael Whitfield at Geisel School of Medicine at Dartmouth College, NH.

8. SPECIAL REPORTING REQUIREMENTS

COLLABORATIVE AWARDS: For collaborative awards, independent reports are required from BOTH the Initiating PI and the Collaborating/Partnering PI. A duplicative report is acceptable; however, tasks shall be clearly marked with the responsible PI and research site. A report shall be submitted to https://ers.amedd.army.mil for each unique award.

An identical final progress report will be sent from Dr. Whitfield.

9. REFERENCES

1. Bunce M, O'Neill CM, Barnardo MC, Krausa P, Browning MJ, Morris PJ, Welsh KI: **Phototyping: comprehensive DNA typing for HLA-A, B, C, DRB1, DRB3, DRB4, DRB5 & DQB1 by PCR with 144 primer mixes utilizing sequence-specific primers (PCR-SSP).** *Tissue Antigens* 1995, **46:**355-367.
2. Ishigame H, Mosaheb MM, Sanjabi S, Flavell RA: **Truncated Form of TGF-betaRII, But Not Its Absence, Induces Memory CD8+ T Cell Expansion and Lymphoproliferative Disorder in Mice.** *J Immunol* 2013, **190:**6340-6350.
3. Barisic-Dujmovic T, Boban I, Clark SH: **Regulation of collagen gene expression in the Tsk2 mouse.** *J Cell Physiol* 2008, **215:**464-471.
4. Christner PJ, Hitraya EG, Peters J, McGrath R, Jimenez SA: **Transcriptional activation of the alpha1(I) procollagen gene and up-regulation of alpha1(I) and alpha1(III) procollagen messenger RNA in dermal fibroblasts from tight skin 2 mice.** *Arthritis Rheum* 1998, **41:**2132-2142.
5. Sargent JL, Milano A, Bhattacharyya S, Varga J, Connolly MK, Chang HY, Whitfield ML: **A TGF beta-Responsive Gene Signature Is Associated with a Subset of Diffuse Scleroderma with Increased Disease Severity.** *Journal of Investigative Dermatology* 2010, **130:**694-705.
6. Sargent JL, Li Z, Aliprantis AO, Greenblatt M, Lemaire R, Wu M-h, Wei J, Harris A, Long K, Burgwin C, et al: **Interspecies Comparative Genomics Identifies Optimal Mouse Models of Scleroderma Subsets.** *Submitted* 2014.
7. Milano A, Pendergrass SA, Sargent JL, George LK, McCalmont TH, Connolly MK, Whitfield ML: **Molecular subsets in the gene expression signatures of scleroderma skin.** *PLoS One* 2008, **3:**e2696.
8. Pendergrass SA, Lemaire R, Francis IP, Mahoney JM, Lafyatis R, Whitfield ML: **Intrinsic Gene Expression Subsets of Diffuse Cutaneous Systemic Sclerosis Are Stable in Serial Skin Biopsies.** *Journal of Investigative Dermatology* 2012, **132:**1363-1373.
9. Hinchcliff ME, Huang CC, Wood TA, Mahoney JM, Martyanov V, Bhattacharya S, Tamaki Z, Carns M, Podlusky S, Sirajuddin A, et al: **Molecular Signatures in Skin Associated with Clinical Improvement During Mycophenolate Treatment in Systemic Sclerosis.** *J Invest Dermatol* 2013, **In Press**.
10. Hinchcliff M, Huang CC, Wood TA, Matthew Mahoney J, Martyanov V, Bhattacharyya S, Tamaki Z, Lee J, Carns M, Podlusky S, et al: **Molecular signatures in skin associated with clinical improvement during mycophenolate treatment in systemic sclerosis.** *J Invest Dermatol* 2013, **133:**1979-1989.
11. Greenblatt MB, Sargent JL, Farina G, Tsang K, Lafyatis R, Glimcher LH, Whitfield ML, Aliprantis AO: **Interspecies comparison of human and murine scleroderma reveals IL-13 and CCL2 as disease subset-specific targets.** *Am J Pathol* 2012, **180:**1080-1094.
12. Milks MW, Cripps JG, Lin H, Wang J, Robinson RT, Sargent JL, Whitfield ML, Gorham JD: **The role of Ifng in alterations in liver gene expression in a mouse model of fulminant autoimmune hepatitis.** *Liver Int* 2009, **29:**1307-1315.

13. Sargent JL, Milano A, Bhattacharyya S, Varga J, Connolly MK, Chang HY, Whitfield ML: **A TGFbeta-responsive gene signature is associated with a subset of diffuse scleroderma with increased disease severity.** *J Invest Dermatol* 2009, **130:**694-705.
14. Oganesian A, Au S, Horst JA, Holzhausen LC, Macy AJ, Pace JM, Bornstein P: **The NH2-terminal propeptide of type I procollagen acts intracellularly to modulate cell function.** *J Biol Chem* 2006, **281:**38507-38518.
15. Zhu Y, Oganesian A, Keene DR, Sandell LJ: **Type IIA procollagen containing the cysteine-rich amino propeptide is deposited in the extracellular matrix of prechondrogenic tissue and binds to TGF-beta1 and BMP-2.** *J Cell Biol* 1999, **144:**1069-1080.
16. Lee YJ, Shin KC, Kang SW, Lee EB, Kim HA, Song YW: **Type III procollagen N-terminal propeptide, soluble interleukin-2 receptor, and von Willebrand factor in systemic sclerosis.** *Clin Exp Rheumatol* 2001, **19:**69-74.
17. Vettori S, Maresca L, Cuomo G, Abbadessa S, Leonardo G, Valentini G: **Clinical and subclinical atherosclerosis in systemic sclerosis: consequences of previous corticosteroid treatment.** *Scand J Rheumatol* 2010, **39:**485-489.
18. Nagy Z, Czirják L: **Increased levels of amino terminal propeptide of type III procollagen are an unfavourable predictor of survival in systemic sclerosis.** *Clin Exp Rheumatol* 2005, **23:**165-172.

10. APPENDIX

1. Manuscript by Long, Artlett, and Blankenhorn follows this page (Matrix Biology in press, 2014).
2. Manuscript by Long^, Burgwin^, Huneke, Artlett, and Blankenhorn (Adv. In Wound Care, 2014).
3. Manuscript by Long, Li, Burgwin, Choe, Martyanov, Sassi-Gaha, Earl, Eutsey, Ahmed, Ehrlich, Artlett, Whitfield, and Blankenhorn, (Journal of Investigative Dermatology, in press, 2014).
4. Manuscript by Sargent, Li, Aliprantis, Greenblatt, Lemaire, Wu, Wei, Harris, Long, Burgwin, Artlett, Blankenhorn, Lafyatis, Varga, Clark, and Whitfield, submitted 2014.

Matrix Biology xxx (2014) xxx–xxx

Contents lists available at ScienceDirect

Matrix Biology

journal homepage: www.elsevier.com/locate/matbio

Tight skin 2 mice exhibit a novel time line of events leading to increased extracellular matrix deposition and dermal fibrosis

Kristen B. Long, Carol M. Artlett, Elizabeth P. Blankenhorn *

Department of Microbiology and Immunology, Drexel University College of Medicine, Philadelphia, PA, USA

ARTICLE INFO

Article history:
Received 25 October 2013
Received in revised form 30 April 2014
Accepted 2 May 2014
Available online xxxx

Keywords:
Tight skin 2 mouse
Systemic sclerosis
Skin
Collagen
Elastic fibers

ABSTRACT

The tight skin 2 (Tsk2) mouse model of systemic sclerosis (SSc) has many features of the human disease including tight skin, fibrosis, extracellular matrix abnormalities, and reported antinuclear antibodies (ANA). Here we report that Tsk2/+ mice develop excess dermal fibrosis with age, as skin is not significantly fibrotic until 10 weeks, a full eight weeks after the development of the physical tight skin phenotype. Concomitantly with the tight skin phenotype at two weeks of age, Tsk2/+ mice demonstrate increased levels of total transforming growth factor beta 1 (TGF-β1) and excessive accumulation of dermal elastic fibers. The increase in elastic fibers is not responsible for tight skin, however, because Tsk2/+ mice genetically engineered to lack skin elastic fibers nevertheless have tight skin and fibrosis. Finally, about two months after the first measurable increases of total collagen, a portion of Tsk2/+ mice produce ANAs, but at a similar level to wild-type littermates. The timeline of disease development in the Tsk2/+ mouse shows that fibrosis is progressive, with elastic fiber alterations and TGF-β1 over-production occurring at least two months before *bona fide* fibrosis, that is not dependent on ANA production.

1. Introduction

Systemic sclerosis (SSc) is an autoimmune disorder of unknown origin, characterized by excess accumulation of the extracellular matrix (ECM), primarily collagen, in skin and other internal organs, vascular alterations, and production of antinuclear antibodies (ANAs) (LeRoy et al., 1988; Okano, 1996). Recently, classification of SSc has been redefined. Patients presenting with "skin thickening of the fingers of both hands extending proximal to the metacarpophalangeal joints" fulfills the new major criterion, and alone is enough for a diagnosis. If absent, a score is calculated based on seven additional criteria, and if patients score at or above the threshold (a score of 9), they are classified as having SSc (van den Hoogen et al., 2013). SSc is divided into two major subsets based on total skin involvement. Limited cutaneous SSc involves dermal thickening of skin below the elbows and knees, with or without facial involvement, while diffuse cutaneous SSc manifests as dermal thickening of skin in the extremities, face, and trunk, as well as involvement of at least one internal organ, including the lungs, kidneys, heart, esophagus, and gastrointestinal tract (LeRoy et al., 1988). Survival rates vary significantly between and within subsets of disease, and are usually determined by the severity of the internal organ involvement (Ferri et al., 2002; Scussel-Lonzetti et al., 2002; Steen, 2005). Currently, there are no effective treatments for this disease.

There are several animal models of disease, but while mouse models have proved useful in studying various clinical features, no one mouse model exhibits all the signs of SSc (Artlett, 2010; Yamamoto, 2010). Two main genetic mouse models of disease are the tight skin (Tsk) 1 (Green et al., 1976) mouse and the Tsk2 (Peters and Ball, 1986). Each mouse strain bears a different homozygous lethal mutation that requires mice to be bred and evaluated as heterozygotes (e.g., Tsk1/+ and Tsk2/+). The cause of disease in Tsk1/+ mice is a mutation in the fibrillin 1 gene on chromosome 2 (Siracusa et al., 1996), whereas the cause of scleroderma-like signs in Tsk2/+ mice is a mutation in the collagen type III, alpha I gene (*Col3a1*) on chromosome 1 (Long, unpublished observations). The Tsk1/+ model, while valuable, has several disease signs that differ from SSc, including hypodermal collagen accumulation (Baxter et al., 2005) and an emphysema-like lung pathology (Szapiel et al., 1981).

By contrast, Tsk2/+ mice have increased collagen and ECM changes in the dermis. However, the timing of these changes is controversial. Studies by Christner et al. demonstrate a marked increase in collagen accumulation in the dermis of 10 day old Tsk2/+ mice, which was still present at seven to eight months of age compared to wild-type (WT) littermates. In addition, they observed a mononuclear inflammatory cell

Abbreviations: ANA, antinuclear antibody; αSMA, alpha smooth muscle actin; B6, C57Bl/6J; Col1a1, collagen, type 1, alpha 1; Col3a1, collagen, type 3, alpha 1; Fbln5, fibulin 5; SSc, systemic sclerosis; TGF-β1, transforming growth factor beta-1; Tsk, tight skin; WT, wild-type.

* Corresponding author at: Department of Microbiology and Immunology, Drexel University College of Medicine, 2900 Queen Lane, Philadelphia, PA 19129, USA. Tel.: +1 215 991 8392; fax: +1 215 848 2271.
E-mail address: Eblanken@Drexelmed.edu (E.P. Blankenhorn).

http://dx.doi.org/10.1016/j.matbio.2014.05.002

infiltrate (Christner et al., 1995). However, a subsequent report failed to confirm these findings (Barisic-Dujmovic et al., 2008). Christner et al. showed increased transcription of *Col1a1* and *Col3a1* and up-regulation of collagen production in fibroblasts isolated from Tsk2/+ mice of unstated sex and age (Christner et al., 1998). In agreement, Barisic-Dujmovic et al. (2008) showed that cultured Tsk2/+ fibroblasts had increased expression of a collagen I-promoter-driven GFP reporter compared to control WT fibroblasts, but together these findings do not address the timing of up-regulation of collagen in vivo. This group also noted that Tsk2/+ mice have decreased dermal adipose tissue, a significant reduction in body size and mass, yet normal lung morphology at two to three months of age (Barisic-Dujmovic et al., 2008). Finally, studies by Gentiletti et al. (2005) reported that aged Tsk2/+ mice, on a C3HxC57Bl/6J background, produce numerous antinuclear antibodies (ANAs) that are also observed in SSc.

In the present study, we examined disease pathology and progression over time in Tsk2/+ male and female mice bred to a standard C57Bl/6J (B6) background. We report a novel timeline of events in Tsk2/+ disease development and show that the signs of fibrotic disease are progressive, starting from two weeks of age. Our study also demonstrates that Tsk2/+ mice have excessive elastic fiber accumulation at two weeks; however, analyses of fibulin-5 knockout mice (with a defect in skin elastic fiber formation) demonstrate that elastic fibers are not responsible for the tight skin phenotype or later fibrosis. Also at this age, increased levels of TGF-β1 were observed, and eight weeks later measurable increases in total collagen protein levels were detected, suggesting that the slow accumulation of collagen is TGF-β1 dependent. In addition, we demonstrate that ANAs are present in Tsk2/+ mice only after disease is well established.

2. Results

2.1. Footpad thickness predicts the tight skin phenotype in Tsk2/+ mice

The tight skin phenotype in Tsk2/+ mice is physically evident and felt upon pinching the interscapular skin of young mice as early as two weeks of age (Christner et al., 1995), but this assessment is variable and subjective (Baxter et al., 2005). To provide a more quantitative assay for the Tsk2/+ trait, we assessed the thickness of mouse footpads corrected for body weight. Body weight must be factored due to changes in weight that characterize normal mouse development, weight differences between male and female mice, or between members of different litters. For all ages, weight differences were observed between male and female mice ($p < 0.0001$), as well as between same-sex Tsk2/+ vs. WT mice ($p < 0.001$); mice carrying the *Tsk2* mutation were noted to weigh significantly less than their WT littermates (Fig. 1A) (Barisic-Dujmovic et al., 2008). Footpad thicknesses were highly significantly associated with inheritance of the *Tsk2* gene, with low variance and excellent reproducibility (Fig. 1B and C). At four to six weeks of age, Tsk2/+ male and female mice have significantly thicker footpads than WT mice

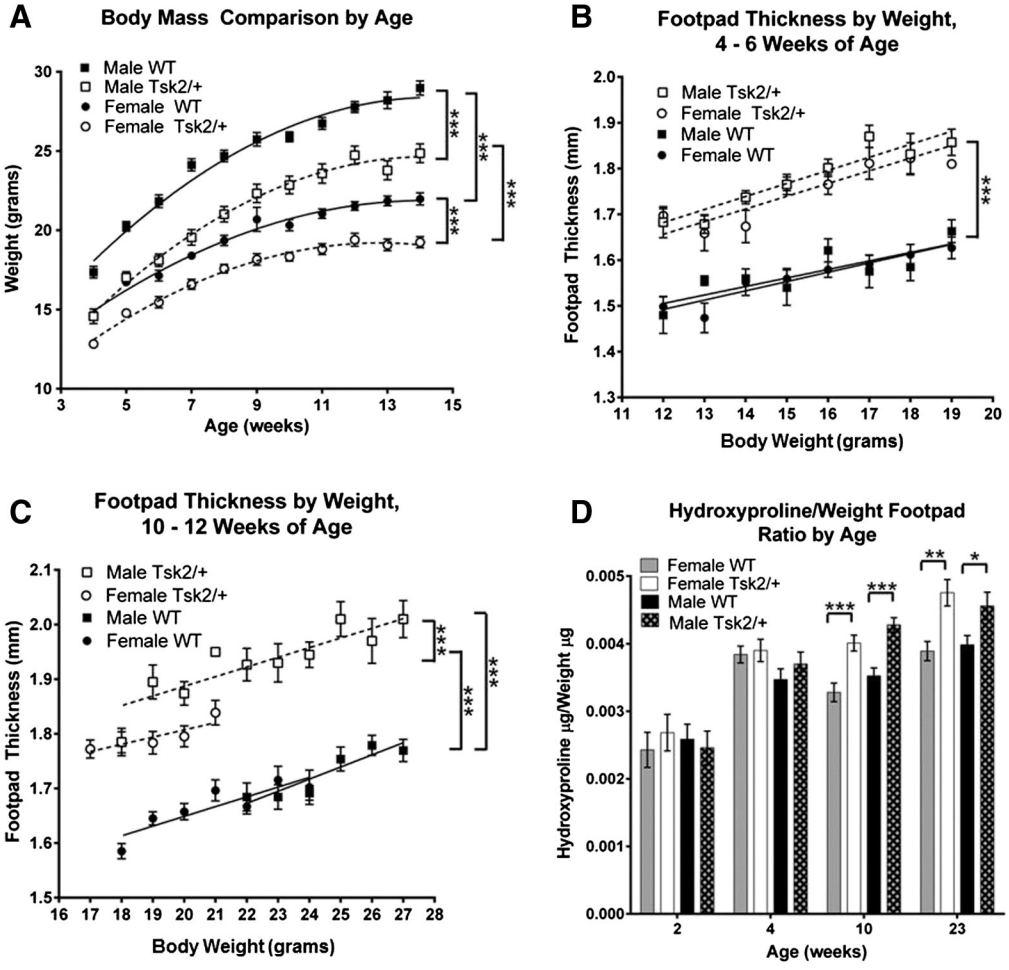

Fig. 1. Tsk2/+ mice have smaller bodies but thicker footpads. Body mass and footpad thickness comparison by age between Tsk2/+ and WT littermates (A–C). Mice were weighed and footpad thickness was measured weekly. A, Body mass was compared directly over time. B and C, Footpad thickness was binned by weight and compared by ages four to six weeks (B) and 10 to 12 weeks (C). Hydroxyproline content of the footpad by age between Tsk2/+ and WT littermates. D, Hydroxyproline (µg)/total weight (µg) was determined from footpads. A–C, $n > 32$ mice per group; D, $n = 9$–12 mice per group. $^{*}p < 0.05$, $^{**}p < 0.01$, $^{***}p < 0.001$.

Please cite this article as: Long, K.B., et al., Tight skin 2 mice exhibit a novel time line of events leading to increased extracellular matrix deposition and dermal fibrosis, Matrix Biol. (2014), http://dx.doi.org/10.1016/j.matbio.2014.05.002

at the same weight ($p < 0.0001$), with no sex difference (Fig. 1B). At 10 to 12 weeks of age (Fig. 1C) and ≥17 weeks of age (data not shown), Tsk2/+ male mice had significantly thicker footpads than Tsk2/+ female mice of the same weight ($p = 0.0004$ and $p < 0.0001$ respectively). At all stages (binned by weight), Tsk2/+ mice had thicker footpads than WT mice of the same sex.

2.2. Protein content of footpads shows that total collagen accumulation occurs with age in Tsk2/+ mice

To assess total collagen accumulation in the footpad with age, we used the hydroxyproline assay. Hydroxyproline makes up about 13% of collagen (Neuman and Logan, 1950), and therefore served as an indicator of the amount of collagen present in the footpad. Individual footpads were weighed from Tsk2/+ and WT mice. Tsk2/+ mice had significantly lighter footpads ($p < 0.004$, data not shown) although they are thicker (Fig. 1B and C) than those of WT mice when compared to animals of the same body weight beginning at two weeks of age. However, assessment of hydroxyproline content of the footpad, normalized to its weight, revealed no difference between Tsk2/+ and WT mice or between male and female mice at two or four weeks of age. Only at 10 weeks of age, there was a significant increase in the amount of footpad total collagen in Tsk2/+ mice, resulting in fibrosis, that continued into adulthood (Fig. 1D). Thus, the increase of collagen in the footpad occurs over time and does not account for the difference in thickness in the early postnatal period.

2.3. Dermal total collagen accumulation occurs with age in Tsk2/+ mice

Skin sections from Tsk2/+ and WT mice from three ages were analyzed visually for total collagen content by Masson's trichrome staining (Fig. 2A). At four to five weeks of age, there was no significant difference in skin thickness between Tsk2/+ and WT mice, although male mice have increased collagen thickness compared to female mice (Fig. 2B). At 10 weeks of age, the amount of stained collagen in Tsk2/+ mice compared to WT littermate mice (roughly 25–50% more) was significant in both male and female mice ($p < 0.01$ and $p < 0.05$, respectively) and this significant difference continues to 17 + weeks of age ($p < 0.001$ and $p < 0.01$, respectively; Fig. 2B). There is also compaction and loss

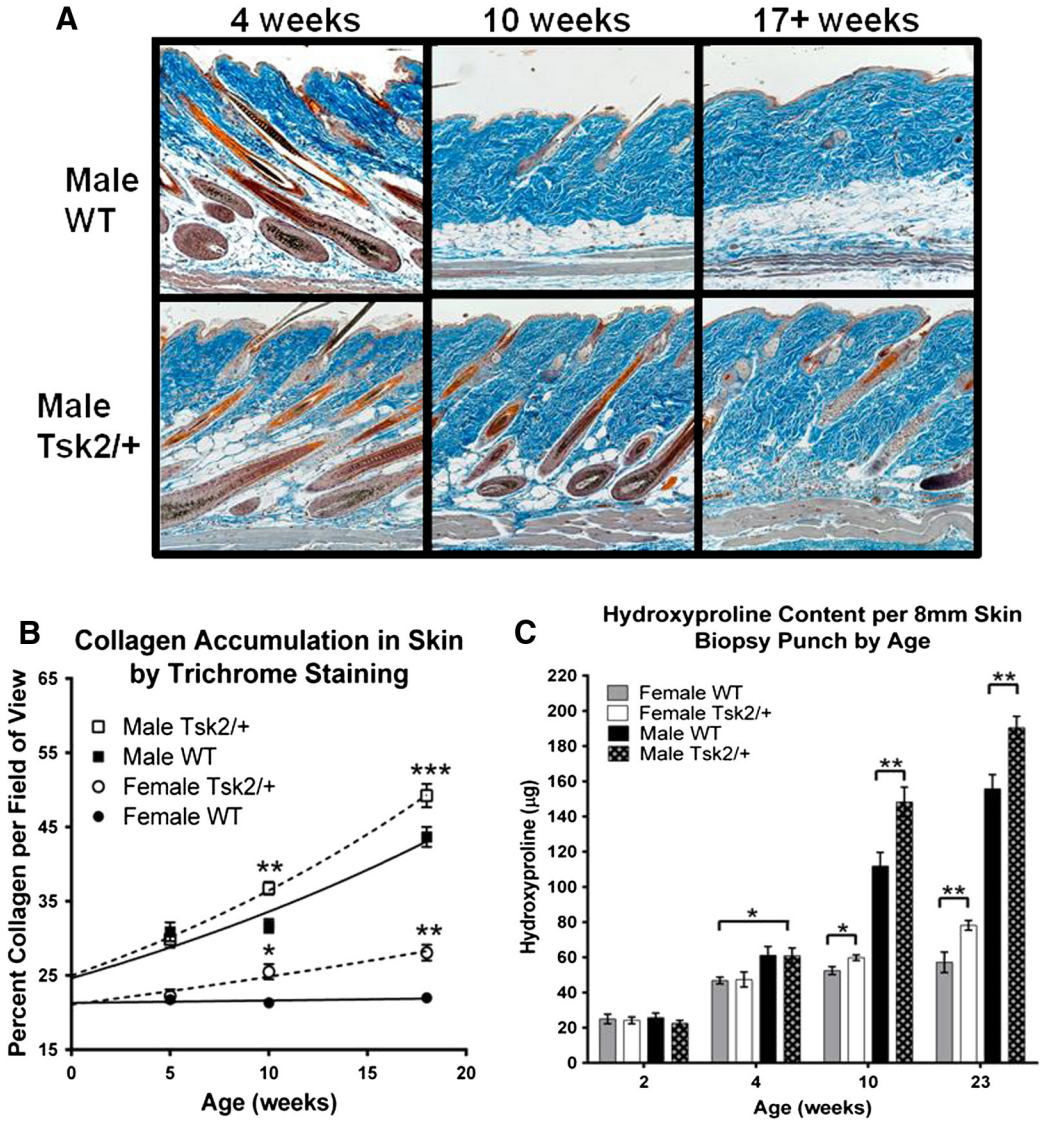

Fig. 2. Collagen content in skin does not differ until 10 weeks of age. A, Skin samples were obtained from the lower dorsal back and processed for paraffin embedding. Samples were stained with Masson's trichrome stain and collagen percentage per field of view (100× magnification) was calculated. B, Quantitative percentage of collagen per 100× magnification over time. C, Hydroxyproline content of skin by age between Tsk2/+ and WT littermates. 8 mm biopsy punches were used to remove a standard area of skin per mouse at two, four, 10, and 23 weeks of age and hydroxyproline content was determined. B, n = 3–4 mice per group, 4–6 images per slide; C, n = 9–12 mice per group. $^{*}p < 0.05$, $^{**}p < 0.01$, $^{***}p < 0.001$.

Please cite this article as: Long, K.B., et al., Tight skin 2 mice exhibit a novel time line of events leading to increased extracellular matrix deposition and dermal fibrosis, Matrix Biol. (2014), http://dx.doi.org/10.1016/j.matbio.2014.05.002

of dermal adipose tissue in Tsk2/+ males at 17 + weeks of age, as was previously reported (Barisic-Dujmovic et al., 2008).

Skin samples across the same age ranges were analyzed for total collagen content by the hydroxyproline assay. At younger ages (two to four weeks) stratified by sex, there was no difference in skin hydroxyproline content between Tsk2/+ and WT mice. However, at 10 and 23 weeks of age, Tsk2/+ skin had significantly more hydroxyproline than WT skin (Fig. 2C). At all ages except two weeks, male skin had significantly more hydroxyproline than female skin ($p < 0.05$ at four and 10 weeks and $p < 0.01$ at 23 weeks). These data show that the measurable increase of collagen, and concomitant fibrosis, in the skin of Tsk2/+ mice occurs after the appearance of the physical tight skin phenotype.

2.4. Histological assessment of cells in the pre-fibrotic and fibrotic skin of Tsk2/+ mice

The unusual tight skin phenotype, evident by pinching the interscapular skin, in Tsk2/+ mice could be due to a cellular infiltrate that drives collagen accumulation and fibrosis. For this, we studied male mice, because Tsk2/+ male mice are significantly more fibrotic than female mice. Skin samples from male mice at two, four, 10, and 23 weeks of age were examined for presence of infiltrating cells. Weigert's hematoxylin staining demonstrated no overt mononuclear cell infiltrate difference at any age (data not shown). Additionally, toluidine blue staining showed that while mast cells decrease with age, they do not differ between Tsk2/+ mice and WT littermates at any age tested (Fig. 3A). Immunofluorescence staining of CD3 + T cells showed a significant but small increase in CD3 + T cells in the epidermis and surrounding the hair follicle in Tsk2/+ mice at four, 10 and 23 weeks of age but not at two weeks of age (Fig. 3B). Immunofluorescence staining of iNOS + inflammatory macrophages showed no difference in total number of infiltrating cells between Tsk2/+ and WT mice. These data suggest that an inflammatory cell infiltrate is not driving the fibrotic phenotype in Tsk/2 + mice.

2.5. NLRP3 inflammasome activation is not required for skin fibrosis

We tested whether an inflammatory immune response was necessary for fibrosis development, as seen in the bleomycin-induced mouse model of SSc (Artlett et al., 2011). Similar to Artlett et al.'s study, Tsk2/+ mice were bred to a NOD-like receptor family, pyrin domain containing 3 (NLRP3) deficient background, which lacks a functional inflammasome and consequently displays defects in neutrophil and macrophage infiltration of tissues and reduced inflammation (Chen and Nunez, 2010). The tight skin phenotype is retained in Tsk2.*NLRP3*KO mice, which is evident upon pinching the interscapular skin of weanlings through to adulthood (not shown). We assessed the thickness of mouse footpads corrected for body weight, as a predictor of fibrosis (Fig. 1B, C), and found that at four to six weeks of age and 10 to 12 weeks of age Tsk2.*NLRP3*KO male and female mice have significantly thicker footpads than B6.*NLRP3*KO mice at the same weight ($p < 0.01$, Fig. 4A, B). At 10 to 12 weeks of age (Fig. 4B), Tsk2/+ male mice have significantly thicker footpads than Tsk2/+ female mice of the same weight ($p < 0.05$), similar to what was noted previously on the *NLRP3* sufficient background (Fig. 1C). We visually analyzed the total collagen content of skin sections from Tsk2.*NLRP3*KO and B6.*NLRP3*KO male mice from the two age groups that have evident fibrosis: 10–12 weeks and 23 weeks of age. At 10 to 12 weeks of age, the amount of stained collagen in Tsk2.*NLRP3*KO mice compared to B6.*NLRP3*KO littermate mice trends toward Tsk2.*NLRP3*KO mice having increased accumulation, but does not reach statistical significance ($p = 0.0503$). At 23 weeks of age, Tsk2.*NLRP3*KO mice have significantly more collagen in their skin compared to B6.*NLRP3*KO littermates ($p < 0.05$, Fig. 4C).

2.6. Tsk2/+ mice have increased levels of total TGF-β1 in skin and yet no difference in the numbers of α-smooth muscle actin (αSMA) positive cells

Skin samples at varying ages from Tsk2/+ and WT mice were examined for the presence of total TGF-β1 and αSMA, a marker of myofibroblasts, as both are associated with increased production of collagen. Staining revealed that total TGF-β1 levels were increased in Tsk2/+ skin at two and 10 weeks of age in male mice (Fig. 5A and B). Staining showed that αSMA-positive cells decrease with age, but do not differ between Tsk2/+ mice and WT littermates at any age tested (Fig. 5C).

2.7. Tsk2/+ mice have increased elastic fibers in the dermis

Because the physical tight skin phenotype is readily observable in Tsk2/+ mice at two to three weeks of age, yet there is no measurable excess collagen, nor a remarkable cellular infiltrate, we sought another explanation for their tight skin. In addition to increased collagen accumulation, studies have shown that patients with SSc have elastic fiber alterations (Quaglino et al., 1996). Similarly, Tsk1/+ mice have dysregulated elastic fibers beneath the panniculus carnosus, which causes tethering of the skin and contributes to their tight skin phenotype (Lemaire et al., 2004). Therefore, we hypothesized that altered elastic fibers may contribute to the tight skin phenotype in Tsk2/+ mice. We examined skin elastic fibers at the histological level from Tsk2/+ and WT littermate mice, and found that as early as two weeks of age, Tsk2/+ skin has significantly more elastic fibers in the dermis compared to WT mice (Fig. 6B, $p < 0.05$). These fibers appear longer, thicker, and

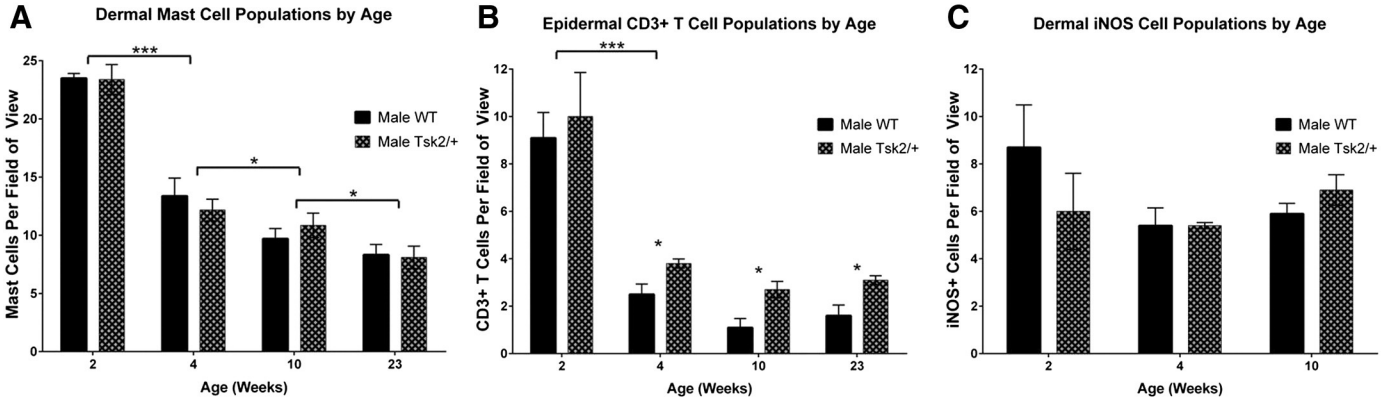

Fig. 3. Examination of resident and infiltrating cell populations in Tsk2/+ and WT male mice. Skin samples were stained with toluidine blue for dermal mast cells (A), anti-CD3 antibody for epidermal CD3 + T cells (B), or anti-iNOS antibody for inflammatory macrophages (C). The total number of positive cells per field of view at 100× (A and C) or 400× (B) magnification was counted. Significance was calculated by student's t-test. n = 3–6 mice per group, 4–12 fields of view per slide. $^{*}p < 0.05$, $^{**}p < 0.01$, $^{***}p < 0.001$.

Please cite this article as: Long, K.B., et al., Tight skin 2 mice exhibit a novel time line of events leading to increased extracellular matrix deposition and dermal fibrosis, Matrix Biol. (2014), http://dx.doi.org/10.1016/j.matbio.2014.05.002

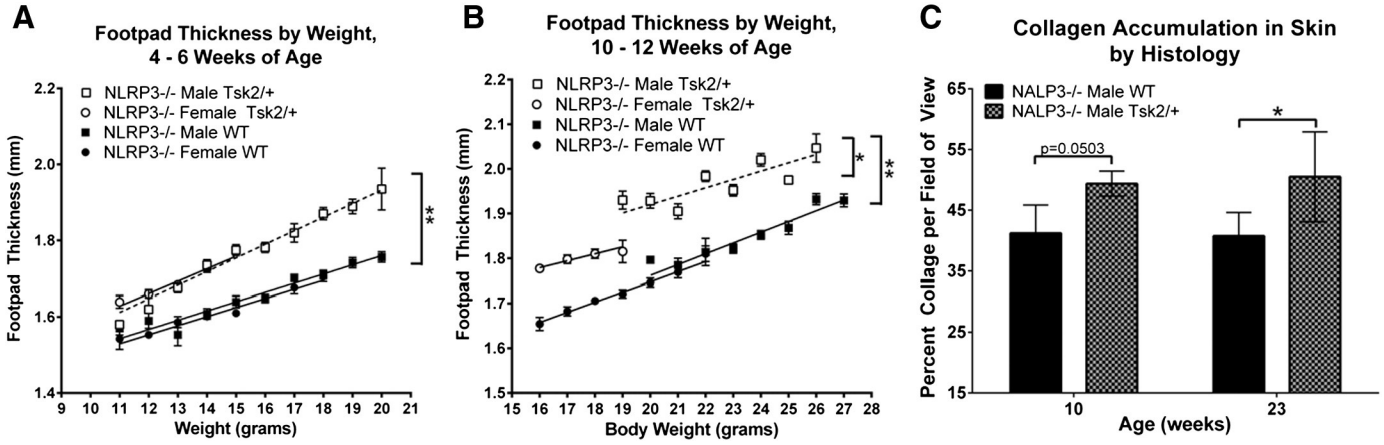

Fig. 4. Tsk2.*NLRP3*KO mice thicker footpads and increased dermal collagen accumulation compared to B6.*NLRP3*KO mice. Weekly, footpad thickness was measured and binned by weight and compared by ages four to six weeks (A) and 10 to 12 weeks (B). Skin samples were stained and collagen percentage per field of view (100× magnification) was calculated. C, Quantitative percentage of collagen per 100× magnification over time. A–B, n > 20 mice per group; C, n = 3–4 mice per group, 6 fields of view per slide. $^{*}p < 0.05$, $^{**}p < 0.01$.

more frequently in Tsk2/+ skin compared to WT skin. Interestingly, there is no phenotypic difference in the elastic fibers beneath the panniculus carnosus in Tsk2/+ mice; in this locality they appear quite similar to the elastic fibers in WT mice. This is in contrast to Tsk1/+ mice (Fig. 6A) (Lemaire et al., 2004). We found that this Tsk2-specific increase in elastic fibers in the skin is maintained throughout all ages tested (Fig. 6C).

2.8. The increase in elastic fibers in the dermis is not responsible for the tight skin phenotype

To determine whether the increase in dermal elastic fibers causes the tight skin phenotype, Tsk2/+ mice were bred to a mouse deficient in fibulin-5 (*Fbln5*-KO). While *Fbln5* −/+ heterozygous mice bear normal elastic fibers, *Fbln5*-KO mice, deficient on both alleles, lack mature elastic fibers specifically in the skin, resulting in very loose skin (Yanagisawa et al., 2002; Choi et al., 2009). Therefore, if increased elastic fibers are responsible for the tight skin observed in Tsk2/+ mice, then their absence should result in normal skin. However, despite the lack of dermal elastic fibers (Fig. 7A), Tsk2.*Fbln5*-KO mice retain their tight skin phenotype as demonstrated by the physical skin pinch test (Fig. 7B). Additionally, we assessed the thickness of footpads corrected for body weight from Tsk.*Fbln5*-KO, Tsk.*Fbln5* +/−, B6.*Fbln5*-KO and B6.*Fbln* +/− male mice, again using footpad thickness as a predictor of skin fibrosis (Fig. 1B, C). Similar to mice bearing WT *Fbln5*, Tsk2/+ mice bearing one or both deleted copies of *Fbln5* have significantly thicker footpads than B6 mice bearing one or both deleted copies of *Fbln5* at four to six and 10 to 12 weeks of age ($p < 0.01$, Fig. 7C, D).

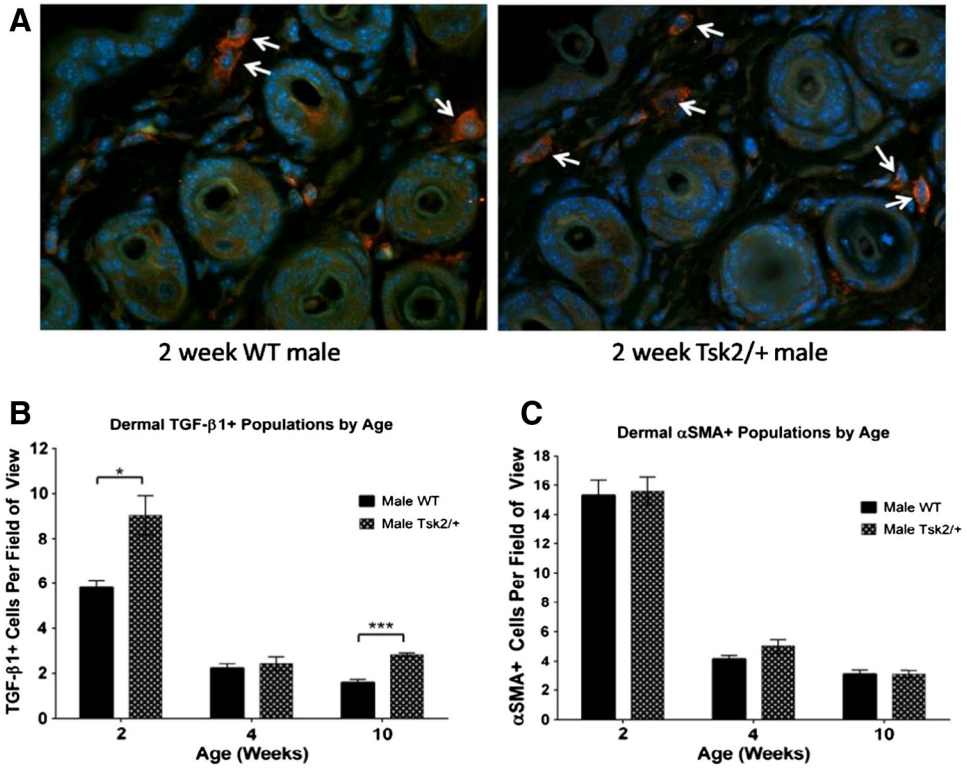

Fig. 5. TGF-β1 but not αSMA positive cells are increased in the skin of Tsk2/+ male mice. Skin samples were evaluated by immunofluorescence for the presence of TGF-β1 (A and B) or αSMA positive cells (sections not shown, C). The total number of TGF-β1 (B) or αSMA (C) positive cells per field of view (400× magnification) was counted. Significance was calculated by student's t-test. n = 3–4 mice per group, 5–9 field of view per slide. $^{*}p < 0.05$, $^{***}p < 0.001$.

Please cite this article as: Long, K.B., et al., Tight skin 2 mice exhibit a novel time line of events leading to increased extracellular matrix deposition and dermal fibrosis, Matrix Biol. (2014), http://dx.doi.org/10.1016/j.matbio.2014.05.002

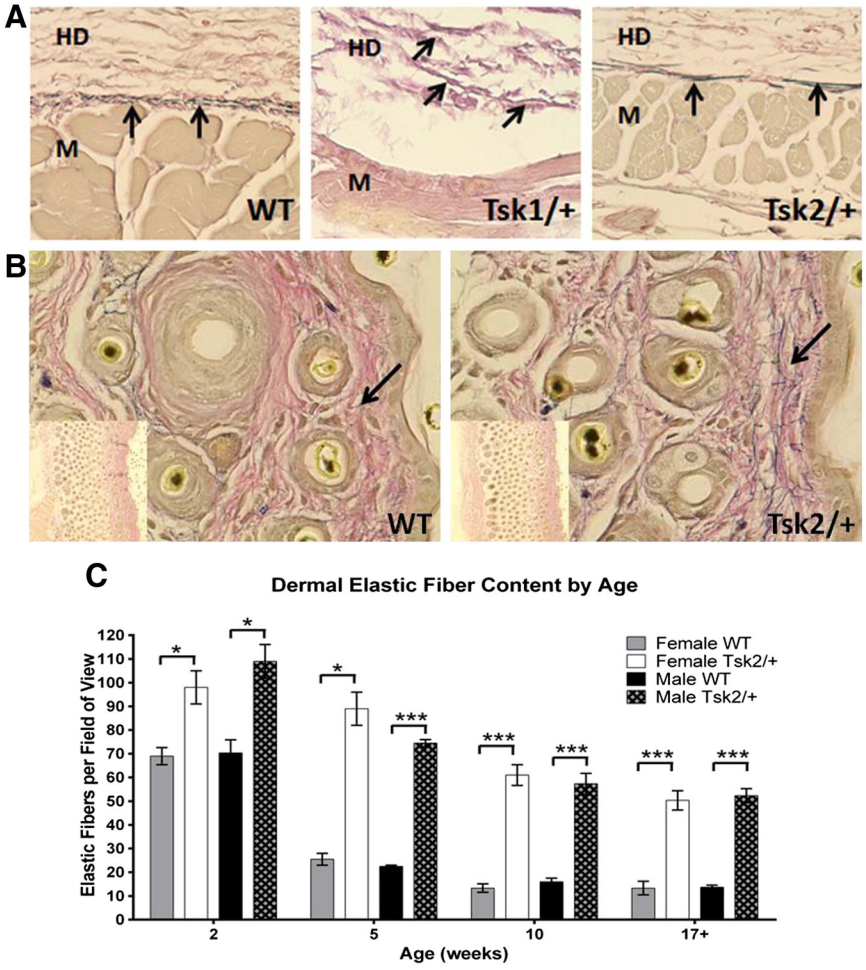

Fig. 6. Tsk2/+ mice have more elastic fibers in the dermis. Skin samples were stained with Weigert's Resorcin Fuchsin Stain. A, Elastic fibers from WT (left), Tsk1/+ (middle) and Tsk2/+ (right) male mice at four weeks of age (400× magnification) shown between the hypodermal muscle (M) and the hypodermal connective tissue (HD). Distinct elastic fibers are marked with arrows. B, Elastic fibers in the dermis from WT (left) and Tsk2/+ (right) female mice at five weeks of age. C, Quantitative amount of elastic fibers per field of view over time. n = 4–6 mice per group, 5–9 fields of view per slide. $^{*}p < 0.05$, $^{**}p < 0.01$, $^{***}p < 0.001$.

2.9. Tsk2/+ mice produce ANAs after disease signs are initiated

We evaluated the timing of the production of ANAs. There was no difference in the occurrence of ANAs between Tsk2/+ mice and their WT littermates although more female mice produced ANAs than male mice ($p = 0.02$). However, all ANA production occurred after 14 weeks of age, well after the development of both tight skin and measurable fibrosis (Fig. 8).

3. Discussion

Previous studies have shown that Tsk2/+ mice develop skin fibrosis, display ECM anomalies, and produce high levels of ANAs (Christner et al., 1995; Gentiletti et al., 2005); however, the progression of such disease signs during aging has never been examined or quantified and a causative role for the collagen accumulation in the fibrotic trait has not been proven. In order to determine disease progression, we needed a reliable method to quantify disease severity. To eliminate the variability inherent in the physical skin pinch method (Baxter et al., 2005), we quantified disease severity by measuring the footpad thickness. Tsk2/+ mice have noticeably tighter scapular skin than WT littermates at two weeks of age, and significantly thicker footpads at three weeks of age (Fig. 1B), yet footpad collagen content is not increased in Tsk2/+ mice until 10 and 23 weeks of age (Fig. 1D). The collagen levels as detected by hydroxyproline content do not correlate with disease as well as the caliper assay of footpads, corrected for body weight. We do not know the reason for this, but we speculate that it may be due to the physically smaller stature of Tsk2/+ mice compared to their WT littermates. Their bones in particular are lighter and smaller, and the foot itself weighs less. Because the Tsk2/+ mouse body weighs less, the necessity of correcting foot thickness for body weight gives the appearance that they have relatively thicker feet, yet the difference is likely more a result of the lighter body weight of the Tsk2/+ mice. Thus, the footpad assay actually is an indicator of the lighter weight of the mouse (itself a highly accurate predictor of animals bearing the *Tsk2* mutation) and not an increase in fibrosis in the feet.

By two independent methods, we found that the observed significant increase in collagen accumulation in the skin of Tsk2/+ mice does not occur until approximately 10 to 12 weeks of age (Fig. 2). This is well after the appearance of positive skin pinch tests (the tight skin phenotype) and thicker footpad measurements distinguish the Tsk2/+ phenotype among littermates, suggesting a slow and steady accumulation of collagen (fibrosis), which is not measurable by our assays until 10 weeks of age. At all ages except 2 weeks, both WT and Tsk2/+ male mice had significantly more dermal collagen than female mice, as expected by androgen sensitivity of skin collagen genes (Markova et al., 2004).

One factor that could explain the unusual tight skin phenotype might be a cellular infiltrate in Tsk2/+ skin, with concomitant inflammation. Because some SSc patients have increased levels of active mast cells (Hugle et al., 2011), infiltrating T cells (Milano et al., 2008)

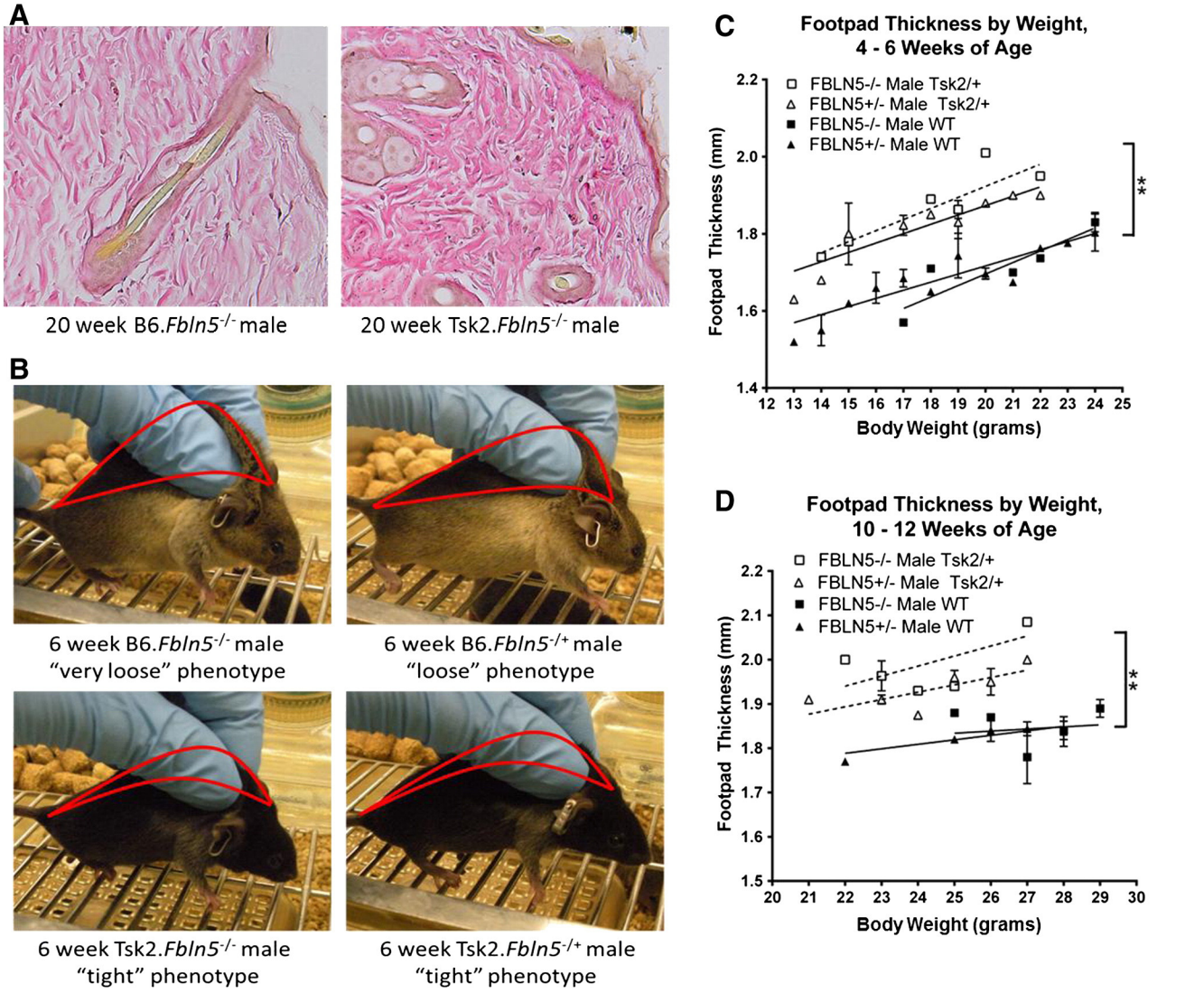

Fig. 7. Excess elastic fibers in Tsk2/+ mice are not responsible for the tight skin phenotype. A, Skin samples were stained with Weigert's Resorcin Fuchsin stain to verify the loss of dermal elastic fibers in B6- and Tsk2.*Fbln5*-KO mice. B, The tight skin phenotype of six week old *Fbln5*-KO mice was determined by skin pinching. Both B6- and Tsk2.*Fbln5*-KO mice lack mature elastic fibers yet Tsk2.*Fbln5*-KO mice still retain their tight skin phenotype. C and D, Weekly, mice were weighed and the footpad thickness was binned by weight and compared at ages four to six weeks (C) and 10 to 12 weeks (D). n = 5–14 mice per group. **Difference between Tsk2/+ and WT littermates of either FBLN5 genotype, $p < 0.01$.

and macrophages (Christmann and Lafyatis, 2010) in diseased skin compared to healthy controls, and because all three cell types can produce TGF-β1, we examined their presence in the skin of Tsk2/+ mice. However, we found no substantial differences in the number of resident or infiltrating cells in the skin of Tsk2/+ mice. Mast cells were seen in equivalent numbers in Tsk2/+ and WT mice across all ages (Fig. 3A). CD3 + T cell analysis showed a small, yet significant increase in the number of cells in the Tsk2/+ epidermis compared to WT littermates starting at four weeks of age (Fig. 3B). Importantly, there was no difference in CD3 + T cell number at two weeks of age, when TGF-β1 levels are increased in Tsk2/+ skin. There was also no difference in the macrophage population (Fig. 3C). We conclude that there is a very subtle increase in the number of infiltrating T cells in the skin of Tsk2/+ mice, but the physiological impact of this infiltrate is questionable as it occurs after the tight skin phenotype is detectable by the physical skin pinch. Because a substantial cellular infiltrate was not observed in Tsk2/+ skin samples, we used another method to verify that skin fibrosis in Tsk2/+ mice is not dependent on the innate immune response by breeding Tsk2/+ mice to NLRP3KO mice. NLRP3KO animals are deficient in an inflammasome and thereby have defective tissue cellular infiltrates and reduced inflammation (Chen and Nunez, 2010). Tsk2.*NLRP3*KO mice retained the tight skin phenotype and developed dermal fibrosis (Fig. 4) similar to what was observed in *NLRP3* sufficient littermates. Taken together, these results indicate that the NLRP3 inflammasome is not necessary for disease development in Tsk2/+ mice and the fibrosis observed in their skin is independent of the innate immune infiltrate.

Because TGF-β1 is believed to drive skin fibrosis in SSc through the activation of fibroblasts (Leroy et al., 1989; Cotton et al., 1998; Varga, 2004) and increased levels have been noted in skin samples from SSc patients (Gabrielli et al., 1993; Sfikakis et al., 1993), dermal levels of TGF-β1 in Tsk2/+ skin were examined by immunofluorescence. Notably, Tsk2/+ male mouse skin has elevated levels of total TGF-β1 protein at two weeks of age (Fig. 5A and B) compared to WT males. Overall, because of this increase in TGF-β1 + cells prior to demonstrable fibrosis, it is possible that collagen accumulation in Tsk2/+ mice is dependent on a pulse of TGF-β1 at approximately two weeks and 10 weeks of age (Fig. 5B) and that these signaling events stimulate the fibroblasts to secrete additional collagen for weeks afterward, resulting in the increases in dermal thickness observed in the mouse (Fig. 2). Surprisingly, there was no difference in the number of αSMA + cells, key producers of TGF-β1, as detected by immunofluorescence at any age (Fig. 5C). Because Tsk2/+ and WT littermates have a similar proportion of

Please cite this article as: Long, K.B., et al., Tight skin 2 mice exhibit a novel time line of events leading to increased extracellular matrix deposition and dermal fibrosis, Matrix Biol. (2014), http://dx.doi.org/10.1016/j.matbio.2014.05.002

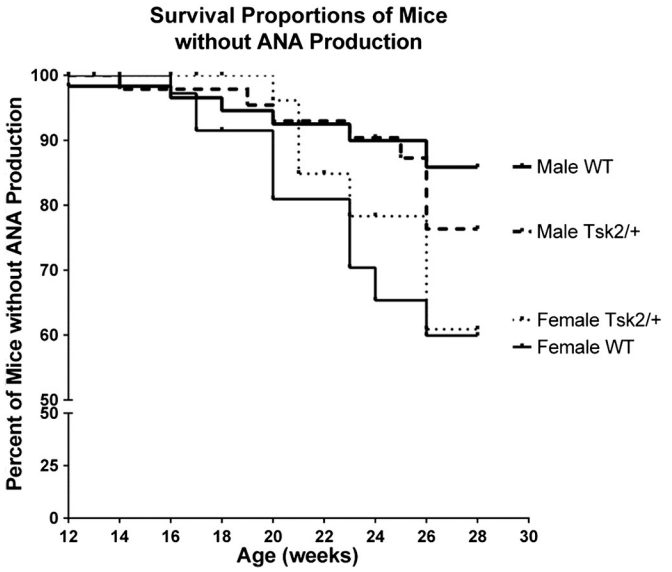

Fig. 8. Total ANA production in Tsk2/+ mice is similar to WT mice. Blood samples were collected every other week from mice between 12 and 26 weeks of age. Proportions of ANA-negative Tsk2/+ and WT mice over time are shown as a survival curve.

infiltrating cells (Figs. 3 and 4) and because there is no difference between them in the number of myofibroblasts (Fig. 5), we hypothesize that a resident skin cell population is responsible for the increased levels of TGF-β1 in Tsk2/+ mice. Perhaps epidermal dendritic cells are critical producers of TGF-β1 in Tsk2/+ skin (Gruschwitz and Hornstein, 1992). The proposed causal relationship of TGF-β1 to skin fibrosis and the physical phenotype of tight skin in Tsk2/+ mice needs verification, but we note that at two weeks, skin from male Tsk2/+ mice expresses 170%–300% more mRNA for five TGF-β1 signature proteins (collagen type V, alpha 2; elastin; fibulin-2; α-smooth muscle actin; and cartilage oligomeric protein) (Piscaglia et al., 2009; Kurpinski et al., 2010; Sargent et al., 2010) as assessed by quantitative real-time PCR (data not shown).

To investigate changes in other ECM proteins that are observed to be altered in both Tsk1/+ mice and human disease, we examined the phenotype of elastic fibers present in the dermis of Tsk2/+ mice. Two-week old Tsk2/+ mice (an age when there is no collagen accumulation difference) exhibit almost two-fold more elastic fiber protein in the dermis than WT littermates (Fig. 6B and C). Additionally, the fibers appear longer and thicker. This difference remains significant across all ages of Tsk2/+ mice, suggesting that elastic fiber dysregulation precedes other signs of fibrosis. The difference between Tsk2/+ and WT littermates in elastic fiber expression is one of the earliest and most reliable signatures of the Tsk2/+ phenotype in the skin and, unlike collagen deposition two weeks of age, predicts fibrosis in Tsk2/+ skin as early as the skin pinch and foot caliper assays. It was therefore tempting to speculate that elastic fiber differences account for the initial tight skin phenotype at weaning. However, breeding the *Fbln5*-KO mutation onto the Tsk2/+ background proved that the loss of elastic fibers did not result in a loss of the physical tight skin phenotype (Fig. 7B) or a decrease in the thickness of footpads from Tsk2/+ mice (Fig. 7C, D).

Previously, Gentiletti et al. (2005), demonstrated that Tsk2/+ mice have increases in ANAs, but the mice they evaluated were older and already had established disease. We therefore quantified ANA production in younger mice to determine whether ANAs drive Tsk2/+ fibrosis or if ANA production is instead a result of disease development. Our antibody study revealed that there were no differences in the occurrence of ANAs between Tsk2/+ and WT mice (Fig. 8). The differences in our findings compared to the Gentiletti et al. report could be due to the age of the mice and the genetic background of the control mice, as the control mice used for the Gentiletti et al. report were CAST/Ei and C3H/HeJ, whereas our control mice are littermates on the B6 background. Because ANAs are seen after the initiation of fibrosis, we argue that antibody production is at most a marker of disease progression and severity, and not the cause of disease.

We recently found by linkage analysis, coupled with cDNA and genomic DNA sequencing, that the causal mutation in the Tsk2/+ mouse is a non-synonymous change in the procollagen III amino terminal propeptide (PIIINP) segment of the protein (Long, unpublished observations). We speculate that, when homozygous, this change dramatically alters the character of type III collagen in utero leading to fetal demise. In heterozygous Tsk2/+ mice, because collagen is a triple helix, stoichiometry suggests that up to 75% of the type III collagen fibers may contain an abnormal fibril derived from the mutated collagen. Studies are currently underway to understand the signaling difference(s) due to this collagen mutation as it drives dermal fibrosis and if it indeed requires TGF-β1.

Overall, this study allowed for the development of a novel time line of disease progression in Tsk2/+ mice (Fig. 9), leading to the investigation of alterations in the ECM during the establishment of dermal fibrosis. We have demonstrated that elastic fiber accumulation occurs weeks prior to collagen accumulation, concomitant with increased levels of TGF-β1, suggesting that disease development in Tsk2/+ mice could be driven by TGF-β1. This presents a novel pathway of disease development in Tsk2/+ mice and a valuable model for tracing the development of a naturally occurring fibrotic disease from its origins.

4. Materials and methods

4.1. Mice

Tsk2/+ mice were obtained from Dr. Paul Christner (Thomas Jefferson University, Philadelphia PA) with permission from the MRC Radiobiology Unit Laboratory, Chilton, UK and were housed at Drexel University College of Medicine. The Tsk2/+ mice were originally bred onto the hybrid (C3H × B6) background. At Drexel, they were serially backcrossed to B6 mice, and mice used in this study were at generation N4–N5. NLRP3-KO mice were obtained from Dr V. Dixit (Genentech) and had a C57BL/6 background (Artlett et al., 2011). Fibulin-5 deficient mice were a kind gift from Dr. Hiromi Yanagisawa (University of Texas Southwestern Medical Center). Each deficient strain was bred to B6.Tsk2/+ mice. For each experiment, age- and sex-matched WT littermates were used as controls. All studies were approved by the Institutional Animal Care and Use Committee at Drexel University College of Medicine.

4.2. Footpad measurement of disease severity

The mice were restrained with the left leg extended and a Starrett Catch and Release Analog Caliper was placed in the middle of the footpad and the resulting thickness of the pad was recorded. Because footpad size and thickness increases with age and body size, footpad thickness was binned by body weight at three different age ranges: four–six, 10–12, and 17 + weeks of age.

4.3. Determination of hydroxyproline content in skin and footpad tissue

Mice were sacrificed and the lower dorsal fur was removed by shaving. Two 8 mm punches were excised from each piece of skin, snap-frozen, weighed, and stored at −80 °C. Footpads were cut just above the pad and processed in the same manner. Protein was isolated for hydroxyproline assays (Kuperman et al., 2002). Briefly, footpads and skin punches were homogenized in water and a 2:1 chloroform/methanol mixture was added to remove lipids. The homogenate mixture was shaken and then centrifuged to separate the phases. The organic and aqueous phases were discarded, and the interphase was resuspended in water, and 50% TCA was added to precipitate the protein, and the protein was collected by centrifugation. The protein pellet was hydrolyzed

Please cite this article as: Long, K.B., et al., Tight skin 2 mice exhibit a novel time line of events leading to increased extracellular matrix deposition and dermal fibrosis, Matrix Biol. (2014), http://dx.doi.org/10.1016/j.matbio.2014.05.002

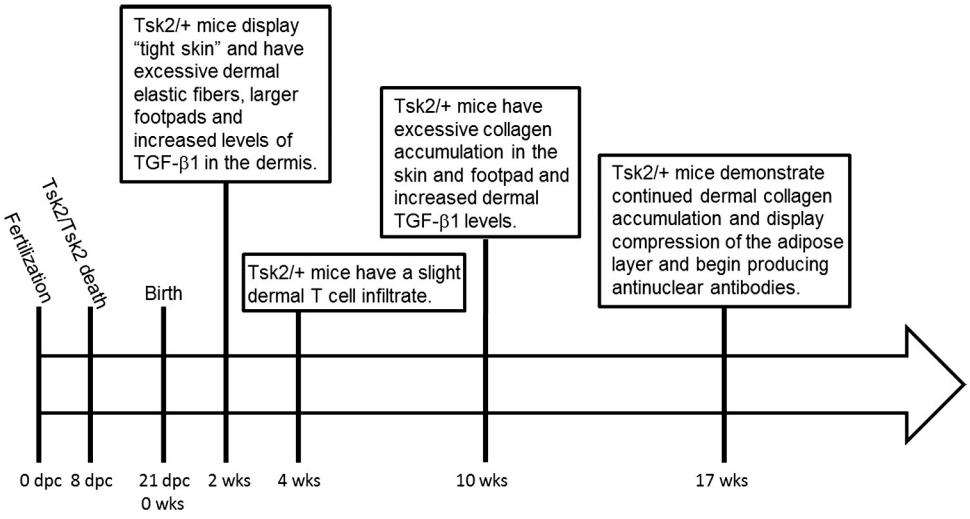

Fig. 9. Time line for the development of fibrosis in the Tsk2/+ mouse. Abbreviations: dpc, days post conception; wks, weeks.

with 12 M HCl for 16 h at 110 °C under vacuum and then reconstituted in water. Chloramine T solution was added to each sample, followed by the addition of Ehrlich's solution. The optical density was read at 550 nm in triplicate and the hydroxyproline content was determined against a standard curve of hydroxyproline (Sigma-Aldrich, St. Louis, MO).

4.4. Histological assessment of dermal fibrosis and ECM abnormalities

Skin samples were placed in 4% paraformaldehyde and paraffin embedded. Sections were stained with Masson's trichrome stain (Trichrome Stain (Masson), Sigma-Aldrich, St. Louis, MO) to visualize collagen. Each section was standardized for the photographic area (1200 × 1200 pixels) allowing a direct comparison between images. The collagen area was traced and measured using Image J software (http://rsbweb.nih.gov/ij/) and the percentage of collagen per standardized field of view (100× magnification) was calculated.

Elastic fibers in the skin were visualized using Weigert's Resorcin Fuchsin stain (Electron Microscopy Sciences, Hatfield, PA). The number of elastic fibers per 400× field of view was quantified.

4.5. Histological assessment of infiltrating cells, αSMA positive cells and TGF-β1

To visualize mast cells, paraffin embedded sections were stained with toluidine blue (0.05% toluidine/3.5% ethanol/1% NaCl, pH 2.3) for 2–3 min, rinsed in three changes of water, dehydrated in increasing concentrations of ethanol with a final rinse in xylene, then a coverslip fixed with Cytoseal Mounting media (Thermo Scientific Inc, Rockford, IL). Immunofluorescence was used to visualize CD3 + T cells, macrophages, αSMA cells and TGF-β1. Antigens were unmasked with 10 mM citrate buffer at 100 °C for 30 min, and then blocked with 5% goat serum. Rabbit anti-CD3 polyclonal antibody (1:250) (Abcam, Cambridge, MA), rabbit anti-iNOS polyclonal antibody (1:100) (Abcam, Cambridge, MA), rabbit anti-TGF-β1 polyclonal antibody (1:100) (Santa Cruz Biotechnology, Inc, Santa Cruz, CA), and mouse anti-αSMA monoclonal antibody (1:5000) (Lab Vision IHC System Solutions, Kalamazoo, MI) in blocking buffer were applied to the sections for 40 min. The unbound antibody was removed from the sections with three changes of PBS and Cy3-conjugated goat anti-rabbit IgG (1:500) (Jackson ImmunoResearch Laboratories, West Grove, PA) was used to visualize CD3 + cells, iNOS + macrophages, and TGF-β1, or Cy3-conjugated goat anti-mouse IgG (1:10,000) (Jackson ImmunoResearch Laboratories) to visualize αSMA. DAPI (Invitrogen, Carlsbad CA) was used to visualize the nuclei.

4.6. Immunofluorescence assay for ANAs

Plasma was obtained by submandibular bleeding of Tsk2/+ and WT mice, diluted 1:20 in PBS, applied to slides pre-coated with HEp-2 cells (Bio-Rad, Redmond, WA) and washed, and then a FITC-conjugated goat anti-mouse IgG (Jackson ImmunoResearch Laboratories) diluted 1:100 was applied (Gentiletti et al., 2005).

4.7. Statistics

Significance of the biological differences between Tsk2/+ and WT littermates was calculated using non-linear regression (Fig. 1A), linear regression (Fig. 1B, C) and the student's t-test (all other figures), with $p < 0.05$ taken as significant.

Conflict of interest

The authors state no conflict of interest.

Acknowledgments

This work was funded by a Scleroderma Foundation Grant and awards from the NIH (AR061384) and the U.S. Department of Defense (PR100338). We would like to thank Dr. Hiromi Yanagisawa (University of Texas Southwestern Medical Center) for the generous gift of the fibulin-5 deficient mice, and Dr. Elaine Davis (McGill University) for discussions on creating this dual mutant model.

References

Artlett, C.M., 2010. Animal models of scleroderma: fresh insights. Curr. Opin. Rheumatol. 22, 677–682.
Artlett, C.M., Sassi-Gaha, S., Rieger, J.L., Boesteanu, A.C., Feghali-Bostwick, C.A., Katsikis, P. D., 2011. The inflammasome activating caspase 1 mediates fibrosis and myofibroblast differentiation in systemic sclerosis. Arthritis Rheum. 63, 3563–3574.
Barisic-Dujmovic, T., Boban, I., Clark, S.H., 2008. Regulation of collagen gene expression in the Tsk2 mouse. J. Cell. Physiol. 215, 464–471.
Baxter, R.M., Crowell, T.P., McCrann, M.E., Frew, E.M., Gardner, H., 2005. Analysis of the tight skin (Tsk1/+) mouse as a model for testing antifibrotic agents. Lab. Investig. 85, 1199–1209.
Chen, G.Y., Nunez, G., 2010. Sterile inflammation: sensing and reacting to damage. Nat. Rev. Immunol. 10, 826–837.
Choi, J., Bergdahl, A., Zheng, Q., Starcher, B., Yanagisawa, H., Davis, E.C., 2009. Analysis of dermal elastic fibers in the absence of fibulin-5 reveals potential roles for fibulin-5 in elastic fiber assembly. Matrix Biol. 28, 211–220.
Christmann, R.B., Lafyatis, R., 2010. The cytokine language of monocytes and macrophages in systemic sclerosis. Arthritis Res. Ther. 12, 146.
Christner, P.J., Peters, J., Hawkins, D., Siracusa, L.D., Jimenez, S.A., 1995. The tight skin 2 mouse. An animal model of scleroderma displaying cutaneous fibrosis and mononuclear cell infiltration. Arthritis Rheum. 38, 1791–1798.

Christner, P.J., Hitraya, E.G., Peters, J., McGrath, R., Jimenez, S.A., 1998. Transcriptional activation of the alpha1(I) procollagen gene and up-regulation of alpha1(I) and alpha1(III) procollagen messenger RNA in dermal fibroblasts from tight skin 2 mice. Arthritis Rheum. 41, 2132–2142.

Cotton, S.A., Herrick, A.L., Jayson, M.I., Freemont, A.J., 1998. TGF beta—a role in systemic sclerosis? J. Pathol. 184, 4–6.

Ferri, C., Valentini, G., Cozzi, F., Sebastiani, M., Michelassi, C., La Montagna, G., Bullo, A., Cazzato, M., Tirri, E., Storino, F., Giuggioli, D., Cuomo, G., Rosada, M., Bombardieri, S., Todesco, S., Tirri, G., 2002. Systemic sclerosis: demographic, clinical, and serologic features and survival in 1,012 Italian patients. Medicine (Baltimore) 81, 139–153.

Gabrielli, A., Di Loreto, C., Taborro, R., Candela, M., Sambo, P., Nitti, C., Danieli, M.G., DeLustro, F., Dasch, J.R., Danieli, G., 1993. Immunohistochemical localization of intracellular and extracellular associated TGF beta in the skin of patients with systemic sclerosis (scleroderma) and primary Raynaud's phenomenon. Clin. Immunol. Immunopathol. 68, 340–349.

Gentiletti, J., McCloskey, L.J., Artlett, C.M., Peters, J., Jimenez, S.A., Christner, P.J., 2005. Demonstration of autoimmunity in the tight skin-2 mouse: a model for scleroderma. J. Immunol. 175, 2418–2426.

Green, M.C., Sweet, H.O., Bunker, L.E., 1976. Tight-skin, a new mutation of the mouse causing excessive growth of connective tissue and skeleton. Am. J. Pathol. 82, 493–512.

Gruschwitz, M.S., Hornstein, O.P., 1992. Expression of transforming growth factor type beta on human epidermal dendritic cells. J. Investig. Dermatol. 99, 114–116.

Hugle, T., Hogan, V., White, K.E., van Laar, J.M., 2011. Mast cells are a source of transforming growth factor beta in systemic sclerosis. Arthritis Rheum. 63, 795–799.

Kuperman, D.A., Huang, X., Koth, L.L., Chang, G.H., Dolganov, G.M., Zhu, Z., Elias, J.A., Sheppard, D., Erle, D.J., 2002. Direct effects of interleukin-13 on epithelial cells cause airway hyperreactivity and mucus overproduction in asthma. Nat. Med. 8, 885–889.

Kurpinski, K., Lam, H., Chu, J., Wang, A., Kim, A., Tsay, E., Agrawal, S., Schaffer, D.V., Li, S., 2010. Transforming growth factor-beta and notch signaling mediate stem cell differentiation into smooth muscle cells. Stem Cells 28, 734–742.

Lemaire, R., Korn, J.H., Schiemann, W.P., Lafyatis, R., 2004. Fibulin-2 and fibulin-5 alterations in Tsk mice associated with disorganized hypodermal elastic fibers and skin tethering. J. Investig. Dermatol. 123, 1063–1069.

LeRoy, E.C., Black, C., Fleischmajer, R., Jablonska, S., Krieg, T., Medsger Jr., T.A., Rowell, N., Wollheim, F., 1988. Scleroderma (systemic sclerosis): classification, subsets and pathogenesis. J. Rheumatol. 15, 202–205.

Leroy, E.C., Smith, E.A., Kahaleh, M.B., Trojanowska, M., Silver, R.M., 1989. A strategy for determining the pathogenesis of systemic sclerosis. Is transforming growth factor beta the answer? Arthritis Rheum. 32, 817–825.

Markova, M.S., Zeskand, J., McEntee, B., Rothstein, J., Jimenez, S.A., Siracusa, L.D., 2004. A role for the androgen receptor in collagen content of the skin. J. Investig. Dermatol. 123, 1052–1056.

Milano, A., Pendergrass, S.A., Sargent, J.L., George, L.K., McCalmont, T.H., Connolly, M.K., Whitfield, M.L., 2008. Molecular subsets in the gene expression signatures of scleroderma skin. PLoS One 3, e2696.

Neuman, R.E., Logan, M.A., 1950. The determination of hydroxyproline. J. Biol. Chem. 184, 299–306.

Okano, Y., 1996. Antinuclear antibody in systemic sclerosis (scleroderma). Rheum. Dis. Clin. N. Am. 22, 709–735.

Peters, J., Ball, S.T., 1986. Tight skin-2 (Tsk2). Mouse News Lett. 2.

Piscaglia, F., Dudas, J., Knittel, T., Di Rocco, P., Kobold, D., Saile, B., Zocco, M.A., Timpl, R., Ramadori, G., 2009. Expression of ECM proteins fibulin-1 and -2 in acute and chronic liver disease and in cultured rat liver cells. Cell Tissue Res. 337, 449–462.

Quaglino Jr., D., Bergamini, G., Boraldi, F., Manzini, E., Davidson, J.M., Pasquali Ronchetti, I., 1996. Connective tissue in skin biopsies from patients suffering systemic sclerosis. J. Submicrosc. Cytol. Pathol. 28, 287–296.

Sargent, J.L., Milano, A., Bhattacharyya, S., Varga, J., Connolly, M.K., Chang, H.Y., Whitfield, M.L., 2010. A TGFbeta-responsive gene signature is associated with a subset of diffuse scleroderma with increased disease severity. J. Investig. Dermatol. 130, 694–705.

Scussel-Lonzetti, L., Joyal, F., Raynauld, J.P., Roussin, A., Rich, E., Goulet, J.R., Raymond, Y., Senecal, J.L., 2002. Predicting mortality in systemic sclerosis: analysis of a cohort of 309 French Canadian patients with emphasis on features at diagnosis as predictive factors for survival. Medicine (Baltimore) 81, 154–167.

Sfikakis, P.P., McCune, B.K., Tsokos, M., Aroni, K., Vayiopoulos, G., Tsokos, G.C., 1993. Immunohistological demonstration of transforming growth factor-beta isoforms in the skin of patients with systemic sclerosis. Clin. Immunol. Immunopathol. 69, 199–204.

Siracusa, L.D., McGrath, R., Ma, Q., Moskow, J.J., Manne, J., Christner, P.J., Buchberg, A.M., Jimenez, S.A., 1996. A tandem duplication within the fibrillin 1 gene is associated with the mouse tight skin mutation. Genome Res. 6, 300–313.

Steen, V.D., 2005. Autoantibodies in systemic sclerosis. Semin. Arthritis Rheum. 35, 35–42.

Szapiel, S.V., Fulmer, J.D., Hunninghake, G.W., Elson, N.A., Kawanami, O., Ferrans, V.J., Crystal, R.G., 1981. Hereditary emphysema in the tight-skin (Tsk/+) mouse. Am. Rev. Respir. Dis. 123, 680–685.

van den Hoogen, F., Khanna, D., Fransen, J., Johnson, S.R., Baron, M., Tyndall, A., Matucci-Cerinic, M., Naden, R.P., Medsger Jr., T.A., Carreira, P.E., Riemekasten, G., Clements, P. J., Denton, C.P., Distler, O., Allanore, Y., Furst, D.E., Gabrielli, A., Mayes, M.D., van Laar, J.M., Seibold, J.R., Czirjak, L., Steen, V.D., Inanc, M., Kowal-Bielecka, O., Muller-Ladner, U., Valentini, G., Veale, D.J., Vonk, M.C., Walker, U.A., Chung, L., Collier, D.H., Csuka, M.E., Fessler, B.J., Guiducci, S., Herrick, A., Hsu, V.M., Jimenez, S., Kahaleh, B., Merkel, P.A., Sierakowski, S., Silver, R.M., Simms, R.W., Varga, J., Pope, J.E., 2013. 2013 classification criteria for systemic sclerosis: an American College of Rheumatology/European League against Rheumatism collaborative initiative. Arthritis Rheum. 65, 2737–2747.

Varga, J., 2004. Antifibrotic therapy in scleroderma: extracellular or intracellular targeting of activated fibroblasts? Curr. Rheumatol. Rep. 6, 164–170.

Yamamoto, T., 2010. Animal model of systemic sclerosis. J. Dermatol. 37, 26–41.

Yanagisawa, H., Davis, E.C., Starcher, B.C., Ouchi, T., Yanagisawa, M., Richardson, J.A., Olson, E.N., 2002. Fibulin-5 is an elastin-binding protein essential for elastic fibre development in vivo. Nature 415, 168–171.

Please cite this article as: Long, K.B., et al., Tight skin 2 mice exhibit a novel time line of events leading to increased extracellular matrix deposition and dermal fibrosis, Matrix Biol. (2014), http://dx.doi.org/10.1016/j.matbio.2014.05.002

Tight Skin 2 Mice Exhibit Delayed Wound Healing Caused by Increased Elastic Fibers in Fibrotic Skin

Kristen B. Long,[1,†] Chelsea M. Burgwin,[1,†] Richard Huneke,[2] Carol M. Artlett,[1] and Elizabeth P. Blankenhorn[1,*]

[1]Department of Microbiology and Immunology and [2]University Laboratory Animal Resources, Drexel University College of Medicine, Philadelphia, Pennsylvania.

Elizabeth P. Blankenhorn, PhD

Submitted for publication February 25, 2014. Accepted in revised form March 26, 2014.

*Correspondence: Department of Microbiology and Immunology, Drexel University College of Medicine, 2900 Queen Lane, Philadelphia, PA 19129 (e-mail: eblanken@drexelmed.edu).

Rationale: The Tight Skin 2 (Tsk2) mouse model of systemic sclerosis (SSc) has many features of human disease, including tight skin, excessive collagen deposition, alterations in the extracellular matrix (ECM), increased elastic fibers, and occurrence of antinuclear antibodies with age. A tight skin phenotype is observed by 2 weeks of age, but measurable skin fibrosis is only apparent at 10 weeks. We completed a series of wound healing experiments to determine how fibrosis affects wound healing in Tsk2/+ mice compared with their wild-type (WT) littermates.

Method: We performed these experiments by introducing four 4 mm biopsy punched wounds on the back of each mouse, ventral of the midline, and observed wound healing over 10 days. Tsk2/+ mice showed significantly delayed wound healing and increased wound size compared with the WT littermates at both 5 and 10 weeks of age. We explored the potential sources of this response by wounding Tsk2/+ mice that were genetically deficient either for the NLRP3 inflammasome (a known fibrosis mediator), or for elastic fibers in the skin, using a fibulin-5 knockout.

Conclusion: We found that the loss of elastic fibers restores normal wound healing in the Tsk2/+ mouse and that the loss of the NLRP3 inflammasome had no effect. We conclude that elastic fiber dysregulation is the primary cause of delayed wound healing in the Tsk2/+ mouse and therapies that promote collagen deposition in the tissue matrix in the absence of elastin deposition might be beneficial in promoting wound healing in SSc and other diseases.

INTRODUCTION

Scleroderma (or systemic sclerosis, SSc) is a polygenic, autoimmune disorder of unknown etiology, characterized by the excessive and variable accumulation of extracellular matrix (ECM) proteins, vascular alterations, and production of autoantibodies. It is a rare disease, and a potentially fatal one, due to consequent lung fibrosis with or without pulmonary arterial hypertension.[1] There is no cure for the disease and only palliative treatment is available. One of the factors limiting the treatment of SSc is the lack of understanding of the development of disease. Specific triggers of fibrosis are unclear because patients may have advanced disease before diagnosis, and skin biopsy samples from patients can only be investigated after the disease has been well established, highlighting the need for animal models that will allow investigation of early skin changes before the onset of fibrosis and an exploration of traits associated with SSc.

[†]These authors contributed equally to this work.

DOI: 10.1089/wound.2014.0529

A complex and incomplete literature surrounds the issue of wound healing in people with SSc. Because poor circulation due to Raynaud's syndrome is common in SSc, it is not surprising that many of them develop digital ulcers that exhibit slow and poor quality healing. Malnutrition contributes to poor healing,[2] and persons with SSc often suffer from malnutrition caused by gastrointestinal complications.[3,4] Anecdotally, there are reports of surgical wounds that fail to heal properly in SSc patients, in body regions that are not especially vulnerable to a reduced blood supply. Keloid formation, instead of scarless wound resolution, is seen in individuals with SSc and is considered a wound healing defect.[5,6] Few objective data exist to compare healing in affected versus unaffected skin, and although scleroderma has been characterized as an excessive wound healing response,[7] distinguishing whether fibrosis plays an active role in delayed resolution of an open wound still needs to be determined.

Wound resolution is more appropriately studied in animal models, and there are several fibrotic mouse models of SSc, including chemically induced fibrosis and tight skin with a genetic basis. However, no mouse model is completely faithful to the full range of traits in SSc.[8,9] The two popular genetic mouse models of disease are the Tsk1 mouse[10–12] and the Tsk2 mouse.[13,14] Each mouse strain bears a different homozygous lethal mutation that requires mice to be bred and evaluated as heterozygotes (*e.g.*, Tsk1/+ and Tsk2/+). The Tsk2/+ mouse has a mutation in the *Col3a1* gene that leads to a missense mutation in the N-terminal peptide, marked increase in collagen accumulation, and loss of the subcutaneous fat layer in the dermis at 10 weeks of age compared with wild-type (WT) littermates.[15] Transcription of the *Col1a1* gene and production of COL1A1 are also upregulated in fibroblasts isolated from Tsk2/+ mice[15–17] at this age. The Tsk2/+ mouse recapitulates several facets of the human disease, including increased collagen and autoantibody production late in life.[15,18] The Tsk2/+ mouse also has a classical tight skin phenotype and a small body stature. Most importantly, however, is that we have found that Tsk2/+ mice have dramatically increased elastin in the skin.[15]

Previous work in our laboratory has shown that the cardinal Tsk2/+ traits of fibrosis and tight skin are not dependent on the NOD-like receptor family, pyrin domain containing 3 (NLRP3) activation, or excess elastic fibers.[15] In the present study, we consider the role of NLRP3 and elastic fibers in wound healing independently of fibrosis. We find that Tsk2/+ mice have delayed wound healing as compared with WT littermates that is evident in both prefibrotic (5 weeks old) and postfibrotic (10 weeks old) mice. By crossing Tsk2/+ mice to NLRP3 inflammasome knockout (NLRP3-KO) mice or to elastic fiber knockout mice (Fibulin-5 (*Fbln5)*-KO), we determined that this delayed wound is due to excessive elastic fibers and not differential inflammasome activation.

CLINICAL PROBLEM ADDRESSED

An incomplete picture of wound healing in people with SSc prevents our understanding of the role of fibrosis on wound closure. By using an animal model that can be studied for both wound healing and fibrosis, and one where mice with selected genetic deficiencies can be used to probe individual pathways for healing, we have begun to assemble a more complete list of contributing factors for healing in the setting of dermal abnormalities.

MATERIALS AND METHODS

Ethics statement

All studies and procedures were approved by the Institutional Animal Care and Use Committee (IACUC) of Drexel University, and conducted in accord with recommendations in the "Guide for the Care and Use of Laboratory Animals" (Institute of Laboratory Animal Resources, National Research Council, National Academy of Sciences, 2011).

Mice

Tsk2/+ mice were obtained from Dr. Paul Christner (Thomas Jefferson University, Philadelphia, PA) with permission from the MRC Radiobiology Unit Laboratory and were housed at the Drexel University College of Medicine. The Tsk2/+ mice were originally bred onto the hybrid (C3H x B6) background. At Drexel, they were serially backcrossed to B6 mice. Fibulin-5–deficient mice were a kind gift from Dr. Hiromi Yanagisawa (University of Texas Southwestern Medical Center) and were bred to B6.Tsk2/+ mice. NLRP3-KO mice were obtained from Jackson Laboratories. For each experiment, age- and sex-matched WT littermates were used as controls. Mice were housed in individually ventilated autoclaved cages, fed Purina LabDiet® PicoLab® 5053 and 5058 ad libitum, and provided autoclaved water, acidified to pH 3. All studies were approved by the IACUC of Drexel University.

Tsk2/+ microsatellite genotyping

Mice were genotyped for the *Tsk2* locus using PCR of flanking markers: microsatellites *D1Mit233*, *D1Mit235*, and a microsatellite in the *Glutaminase*

gene (*Gls*). PCR products were separated by electrophoresis on a 3% agarose gel. Genotypes were confirmed by skin tightness assessment of every mouse.

Fibulin-5 deletion genotyping

Fibulin-5 deletion was detected using a two primer set PCR, whereby one primer set detected the WT allele and the other detected the KO allele. WT forward (common) primer 5′-AGCTAAGGATAAC GAGGTGAGG-3′, WT reverse primer 5′-TCAGAT TACAGCGCTCACCA-3′, and KO reverse primer 5′-AGCATCTATCCAAGCAACTACAG-3′PCR products were separated by electrophoresis on a 3% agarose gel.

Wound healing: measurements and quantification

On Day 1, 5- and 10-week-old mice were anesthetized with isoflurane and their back hair removed with wax. On Day 0, mice were again anesthetized with isoflurane and four 4 mm full-thickness skin wounds were created with a sterile 4 mm biopsy punch. Wound pictures were taken from 6 inches directly above the mouse. Over days 1–10, mice were anesthetized daily and pictures taken and the wound area was traced using ImageJ software (http://rsbweb.nih.gov/ij/). After Day 10, mice were euthanized and back skin was taken for histological analysis. Analysis of wound closure was done with GraphPad Prism software.

Hydroxyproline assay

Mice were euthanized and the lower dorsal fur was removed by shaving. Two 8 mm punches were excised from each piece of skin, snap-frozen, weighed, and stored at −80°C. Protein was isolated for hydroxyproline assays.[19] The optical density was read at 550 nm in triplicate and the hydroxyproline content was determined against a standard curve of hydroxyproline (Sigma-Aldrich).

Western blot

Skin was harvested and collagen content was determined by western blot analysis, as previously described.[15] Briefly, skin was homogenized in the RIPA buffer (Sigma-Aldrich) containing 1% phosphatase inhibitor and 1% protease inhibitor (Sigma-Aldrich). The lysate was centrifuged at 8,000 *g* for 10 min at 4°C to pellet debris. The supernatant was collected. Approximately 75 μg of protein per sample was added to a reducing buffer, boiled, and then loaded onto an 8% SDS gel. Proteins were transferred to a polyvinylidene fluoride membrane, blocked in 5% nonfat milk in Tris-buffered saline, probed with goat anti-elastin (sc-17581) or goat anti-β-actin (#sc-1616), probed with a secondary antibody donkey anti-goat (#sc-2020; Santa Cruz Biotechnology, Inc.), and developed using the SuperSignal West Dura ECL reagent (Thermo Scientific, Inc.). Band intensities were measured using ImageQuant TL Software (GE Healthcare Life Sciences).

RESULTS

Tsk2/+ mice have increased wound size and delayed healing

To examine wound healing in the Tsk2/+ mouse, we used two groups: 5- to 6-week-old animals that were considered prefibrotic, and 10-week-old animals that were considered postfibrotic by assessment of total skin collagen.[15] Both male and female Tsk2/+ mice had delayed wound healing (Fig. 1, Table 1). Furthermore, we observed that within 2 days, wounds in Tsk2/+ mice become significantly larger than in WT mice in 5- and 10-week male mice and 10-week female mice. The maximum wound size in Tsk2/+ mice peaks at day 2 postwounding compared with the initial wound (day 0) in WT littermates (Fig. 1). This suggests that a factor relevant to their tight skin syndrome increases the wound size early in wound closure in Tsk2/+ mice.

Wound sizes and the subsequent healing time in mice are dependent on sex and age (Fig. 1). The sex difference is significant between WT mice at 5–6 weeks ($p < 0.0001$) and at 10 weeks ($p = 0.013$); it is even more pronounced between Tsk2/+ males and Tsk2/+ females ($p < 0.0001$). In females, 10-week-old Tsk2/+ mice have larger wounds than 5- to 6-week-old Tsk2/+ mice, yet in males, younger WT mice have larger wounds than older WT mice. The wounds in the majority of WT mice healed by 8 days, whereas most wounds in Tsk2/+ mice failed to close by day 10. As expected, a larger wound was linked to a longer 50% wound closure time (Table 1), however, as demonstrated by the female 5- to 6-week age group, Tsk2/+ mice still had delayed wound healing even when the wounds did not initially expand. Because both the prefibrotic (5–6 weeks) and postfibrotic (10 weeks old) mice display wound healing defects, we can conclude that delayed wound healing in Tsk2/+ mice is not a result of increased total collagen. This leads us to consider what early factors could be responsible for this phenotype.

A deficiency in the NLRP3 inflammasome does not improve wound healing in Tsk2/+ mice

Because fibrosis was likely not the driving factor behind delayed wound healing in Tsk2/+ mice, we explored if an inflammatory factor could be responsible by determining the effect of a deficiency

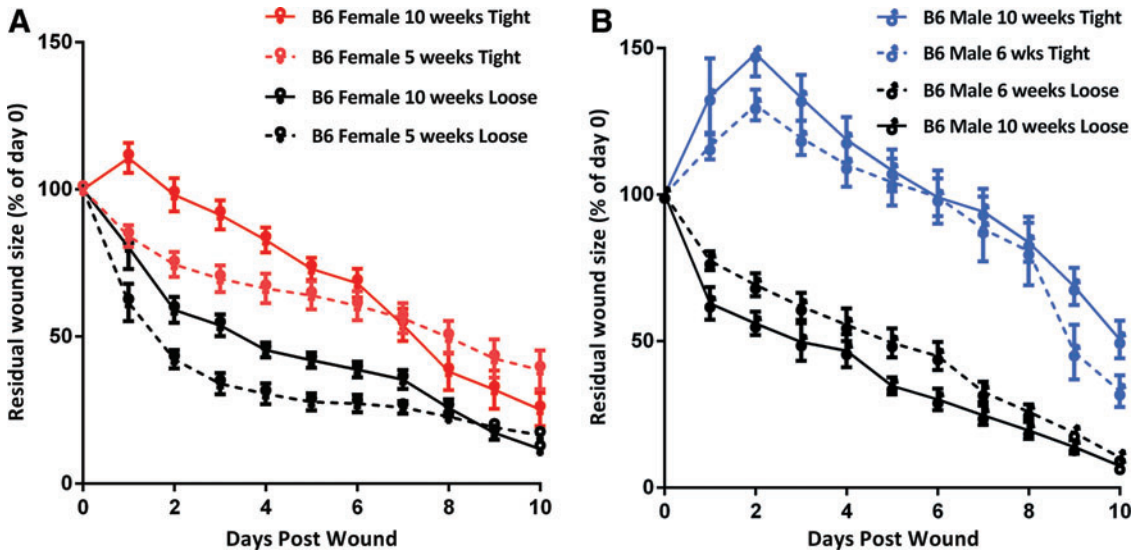

Figure 1. Tsk2/+ mice have delayed wound healing as compared to wild-type littermates at both 5–6 and 10 weeks of age. Female **(A)** and male **(B)** littermates were genotyped as WT (loose skin) or Tsk2/+ (tight skin). At 5–6 weeks or 10 weeks of age, mice had 4 mm wounds made in back skin. Measurements of residual wound size were made daily and are expressed as a percent of day 0. To see this illustration in color, the reader is referred to the web version of this article at www.liebertpub.com/wound

in NLRP3-KO on the wounding phenotype of the Tsk2/+ mouse. NLRP3 inflammasome activation is required for skin fibrosis in the bleomycin-induced model of SSc,[20–22] but not in Tsk2/+ mice.[15] To test if NLRP3 activation contributes to poor wound healing, Tsk2/+ mice were crossed to NLRP3 knockout mice, and progeny with different *Tsk2* and *Nlrp3* genotypes were tested. Dorsal wounds were made at 10 weeks of age. The mice were grouped by genotype (Tsk2.*Nlrp3*-KO, Tsk2.*Nlrp3*-WT, WT.*Nlrp3*-KO, and WT. *Nlrp3*-WT) and stratified by sex. In two groups (female Tsk2.*Nlrp3*-KO and male WT. *Nlrp3*-KO), the complete deficiency of NLRP3 significantly lengthened the time to 50% wound healing (Fig. 2). In male animals, Tsk2.*Nlrp3*-KO mice had the same delayed wound healing and increased early wound size as Tsk2.*Nlrp3*-WT mice ($p = 0.96$, Fig. 2), indicating that the loss of NLRP3 did not restore proper healing; female animals, Tsk2.*Nlrp3*-KO mice had modestly worse healing than female Tsk2.

Table 1. *Mean 50% wound closure time (days)*

	Male	*Female*
WT at 5–6 weeks of age	4.71	2.32
WT at 10 weeks of age	3.22	3.89
Tsk2/+ at 5–6 weeks of age	9.15	7.56
Tsk2/+ at 10 weeks of age	9.85	7.51

Littermates were genotyped as WT (loose skin) or Tsk2/+ (tight skin), and 4 mm full thickness skin wounds made at 5–6 weeks or 10 weeks of age and assessed daily. A best fit nonlinear regression was performed and the 50% wound closure time (in days) was interpolated for each group.

Nlrp3-WT mice. In female mice with WT alleles at the *Tsk2* locus, *Nlrp3*-KO had no significant effect on healing times compared with WT.*Nlrp3*-WT ($p = 0.61$). This result shows that the ability to form NLRP3+ inflammasomes does not play a role in the poor wound healing of Tsk2/+ mice.

Elastic fibers are the primary cause of delayed wound healing in the Tsk2/+ mouse

With both fibrosis and inflammasome activation eliminated as probable causes of delayed wound healing, we explored if elastic fiber dysregulation plays a role in Tsk2/+ wound healing. We bred Tsk2.*Fbln5*-KO mice, and confirmed our previous report[15] that elastic fiber loss had no effect on fibrosis as assessed by hydroxyproline at 20 weeks (Fig. 3). *Fbln5*-KO mice can make elastin, but do not assemble elastic fibers in the skin in either WT[23] or Tsk2/+ mice.[15]

Dorsal wounds were made at 10 weeks of age in mice with the following genotypes: Tsk2.*Fbln5*-KO, Tsk2.*Fbln5*-WT, WT.*Fbln5*-KO, and WT.*Fbln5*-WT. The loss of *Fbln5* restored normal wound healing to Tsk2/+ mice of both sexes (Figs. 4, 5). The wounds in both male and female Tsk2.*Fbln5*-KO mice close at a rate and to a degree that is very similar to WT mice. Furthermore, wounds in the Tsk2.*Fbln5*-KO mice did not expand as much after day 0, as they do in Tsk2.*Fbln5*-WT mice, and instead began closing similar to WT or WT.*Fbln5*-KO mice (Fig. 5). Tsk2.*Fbln5*-HET male and female mice healed similarly to Tsk2.*Fbln5*-WT indicating that hetero-

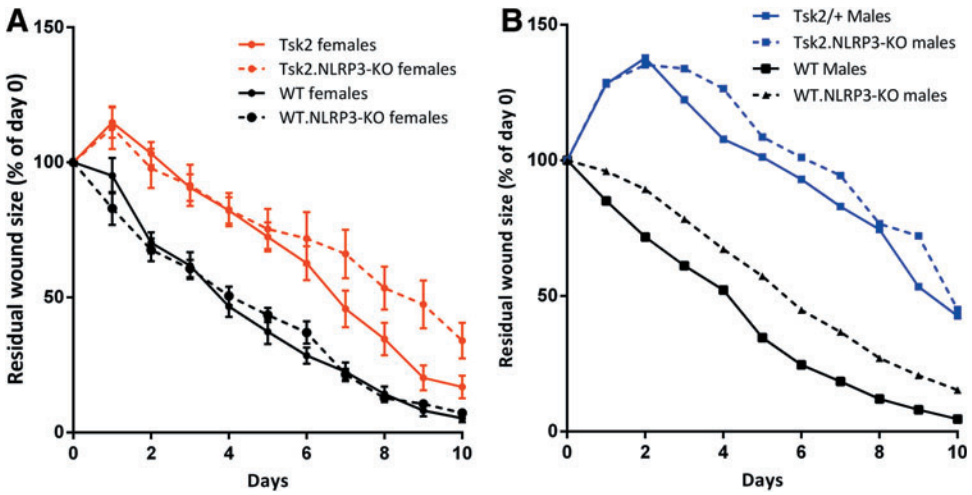

Figure 2. NLRP3 deficiency does not improve poor healing in Tsk2 mice. Female **(A)** and male **(B)** littermates were genotyped as WT (loose skin) or Tsk2/+ (tight skin), and genotyped for expression of NLRP3. Four 4 mm wounds were made in back skin at 10 weeks of age. Measurements of residual wound size were made daily and are expressed as a percent of day 0. As measured in 2-way ANOVA, *Nlrp3*-WT mice did not differ significantly from *Nlrp3*-KO mice within each sex. To see this illustration in color, the reader is referred to the web version of this article at www.liebertpub.com/wound

zygosity for *Fbln5* is sufficient to cause delayed wound healing in Tsk2/+ mice (Fig. 6). Notably, all *Fbln5*-KO groups healed better than their *Fbln5*-WT counterparts (Fig. 4). WT.*Fbln5*-KO healed somewhat better (males) or considerably better (females) than WT.*Fbln5*-WT, indicating that normal skin elastin can inhibit early wound healing, in contrast to previous findings.[23] These results demonstrate that FBLN5 proteins or the skin elastic fibers containing FBLN5 and elastin, are responsible for the two major features of delayed wound healing in Tsk2/+ mice: the expansion of the wound in the first 2 days of wound resolution, and the significantly delayed overall healing.

DISCUSSION

Mammalian wound healing comprises four overlapping phases: the immediate phase; the inflammatory phase; the proliferation, migration/

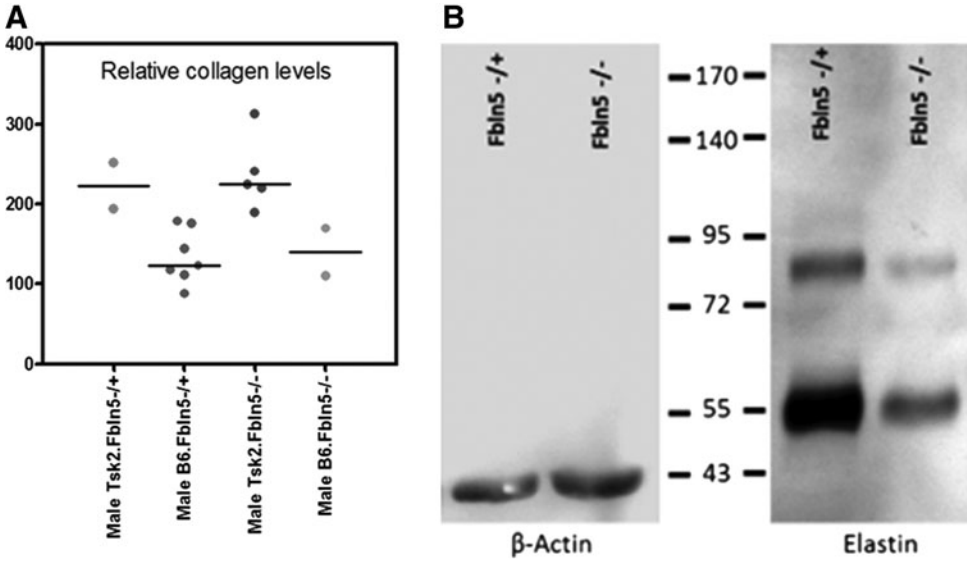

Figure 3. Fibrosis is unchanged in Tsk2.*Fbln5*-KO mice. **(A)** Tsk2.*Fbln5*-KO have the same excess collagen levels as Tsk2.*Fbln5*-HET mice. The 8 mm punches were excised from the back skin of 20 week male mice and analyzed for collagen content by hydroxyproline analysis. The hydroxyproline assay shows no significant difference in total collagen between Tsk2/+ samples either with or without fibulin-5, and significantly elevated collagen in both compared with WT (B6) littermates. **(B)** *Fbln5*-KO mice produce significantly less elastin as compared with *Fbln5*-HET mice. Protein isolated from mouse skin and analyzed by western blot. The gel was transferred to a membrane and probed with anti-elastin and anti-actin antibodies.

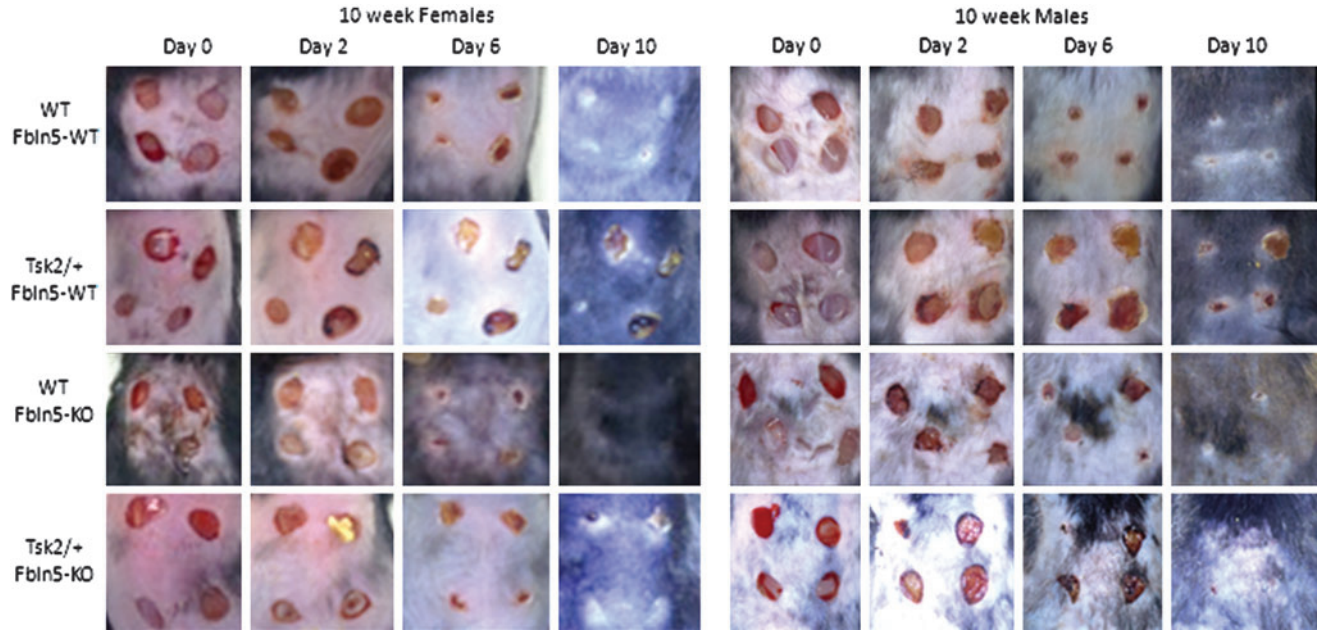

Figure 4. *Fbln5*-KO improves wound healing in both Tsk2/+ and wild-type littermates. Postwound skin pictures of females (left) and males (right) on day 0, 2, 6, and 10. Mice were anesthetized, hair was waxed, and full-thickness excisional wounds were created on the back of each animal with a 4 mm biopsy punch. Wound sizes were calculated using ImageJ. Tsk2/+ male mice with WT *Fbln5* exhibit an initial increase in wound size (maximum at day 2) followed by delayed healing when compared with wild-type mice. To see this illustration in color, the reader is referred to the web version of this article at www.liebertpub.com/wound

contraction phase; and the resolution phase.[24] The immediate phase occurs directly after injury.[25] During this stage, the platelets and surrounding immune cells release cytokines to aid the healing process. Together, immune cytokines, such as IL-1 and colony-stimulating factors, induce the formation of serum response factor, which leads to the increase in transcription of hundreds of genes important for the initiation of wound healing.[26] The inflammatory phase extends from day 0 to 6 postwounding in mice.[24,27] Next, the proliferation/migration/contraction phase begins at day 4 and

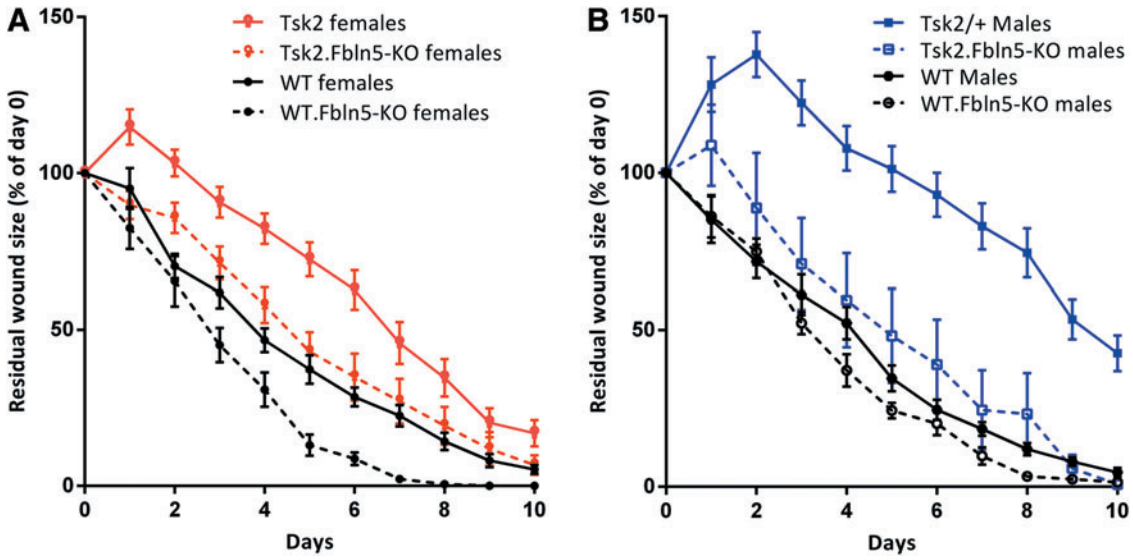

Figure 5. Elastic fiber deficiency improves poor healing in Tsk2/+ mice. Ten-week-old female **(A)** and male **(B)** littermates were genotyped for *Fbln5* and for *Tsk2* and had 4 mm dorsal skin wounds made at this time. Measurements of residual wound size were made daily and are expressed as a percent of day 0. As measured in 2-way ANOVA comparing male mice, the Tsk2/+ fibulin-5–sufficient mice had significantly different healing ($p < 0.0001$) compared with every other strain at each day, and the Tsk2.*Fbln5*-KO is similar to WT mice. In female mice, there is a significant difference due to *Tsk2* ($p < 0.0001$ day 2–8), and loss of *Fbln5* in Tsk2/+ mice rendered them statistically similar to WT.*Fbln5*-WTmice; in addition, there was a small but significant difference after day 5 between WT mice and WT mice bearing the *Fbln5*-KO. To see this illustration in color, the reader is referred to the web version of this article at www.liebertpub.com/wound

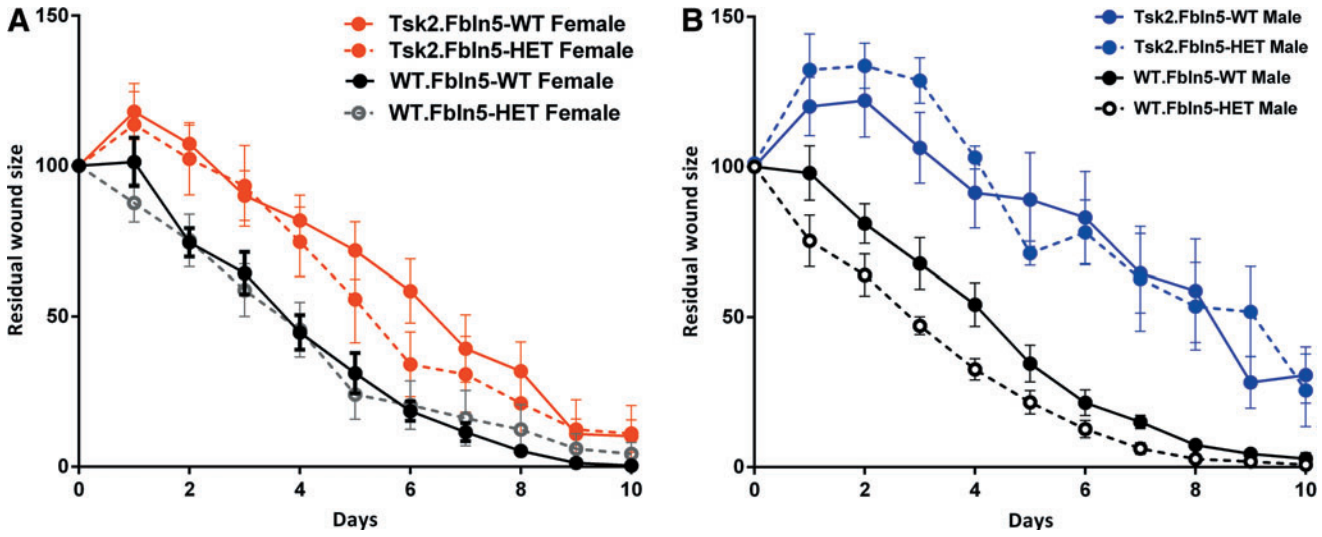

Figure 6. Wound healing in *Fbln5*-heterozygotes compared with *Fbln5*-WT littermates shows that one copy of *Fbln5* is sufficient to promote healing defect. Female **(A)** and male **(B)** littermates were genotyped as WT (loose skin) or Tsk2/+ (tight skin) and genotyped for *Fbln5*. Measurements of residual wound size in 10-week-old mice were made daily and are expressed as a percent of wound size on day 0. Wound healing of *Fbln5*-HET mice was graphed against Tsk2.*Fbln5*-WT mice and stratified by sex and Tsk2 genotypes. A nonlinear regression determined that Tsk2.*Fbln5*-HET mice and Tsk2.*Fbln5*-WT mice heal at similar rates. To see this illustration in color, the reader is referred to the web version of this article at www.liebertpub.com/wound

stretches to day 14,[27] and is necessary for the permanent closure of the wound and the repair of damaged tissue. Alterations and inhibition of components in this process at any point can impede wound healing, and our studies attempted to determine which of these factors contributes to the significantly impaired healing seen in Tsk2/+ mice.

Collagen has a well-established role in early wound healing. During the proliferative phase, type III collagen (COL3A1) is secreted by migrating and proliferating fibroblasts, in and around the wound bed.[27] This collagen is vital for creating the provisional matrix during this phase.[27] Because the *Tsk2* mutation is in *Col3a1* (Long *et al.*, in revision, 2014), we anticipated that fibrosis itself would account for the poor wound healing in this strain, but deficient wound closure is seen before the accumulation of collagens in the skin, as reflected by the poor wound closure in 5-week-old Tsk2/+ mice, which do not yet display skin fibrosis.[15] Type I collagen (COL1A1) is also important during the maturation stage when COL1A1 replaces the COL3A1 laid down in the granuloma tissue—COL1A1 fibrils are stronger and the most prevalent collagen in unwounded skin.[27] Mice bearing a mutant COL1A1 that is resistant to metalloproteinase cleavage are very deficient in wound healing.[28] However, excess collagen of this type is not the cause of the impaired wound healing in Tsk2/+ mice, as young, prefibrotic Tsk2/+ mice are not able to close dorsal wounds as well as their WT littermates.

Nlrp3 is a gene that encodes a pyrin-like protein, NLRP3, which interacts with apoptosis-associated proteins containing a caspase recruitment domain.[29] Activation of the NLRP3 inflammasome contributes to bleomycin-induced tissue injury because *Nlrp3*-KO mice injected with bleomycin do not develop fibrosis in the skin or lungs.[20–22] During wound healing, the inflammasomes become activated and IL-1β is cleaved when caspase-1 is processed to its mature form.[29] This process can occur in numerous cell types in the wound bed, including platelets and endothelial cells.[27] IL-1β has many proinflammatory effects, including upregulating the expression of collagens and TGF-β1, required for wound healing. In the setting of excess fibrosis seen in Tsk2/+ mice, it might be expected that NLRP3 could contribute to poor wound healing by exaggerating the fibrotic response. However, Tsk2.*Nlrp3*-KO mice have the same amount of fibrosis as Tsk2.Nlrp3-WT littermates, and Tsk2.*Nlrp3*-KO still have impaired wound healing, not improved. Thus, the wound healing defect characteristic of Tsk2/+ mice is the same in tight skin animals whether or not they express NLRP3.

Elastic fibers have a less well-defined role in wound healing. *Fbln5* mRNA and elastic fibers appear late, after 14 days, in the wound healing process.[23] Work in a rabbit model found that ectopic elastin applied to the wound bed can decrease wound healing time[30]; however, reduction of elastin fiber formation in *Fbln5*-KO mice either had no effect on mouse wound healing[23] or, in the present

study, genetic deletion of *Fbln5* significantly enhanced healing, and reduced the time to 50% wound closure (Fig. 5). Taken together, these results indicate that reducing elastic fibers can be beneficial to wound healing in mice, promoting earlier wound closure. Furthermore, we show that an overabundance of elastic fibers in Tsk2/+ skin has a detrimental effect on wound healing. Of course, further studies would be required to extend these results directly to people with fibrosis, as the Tsk2/+ model is a single-gene defect, and mouse skin has a substantially different architecture that does not adequately model the complexity of healing in the human being.

KEY FINDINGS

- The delayed wound healing in Tsk2/+ mice (a model of systemic sclerosis) is not related to their fibrosis *per se* because it is evident at ages when substantial fibrotic accumulation of the ECM has not yet occurred.
- The delayed wound healing in the Tsk2/+ mice is not due to the presence of inflammation that is dependent on the NLRP3 inflammasome. However, as might be predicted from the theory that a modest level of inflammation is required for optimal healing, all mice healed more slowly, sometimes significantly so, when they could not activate the NLRP3 pathway.
- The delayed wound healing in Tsk2/+ mice is due to excessive elastin- and fibulin-5–containing elastic fibers, because the *Fbln5*-KO restores healing kinetics and closure to near normal levels in Tsk2/+ male and female mice.

Whereas little is known regarding the rate of healing in SSc patients, it is known that SSc patients, especially those with severe, diffuse disease, are at a greater risk for developing skin ulcers[31] and they show dysregulation of elastic fibers in their skin.[32,33] Our studies in mice suggest that elastic fiber dysregulation can increase both the initial wound size and healing time. This is the first time elastic fibers have been shown to have a role in early wound healing processes, indicating that the overall health of the ECM and not just vascular insufficiency should be taken into account when considering the explanation for poor quality wound healing. Thus, therapies that promote collagen deposition in the tissue matrix in the absence of elastin deposition might be beneficial in promoting wound healing in SSc and other diseases characterized by chronic wounds.

INNOVATION

The ability to study wound closure in the Tsk2/+ model of a severe, fibrotic autoimmune human disease is novel, especially because we discovered that these mice exhibit a very significantly delayed dorsal wound response. Using this model, we teased apart the various factors that contribute to poor quality wound healing using genetic approaches and found that dermal elastic fibers, contrary to expectation, can impede wound closure when in great excess compared with normal skin.

ACKNOWLEDGMENTS AND FUNDING SOURCES

The authors gratefully acknowledge the gift of Tsk2/+ mice from Dr. Paul Christner and the Fibulin-5 knockout mice from Dr. Hiromi Yanagisawa. The research in this report was supported by the Scleroderma Foundation, the National Institutes of Health, and the Department of Defense.

AUTHOR DISCLOSURE AND GHOSTWRITING

No competing financial interests exist. The content of this article was expressly written by the authors listed. No ghostwriters were used to write this article. All authors contributed to the writing and the review of the article.

ABOUT THE AUTHORS

Kristen B. Long and **Chelsea M. Burgwin** contributed equally to this work. Kristen did her doctoral thesis on the Tsk2/+ mouse model in the Blankenhorn laboratory, and is currently a postdoctoral researcher at the University of Pennsylvania. Chelsea Burgwin is studying this mouse model for her doctoral dissertation work at the Drexel University in the Molecular Cell Biology and Genetics graduate program. **Dr. Richard Huneke** is a veterinarian and head of the University Laboratory Animal Resources at Drexel University College of Medicine, and was very helpful in assisting us in the practice of wound instillation and measurement in an ethical and humane manner. **Dr. Carol M. Artlett** is a contributing author with a long and substantial interest in SSc and fibrosis, and is currently Associate Professor in the Department of Microbiology and Immunology at Drexel University College of Medicine. **Dr. Elizabeth P. Blankenhorn** has a long-standing interest in genetics and animal models of complex diseases. She heads the Research Center of Excellence in Immunogenetics & Inflammatory Disease in the Institute for Molecular Medicine and Infectious Disease at Drexel University College of Medicine and is a Professor in the Department of Microbiology and Immunology.

REFERENCES

1. Steen VD and Medsger TA: Changes in causes of death in systemic sclerosis, 1972–2002. Ann Rheum Dis 2007; **66:** 940.
2. Young ME: Malnutrition and wound healing. Heart Lung 1988; **17:** 60.
3. Caporali R, Caccialanza R, Bonino C, *et al.*: Disease-related malnutrition in outpatients with systemic sclerosis. Clin Nutr 2012; **31:** 666.
4. Gyger G and Baron M: Gastrointestinal manifestations of scleroderma: recent progress in evaluation, pathogenesis, and management. Curr Rheumatol Rep 2012; **14:** 22.
5. Heath CR, David JN, and Taylor SC: Nodular scleroderma presenting as multiple spontaneous keloidal scars. J Am Acad Dermatol 2012; **66:** e245.
6. Le EN, Junkins-Hopkins JM, Sherber NS, and Wigley FM: Nodular/keloidal scleroderma: acquired collagenous nodules in systemic sclerosis. J Rheumatol 2012; **39:** 660.
7. Elkon KB and Rhiannon JJ. Scleroderma. From Pathogenesis to Comprehensive Management. In: *Innate Immunity*, edited by Varga J, Denton C, and Wigley F. New York: Springer, 2012.
8. Yamamoto T: Animal model of systemic sclerosis. J Dermatol 2010; **37:** 26.
9. Artlett CM: Animal models of scleroderma: fresh insights. Curr Opin Rheumatol 2010; **22:** 677.
10. Baxter RM, Crowell TP, McCrann ME, Frew EM, and Gardner H: Analysis of the tight skin (Tsk1/+) mouse as a model for testing antifibrotic agents. Lab Invest 2005; **85:** 1199.
11. Green MC, Sweet HO, and Bunker LE: Tight-skin, a new mutation of the mouse causing excessive growth of connective tissue and skeleton. Am J Pathol 1976; **82:** 493.
12. Szapiel SV, Fulmer JD, Hunninghake GW, *et al.*: Hereditary emphysema in the tight-skin (Tsk/+) mouse. Am Rev Respir Dis 1981; **123:** 680.
13. Christner PJ, Peters J, Hawkins D, Siracusa LD, and Jimenez SA: The tight skin 2 mouse. An animal model of scleroderma displaying cutaneous fibrosis and mononuclear cell infiltration. Arthritis Rheum 1995; **38:** 1791.
14. Peters J and Ball ST: Tight skin-2 (Tsk2). Mouse News Lett 1986; **74:** 91.
15. Long K, Artlett C, and Blankenhorn E: Tight Skin 2 Mice exhibit a novel time line of events leading to increased extracellular matrix deposition and dermal fibrosis. Matrix Biol 2013 [Epub ahead of print]; DOI: 10.1016/j.matbio.2014.05.002.
16. Christner PJ, Hitraya EG, Peters J, McGrath R, and Jimenez SA: Transcriptional activation of the alpha1(I) procollagen gene and up-regulation of alpha1(I) and alpha1(III) procollagen messenger RNA in dermal fibroblasts from tight skin 2 mice. Arthritis Rheum 1998; **41:** 2132.
17. Barisic-Dujmovic T, Boban I, and Clark SH: Regulation of collagen gene expression in the Tsk2 mouse. J Cell Physiol 2008; **215:** 464.
18. Gentiletti J, McCloskey LJ, Artlett CM, Peters J, Jimenez SA, and Christner PJ: Demonstration of autoimmunity in the tight skin-2 mouse: a model for scleroderma. J Immunol 2005; **175:** 2418.
19. Kuperman DA, Huang X, Koth LL, *et al.*: Direct effects of interleukin-13 on epithelial cells cause airway hyperreactivity and mucus overproduction in asthma. Nat Med 2002; **8:** 885.
20. Artlett CM, Sassi-Gaha S, Rieger JL, Boesteanu AC, Feghali-Bostwick CA, and Katsikis PD: The inflammasome activating caspase 1 mediates fibrosis and myofibroblast differentiation in systemic sclerosis. Arthritis Rheum 2011; **63:** 3563.
21. Artlett CM: The Role of the NLRP3 Inflammasome in Fibrosis. Open Rheumatol J 2012; **6:** 80.
22. Artlett CM: Inflammasomes in wound healing and fibrosis. J Pathol 2013; **229:** 157.
23. Zheng Q, Choi J, Rouleau L, *et al.*: Normal wound healing in mice deficient for fibulin-5, an elastin binding protein essential for dermal elastic fiber assembly. J Invest Dermatol 2006; **126:** 2707.
24. Shaw TJ and Martin P: Wound repair at a glance. J Cell Sci 2009; **122(Pt 18):** 3209.
25. Nurden AT, Nurden P, Sanchez M, Andia I, and Anitua E: Platelets and wound healing. Front Biosci 2008; **13:** 3532.
26. Iyer VR, Eisen MB, Ross DT, *et al.*: The transcriptional program in the response of human fibroblasts to serum. Science 1999; **283:** 83.
27. Broughton G, 2nd, Janis JE, and Attinger CE: The basic science of wound healing. Plastic Reconstr Surg 2006; **117(7 Suppl):** 12S.
28. Beare AH, O'Kane S, Krane SM, and Ferguson MW: Severely impaired wound healing in the collagenase-resistant mouse. J Invest Dermatol 2003; **120:** 153.
29. Schroder K and Tschopp J: The inflammasomes. Cell 2010; **140:** 821.
30. Lee MJ, Roy NK, Mogford JE, Schiemann WP, and Mustoe TA: Fibulin-5 promotes wound healing *in vivo*. J Am Coll Surg 2004; **199:** 403.
31. Schieir O, Thombs BD, Hudson M, *et al.*: Prevalence, severity, and clinical correlates of pain in patients with systemic sclerosis. Arthritis Care Res (Hoboken) 2010; **62:** 409.
32. Davis EC, Blattel SA, and Mecham RP: Remodeling of elastic fiber components in scleroderma skin. Connect Tissue Res 1999; **40:** 113.
33. Walters R, Pulitzer M, and Kamino H: Elastic fiber pattern in scleroderma/morphea. J Cutan Pathol 2009; **36:** 952.

Abbreviations and Acronyms

B6 = C57Bl/6J
COL1A1 = collagen, type 1, alpha 1
COL3A1 = collagen, type 3, alpha 1
ECM = extracellular matrix
Eln = elastin
Fbln5 = fibulin-5
mRNA = messenger RNA
NLRP3 = NOD-like receptor family, pyrin domain containing 3
SSc = systemic sclerosis
Tsk = tight skin
WT = wild type

The Tsk2/+ mouse fibrotic phenotype is due to a gain-of-function mutation in the PIIINP segment of the *Col3a1* gene

Journal:	*Journal of Investigative Dermatology*
Manuscript ID:	JID-2014-0495.R1
Manuscript Type:	Original Article
Date Submitted by the Author:	n/a
Complete List of Authors:	Long, Kristen; Drexel University College of Medicine, Microbiology and Immunology Li, Zhenghui; Dartmouth Geisel School of Medicine, Genetics Burgwin, Chelsea; Drexel University College of Medicine, Microbiology and Immunology Choe, Susanna; Dartmouth Medical School, Department of Genetics Martyanov, Viktor; 2Geisel School of Medicine at Dartmouth, Genetics Sassi-Gaha, Sihem; Drexel University College of Medicine, Microbiology and Immunology Earl, Joshua; Drexel University College of Medicine, Center for Genomics Sciences, Institute for Molecular Medicine and Infectious Disease; Drexel University College of Medicine, Microbiology and Immunology Eutsey, Rory; Allegheny-Singer Research Institute, Center for Genomic Sciences Ahmed, Azad; Allegheny-Singer Research Institute, Center for Genomic Sciences Ehrlich, Garth; Drexel University College of Medicine, Microbiology and Immunology; Drexel University College of Medicine, Center for Genomics Sciences, Institute for Molecular Medicine and Infectious Disease Artlett, Carol; Drexel University College of Medicine, Microbiology and Immunology Whitfield, Michael; Dartmouth Medical School, Department of Genetics Blankenhorn, Elizabeth; Drexel University College of Medicine, Microbiology and Immunology
Key Words:	scleroderma, fibrosis, animal model, genetics, collagen type 3

DREXEL UNIVERSITY
College of
Medicine
Department of Microbiology & Immunology

Elizabeth P. Blankenhorn, Ph.D.
Professor

September 10, 2014
Editors
Journal of Investigative Dermatology

Dear Editors,

Please find herein our REVISED manuscript titled "The Tsk2/+ mouse fibrotic phenotype is due to a gain-of-function mutation in the PIIINP segment of the *Col3a1* gene" for publication as an Original Article.

We have substantially altered it in response to the request from the expert reviewers. In doing so, I think we have made it a much better paper. I still firmly believe that this manuscript is well-suited for the *Journal of Investigative Dermatology* audience because of its unique and successful positional cloning of a causative gene for skin fibrosis, and because there remains a great need for more substantial and useful scleroderma patient categorization based on animal models of their skin disease. This report makes a major stride in that direction. We have added one new author to account for a revision requesting more substantiation of how the $Col3a1^{Tsk2}$ allele contributes to fibrosis, and the letter with all the authors permission to do this is appended to the manuscript. In order to meet the ~3500 word publication limit, we have had to delete some description, but this should improve, not detract, from the paper. However, all the methods are now in supplementary data, and, more appropriately, cited as references for techniques we have published in the recent past.

The data in the manuscript is original and the manuscript is not under consideration elsewhere. None of the manuscript contents have been previously published except in abstract form. All authors have read and approved all versions of the manuscript, its content, and its submission to the JID.

We thank you for your consideration of our manuscript and hope this revision is satisfactory.

Sincerely,

Elizabeth P. Blankenhorn, Ph. D. for the authors
Professor, Department of Microbiology and Immunology
Drexel University College of Medicine
2900 Queen Lane, Philadelphia, PA, 19129

The Tsk2/+ mouse fibrotic phenotype is due to a gain-of-function mutation in the PIIINP segment of the *Col3a1* gene

Kristen B. Long[1], Zhenghui Li[2], Chelsea M. Burgwin[1], Susanna G. Choe[2], Viktor Martyanov[2], Sihem Sassi-Gaha[1], Josh Earl[3], Rory Eutsey[3], Azad Ahmed[3], Garth D. Ehrlich[3], Carol M. Artlett[1], Michael L. Whitfield[2], and Elizabeth P. Blankenhorn[1,*]

[1]Department of Microbiology and Immunology, Drexel University College of Medicine, 2900 Queen Lane, Philadelphia, PA, USA.

[2]Geisel School of Medicine at Dartmouth, Department of Genetics, Hanover, NH USA.

[3]Center for Genomic Sciences, 320 East North Ave, Pittsburgh, PA, USA.

*To whom correspondence should be addressed.
Email: Elizabeth.Blankenhorn@drexelmed.edu
Telephone: 215-991-8392
Fax: 215-848-2271

Short title: Mutation in *Col3a1* causes fibrosis in Tsk2/+ mice

Abbreviations:

collagen, type III, alpha 1, Col3a1; C57Bl/6, B6; extracellular matrix, ECM; knockout, KO; megabases, Mb; procollagen III amino terminal propeptide segment, PIIINP; systemic sclerosis, SSc; single nucleotide polymorphism, SNP; tight-skin, Tsk; untranslated region, UTR; wild-type, WT

Abstract

Systemic sclerosis (SSc) is a polygenic, autoimmune disorder of unknown etiology, characterized by the excessive accumulation of extracellular matrix (ECM) proteins, vascular alterations, and autoantibodies. The tight skin (Tsk)2/+ mouse model of SSc demonstrates signs similar to SSc including tight skin and excessive deposition of dermal ECM proteins. By linkage analysis, we mapped the *Tsk2* gene mutation to less than 3 megabases on chromosome 1. We performed both RNA sequencing of skin transcripts and genome capture DNA sequencing of the region spanning this interval in Tsk2/+ and wild-type littermates. A missense point mutation in the procollagen III amino terminal propeptide segment (PIIINP) of *Col3a1* was found to be the best candidate for *Tsk2*, so both *in vivo* and *in vitro* genetic complementation tests were used to prove that this *Col3a1* mutation is the *Tsk2* gene. All previously documented mutations in the human *Col3a1* gene are associated with Ehlers-Danlos syndrome, a connective tissue disorder that leads to a defect in type III collagen synthesis. The *Tsk2* point mutation is the first documented gain-of-function mutation associated with *Col3a1*, which leads instead to fibrosis. This discovery provides insight into the mechanism of skin fibrosis manifested by Tsk2/+ mice.

Introduction

There are multiple animal models of SSc (Artlett, 2010), yet none mimics all facets of SSc disease. Of the genetic models, the cause of disease in tight-skin 1 (Tsk1/+) mice is known to be a tandem duplication in the fibrillin-1 (*Fbn1)* gene (Siracusa *et al.*, 1996). Other models of SSc have employed mice with individual gene deficiencies or overexpression including Fos-related antigen-2 (*Fra2*) (Maurer *et al.*, 2009), endothelin-1 (*Edn1*) (Hocher *et al.*, 2000; Richard *et al.*, 2008) and Friend leukemia integration 1 transcription factor (*Fli1*) (Asano *et al.*, 2010), which have proven useful for understanding the contribution of these proteins to the vasculopathy and/or lung fibrosis seen in SSc. Non-genetic models of SSc include the bleomycin-induced scleroderma model (Yamamoto *et al.*, 1999), which has been used to study many of the initiating events involved in fibrosis.

The Tsk2/+ mouse was first described in 1986, when an offspring of a 101/H mouse exposed to the mutagenic agent ethylnitrosourea was noted to have tight-skin in the interscapular region (Peters and Ball, 1986). The mutagenized gene causing SSc-like signs in Tsk2/+ mice was reported to be located on chromosome 1 between 42.5 and 52.5 megabases (Mb) (Christner *et al.*, 1996); however, the genetic defect was never identified. Like *Tsk1*, *Tsk2* SSc-like traits are highly penetrant in Tsk2/+ heterozygotes and it is homozygous embryonic lethal. Tsk2/+ mice have many features of human disease including tight-skin, dysregulated dermal extracellular matrix (ECM) deposition, and evidence of an autoimmune response (Christner *et al.*, 1995; Gentiletti *et al.*, 2005).

Herein, we report the positional cloning and identity of the *Tsk2* gene. We have discovered that Tsk2/+ mice carry a deleterious gain-of-function missense mutation in *Col3a1,* that exchanges a cysteine for serine in the N-terminal propeptide, PIIINP. The Tsk2/+ mouse

affords a unique opportunity to examine the pathways leading to the multiple clinical parameters of fibrotic disease from birth onward.

Results

Linkage and sequencing studies reveal a SNP mutation in Col3a1

Identification of the *Tsk2* gene was initiated with further mapping of the *Tsk2* interval by genotyping backcross progeny of Tsk2/+ mice bred to C57Bl/6 (B6) mice. Littermate mice were genotyped for informative microsatellites (*D1Mit233*, *D1Mit235*, a microsatellite in *Gls,* and *D1Mit18)* and single nucleotide polymorphism (SNP) genotyping assays used for additional markers. Multiple recombinants were recovered that mapped the interval to between 42.53 and 52.22 Mb on chromosome 1. Recombinants were bred and then backcrossed to a consomic B6.chr 1-A/J mouse to fine-map the region by SNP typing, as A/J mice bear many known SNPs compared to B6 mice. Additional recombinants were recovered and new SNPs from the sequencing projects (see below) were used to narrow the *Tsk2* interval to between 44.67 – 46.27 Mb (**Fig. 1A**), representing a greater than 3-fold reduction of the size of the interval bearing 101/H genomic DNA and *Tsk2*. There are six known genes in this interval (**Fig. 1B**).

To identify the mutation underlying *Tsk2*, we employed both RNA sequencing (RNA-Seq) and genome capture sequencing of the reduced genomic interval. Sequence reads were aligned to the MM9 reference genome (B6) and analyzed for polymorphisms in the *Tsk2* interval. There were 265 SNPs found in both WT and Tsk2/+ littermates that represent differences between the reference B6 genome and the 101/H background; these were excluded from further study. Thirteen SNPs were found in all four Tsk2/+ mice analyzed; ten of these SNPs were also found to be in liver RNA from 101/H strain or in other non-fibrotic mouse strains

(http://phenome.jax.org/), and were also ruled out as candidates for *Tsk2* (**Table 1**). The remaining three SNPs were heterozygous and confirmed to be only in Tsk2/+ mice. One of these, in a *Gulp1* intron, proved useful as a new marker that resides outside the supported linkage interval for Tsk2/+ on the proximal end in an informative recombinant mouse (**Fig. 1A**). A second SNP was also found in an intron of *Gulp1*. The RNA-Seq data did not identify any splicing defects in *Gulp1* mRNA in the Tsk2/+ mice (**Supplementary Fig. 1**), indicating that this SNP does not change *Gulp1* mRNA splicing, and its gene expression in skin is unchanged (**Fig. 2**). Thus the intronic SNP in *Gulp1* is unlikely to play a role in the tight skin phenotype. The remaining mutation was in *Col3a1* that results in a T to A transversion at Chr1:45,378,353, causing a Cys → Ser amino acid change in the procollagen III amino terminal propeptide (PIIINP) segment, a natural cleavage product of COL3A1. The mutant protein is designated COL3A1^{Tsk2} (C33S).

We calculated the Reads per Kilobase per Million mapped reads for each gene and found that of the genes in the reduced genomic interval, *Col3a1* shows the highest absolute expression level with all other genes showing negligible expression levels. RNA-Seq results indicate that there is a trend toward higher *Col3a1* mRNA abundance in 4-week old Tsk2/+ skin samples compared to WT littermates (**Fig. 2A,B**). The *Col3a1*^{Tsk2} (C33S) mutation is unlikely to change the expression levels of the *Col3a1* mRNA directly but will result in a mutated protein that is deposited in the ECM along with the WT protein in mixed heterotrimers, and could result in activation of pathways that impinge on *Col3a1* such as TGFβ (Sargent, et al., s*ubmitted*). Because Tsk2/+ (affected) mice are heterozygous, the *Col3a1*^{Tsk2} (C33S) mutation should account for 50% of the reads assuming equal expression from each allele. We calculated the read count from the RNA-seq data for the reference and alternate alleles for *Col3a1* at

Chr1:45,378,353. In WT mice we find all reads (492 total) contain the reference T allele, whereas in Tsk2/+, we find 48% of reads (273/564 total reads) contain the WT (T) allele and 52% (291/564 total reads) contain the *Col3a1*^{Tsk2} (C33S) allele (T -> A; **Fig. 2C**). As a comparison, we show the intronic *Gulp1* SNP at Chr1:44,833,682 has significantly lower read coverage consistent with its intronic location (11-fold coverage in Tsk2/+ and 2-fold coverage in WT). The intronic *Gulp1* SNP also shows a distribution of reads consistent with heterozygosity in Tsk2/+ and with homozygosity in WT (**Fig. 2D**). These findings show that the *Col3a1*^{Tsk2} (C33S) locus is heterozygous as expected for the *Tsk2* mutation in these animals, and expression occurs equally from each of the alleles.

Because RNA-Seq only captures variation in the transcribed regions of the genome, and thus might miss an important genomic feature that is unique to *Tsk2*, we sequenced captured genomic DNA samples corresponding to the minimal linkage region from B6.Tsk2/+ heterozygotes and 101/H homozygous parental strain mice. Multiple DNA differences between the Tsk2/+ mouse and its parental 101/H strain were detected. A majority of the differences observed were accounted for by non-chromosome 1 repetitive DNA sequences such as LINE, SINE and retroviral elements contained within the *Tsk2* interval on chromosome 1. After filtering repetitive elements from the comparison, there were six single copy DNA sequence differences, of which three were confirmed to be Tsk2/+ specific (**Table 1**). Among these, there is a SNP that proved useful in demarcating the distal end of the *Tsk2* linkage interval (Chr1:46,268,651; **Table 1** and **Fig. 1**) as it was outside the linkage interval. This allowed us to eliminate the only other gene expressed at an appreciable level in the broader interval, *Slc39a10*. In addition, the GULP1 intronic SNP was confirmed and another SNP in an intron of *Col5a2* was observed. Both these latter SNPs are deemed unrelated to the phenotype, again because of

their low overall expression, and the lack of any influence on splicing or expression in the RNASeq results (**Fig. 2A,B; Supplementary Fig. 1**). Most important, however, the heterozygous T-to-A transversion in *Col3A1* at Chr1:45,378,353 was observed in the genomic sequence comparison, and was identical to the mutation identified by RNA-Seq. There were no additional variants that could be validated on the *Tsk2* chromosome within ~535,000 nucleotides proximal to the transcription start site of *Col3a1* gene or closer than 59,732 nucleotides distal of the end of the *Col3a1* 3' untranslated region (UTR). Selective resequencing of the 3'UTR likewise revealed no differences between Tsk2 and 101/H (not shown). Thus, this non-synonymous coding mutation is the most likely to be *Tsk2* by genomic assessment as well as by RNA sequencing.

Mice bearing Col3a1^{Tsk2} and Col3a1^{KO} are not viable

To prove that *Tsk2* is a single nucleotide change in the *Col3A1* coding region required a separate genetic test. Both *Tsk2/Tsk2* (Peters and Ball, 1986) and *Col3a1*-knockout (KO) (Liu *et al.*, 1997) homozygotes exhibit embryonic lethality, which is also seen in our mouse colony **(Table 2).** We therefore designed a genetic complementation test to determine if *Col3a1^{Tsk2}* (from Tsk2 mice) could complement and rescue the null allele for *Col3a1*. Conversely, this same cross would determine if any other gene in the *Col3a1*-homozygous knockout could serve to complement the *Tsk2* mutation.

Tsk2/+ x *Col3a1*-/+ mice were bred together, and 37 progeny mice (**Table 2**) were genotyped. If *Col3a1^{Tsk2}* (C33S) can complement the *Col3a1*-KO, then we would expect to find nine or ten *Col3a1^{Tsk2}*/*Col3a1*-KO compound heterozygotes. In fact, no viable compound heterozygotes were born (**Table 2, Supplementary Fig. 2**). The hybrid bearing *Tsk2/Col3a1*-

null chromosomes was not viable because the *Tsk2* gene on the *Tsk2*-bearing chromosome cannot 'complement' (rescue) the loss of the *Col3a1* gene on the *Col3a1*-KO chromosome. It bears only the allele of *Col3a1*^{Tsk2} at the *Col3a1* locus, which is insufficient to provide a functional COL3A1 protein that is missing in the *Col3a1*-KO. The *Col3a1*-null chromosome likewise cannot complement the *Tsk2* mutation: the remaining genes on the *Col3a1*-KO chromosome cannot prevent the death of (cannot 'complement') mice bearing the *Tsk2* chromosome, whereas hybrids carrying *Tsk2/Col3a1*-**wild type** alleles are alive, but fibrotic. In fact, having the *Tsk2* mutation is more damaging than not expressing COL3A1 at all, because while a few percent of *Col3a1*-KO homozygotes make it to birth, *Tsk2/Tsk2* homozygotes (and *Tsk2/Col3a1*-KO) never do, and whereas *Col3a1*/*Tsk2* mice are viable but small in stature and fibrotic, *Col3a1*-/+ heterozygotes are normal. Therefore, the mutation in Tsk2/+ mice lies within *Col3a1* and, when homozygous, is substantially more deleterious than a complete genetic deficiency of COL3A1.

Col3a1^{Tsk2} *induces increased COL1A1 and ECM production in vitro*

Because the compound heterozygous animals do not survive to accumulate fibrotic levels of ECM, a direct *in vivo* test for fibrosis is impossible, so we performed an '*in vitro* complementation' test, wherein we transfected mutant or wild-type *Col3a1* cDNA into *Col3a1*-KO fibroblasts, harvested from a *Col3a1*-KO/KO homozygote at birth. Using the production of COL1A1 as a measure of fibrosis (shown to be expressed at high levels in Tsk2/+ skin and used as a marker of fibrosis (Barisic-Dujmovic *et al.*, 2008; Christner *et al.*, 1998)), we assessed both protein and mRNA levels in fibroblasts that received DNA from a plasmid containing a single allele of a single *Col3a1* gene. In three independent experiments, COL1A1 protein was

significantly elevated after 48 hours of transfection with *Col3a1*^{Tsk2} relative to transfection with *Col3a1*^{WT} (**Fig. 3A**); mRNA for *Col1a1* was likewise increased in cells transfected with mutant *Col3a1*^{Tsk2} cDNA (**Fig. 3B**). Transfection efficiencies were equal in each of the experiments (**Fig. 3C**).

Given the observation that the production of a major indicator of fibrosis, COL1A1, is increased by the transfection of the *Col3a1*^{Tsk2} gene, we assessed the impact of the mutant gene genome-wide. RNA from the *Col3a1*^{Tsk2} and *Col3a1*^{WT} transfected *Col3a1*-KO fibroblasts and from four week-old Tsk2/+ and WT littermate skin was analyzed by cDNA microarray. Differentially expressed pathways between the two transfections were determined by Gene Set Enrichment Analysis (GSEA). Transfection of *Col3a1*^{Tsk2} results in significant enrichment of genes associated with fibrotic Gene Ontology (GO) terms including *basement membrane*, *extracellular matrix*, *integrin binding*, and *transmembrane receptor protein kinase activity* (**Fig 3D**; GSEA FDR < 5%). The biological processes observed in the skin of four 4-week old female Tsk2/+ mice relative to WT littermates also shows increases in genes associated with GO terms *extracellular matrix*, *integrin binding* and *basal lamina* (ZL, CB, KBL, CA, EPB, MLW, manuscript *in preparation*). The genes that significantly contributed to the GSEA pathway enrichment in the transfected fibroblasts were extracted from microarray data of the transfections, as well as from female Tsk2/+ and WT skin at 4 weeks of age (**Fig. 3E-F**), and were elevated both in the fibroblasts transfected with *Col3a1*^{Tsk2} and in Tsk2/+ mouse skin. These include those genes typically associated with fibrosis including CTGF, THY1, FBN1, the collagens, laminins, TGFB1, TGFBR1, ADAMTS family genes and MMP11. In addition, there was up-regulation in *Col3a1*^{Tsk2}-transfected fibroblasts and Tsk2/+ skin RNA of the VEGF-Receptors *FLT1* and *FLT4*, as well as genes associated with PDGF signaling (PDGFRB and

PDGFRL; **Fig.3F**). These data indicate that expression of the *Col3a1*^{Tsk2} gene alone can induce a substantial fibrotic gene expression program.

Taken together, this means that *Col3a1* and *Tsk2* are almost certainly one and the same gene. *Col3a1*^{Tsk2} (C33S) is therefore deemed a deleterious gain-of-function allele of *Col3a1*, and the *Col3a1*-KO is a classical loss-of-function allele. Mice thus need at least one copy of a functional, normal *Col3a1* gene.

Tsk2/+ mice have increased dermal COL3A1 protein accumulation

The behavior of *Col3a1* in Tsk2/+ mice could reveal the mechanism by which this mutation causes very substantial ECM fibrosis and very tight skin. We measured the level of COL3A1 protein by histological examinations of Tsk2/+ and WT littermate skin. Reticular fibers are composed primarily of COL3A1 and are a structural element in the skin, found in the panniculus carnosus and in the dermis. COL3A1 expression in skin from two-week old mice is high and declines after birth in WT littermates, but does not decline in the Tsk2/+ mice (**Fig. 4A**). As Tsk2/+ mice age, the reticular fibers thicken and become more pronounced compared to their WT littermates reflecting the accumulation of COL3A1. This finding was confirmed in skin from four-week old mice by western blots, which revealed that there is significantly more COL3A1 in the skin of Tsk2/+ mice compared to age- and sex-matched WT littermates (**Fig. 4B-C**). We propose that the excess COL3A1 protein we observe by several measures in Tsk2/+ mice is due to a trend for excess production of *Col3a1* mRNA (**Fig.2A**) rather than reduced degradation of the Col3 protein. Because the PIIINP fragment is removed from the majority of Col3 molecules before natural Col3 turnover degradation takes place in the tissue, mature COL3A1 from Tsk2 is identical to mature COL3A1 from WT mice, and its natural degradation

is unlikely to be affected by any changes in PIIINP. These data show there is an overall increased accumulation of mature COL3A1 protein in the Tsk2/+ mice; in addition, at least half of the type III procollagen and PIIINP trimers produced likely contain one or more strands bearing the *Tsk2* (C33S) mutation.

Discussion

Sequencing of both expressed RNAs and the genomic region in the Tsk2/+ interval, coupled with the genetic complementation study, prove that Tsk2/+ mice harbor a deleterious coding mutation in *Col3a1*, leading to an amino acid change (C33S) in the N-terminal region of the protein (PIIINP). This point mutation is consistent with those expected from ethylnitrosourea-induced mutagenesis, which generates random single-base-pair point mutations by direct alkylation of nucleic acids. The most common mutations are AT-to-TA and AT-to-GC changes (Cordes, 2005; Noveroske *et al.*, 2000); all three Tsk2-specific mutations identified here were T-to-A or T-to-C mutations. The Tsk2/+ allele is expressed in a 1:1 ratio with the WT by RNASeq indicating equal transcription and making a duplication event unlikely.

Effects of the *Tsk2* mutation include: 1) accumulation of COL3A1 protein *in vivo* over time; 2) induction and accumulation of COL1A1 protein *in vivo* and in *in vitro* expression models; 3) a more lethal phenotype than the homozygous genetic loss of *Col3a1*; and 4) a more lethal compound heterozygous phenotype than that of the homozygous gene knockout. The latter two characteristics indicate that $COL3A1^{Tsk2}$ (C33S) has a dominant prenatal lethal effect, although our *in vitro* complementation results suggest that the presence of COL3A1-C33S (or its mRNA) is not lethal to skin fibroblasts *per se*. A major function of the *Col3a1* gene is promoting blood vessel development (Liu *et al.*, 1997), which likely led to the lethality observed in the

complementation experiment. In the *Col3a1*-KO, a few mice are born with the homozygous deficiency, and these mice die of rupture of the major blood vessels (Liu *et al.*, 1997). The possibility that *Col3a1*^{Tsk2} mutation could directly induce a deleterious vascular phenotype in Tsk2/+ mice is intriguing; it is notable that genes encoding vascular features (*Flt1* and *Flt4*, genes for VEGF receptors) are significantly up-regulated in both *Col3a1*^{Tsk2}-transfected skin fibroblasts and in Tsk2/+ skin relative to WT (Fig 3G). It is possible that a complete *Col3a1* deficiency could be compensated by other collagens, but the *Col3a1*^{Tsk2} mutation is a deleterious gain-of-function, and the deposition of COL3A1-C33S may actively prevent other more benign collagen alternatives from functioning in the vasculature. Thus, our theory is that two doses of a damaging protein are worse than no expression of a normal one.

This is the first mutation in *Col3a1* that results in a gain-of-function phenotype instead of Ehlers-Danlos-like syndromes that are due to loss-of-function or antimorphic collagen-poor phenotypes. Ehlers-Danlos is a group of connective tissue disorders characterized by highly elastic, fragile but not fibrotic skin due to a defect in collagen synthesis (Nishiyama *et al.*, 2001). In addition, these patients have a significant risk for aneurism. Ehlers-Danlos syndrome has been associated with 337 mutations in COL3A1 (http://www.le.ac.uk/ge/collagen/), as well as mutations on COL1A1 and COL5A2. These mutations result in amino acid substitutions in the C terminus of the protein, RNA splicing alterations, deletions, or null alleles. Interestingly, in Ehlers-Danlos syndrome type IV (a very different disease than that observed in Tsk2/+ mice), studies have shown that patients bearing a mutated COL3A1 (compared to a null COL3A1) develop more severe disease and succumb to disease prematurely, whereas those with null COL3A1 were able to live a relatively normal life with limited disease (Leistritz *et al.*, 2011). Currently, all reported COL3A1 mutations result in decreased collagen protein secretion leading

to variably thinner skin and defects in the vasculature that are observed in these patients. In contrast to the mutations observed in Ehlers-Danlos, the Tsk2/+ mouse mutation results in thickened skin with no apparent evidence of aneurism. The mutation reported here occurs in the N-terminal PIIINP fragment of the protein, rather than the C-terminal region associated with Ehlers-Danlos.

The PIIINP molecule is a homotrimer with a molecular weight of approximately 42,000 daltons and comprises three domains: a cysteine-rich globular domain (Col 1) containing 79 amino acids with five intrachain disulphide bonds, a triple-helical domain (Col 3) with 12 amino acids and three interchain disulphide bonds, and a non-collagenous domain (Col 2) comprising of 39 amino acids ending with the N-telopeptide that forms a triple helical structure (Bruckner *et al.*, 1978). The mutation in *Col3a1*^{Tsk2} substitutes a serine for the cysteine in one of the five Col 1-domain cysteines involved in disulphide bonds (Bruckner *et al.*, 1978).

Features shared by Tsk2/+ mice and people with fibrotic diseases (scleroderma, liver fibrosis, kidney fibrosis) include the dysregulation of PIIINP (Abignano and Del Galdo, 2014; Del Galdo and Matucci-Cerinic, 2014; Majewski *et al.*, 1999; Quillinan *et al.*, 2014; Sondergaard *et al.*, 1997). The PIIINP fragment is a clinically validated biomarker of liver fibrosis (Leroy *et al.*, 2004; Rosenberg *et al.*, 2004) and scleroderma (Majewski *et al.*, 1999; Sondergaard *et al.*, 1997) and it has been used as a surrogate marker of fibrosis in clinical trials of potential SSc therapies (Denton *et al.*, 2009; Majewski *et al.*). Our finding of a point mutation in the protein that likely has a deleterious effect on PIIINP function is consistent with these clinical results and the fibrotic phenotype in the Tsk2/+ mouse.

Its high level in the sera of such patients may not merely be a benign biomarker. Support for this hypothesis derives from our *in vitro* complementation results showing that the presence

of COL3A1-C33S is sufficient to up-regulate the synthesis and secretion of COL1A1, consistent with the increased activity of the *Col1a1* promoter and excess production of COL1A1 in Tsk2/+ mice (Barisic-Dujmovic *et al.*, 2008; Christner *et al.*, 1998). It is likely that higher levels of or altered COL3A1 protein or PIIINP fragment also directly influence the composition and size of COL1A1/A2- and COL3A1-containing fibers, and that these features indirectly up-regulate TGF-β1 signaling, an important mediator of collagen production. A previous report from our laboratory has demonstrated increased dermal elastic fibers and TGF-β1 accumulation in the skin of Tsk2/+ mice beginning at two weeks of age, lending further support to our hypothesis (Long *et al.*, 2014). In addition, our gene expression analyses show that similar global impact of the *Col3a1*^{Tsk2} gene occurs both *in vitro* and *in vivo*, and in both settings, there are fundamental changes in the extracellular matrix and in fibroblasts due to the presence of this mutation. The hypothesis that *Col3a1*^{Tsk2} (or PIIINP^{Tsk2}) directly causes dermal fibrosis and scleroderma-like characteristics is attractive: it would likely be dominant within the heterozygote, as collagen III is a homotrimeric triple helix (Ramachandran and Kartha, 1955), and the gene product of the mutant chromosome could be expected to contribute to alteration of a majority of collagen helices even in the presence of 50% normal collagen (Strachan and Read, 1999).

Materials and Methods

All studies and procedures were approved by the Institutional Animal Care and Use Committee at Drexel University College of Medicine, and conducted in accord with recommendations in the "Guide for the Care and Use of Laboratory Animals" (Institute of Laboratory Animal Resources, National Research Council, National Academy of Sciences). Detailed methods are provided in the supplemental materials.

Competing interests: The authors state no conflict of interest.

Acknowledgments: We thank Dr. Paul Christner for providing the breeding pairs of the original Tsk2/+ mice, and Dr. Xianhua Piao at Harvard University for the *Col3a1*-KO mice.

Funding: This work was supported by a Scleroderma Foundation Grant and awards from the NIH (AR061384) and the Department of Defense (PR100338).

Author contributions: KBL and CMB bred and genotyped the B6.Tsk2 mice and all the derivative animals in this report; KBL, CMA, CMB and SSG conducted the histology on skin and transfections on fibroblasts; EPB was responsible for the design and interpretation of the research including the genetic analyses; ZL and MLW conducted the expression analyses and interpreted the results, VM conducted GSEA analysis, SGC constructed the plasmids containing the mutant Col3a1 cDNA; GDE, JE, RE, AA performed the genomic DNA capture and sequencing and interpreted these results; KBL, EPB, CMA and MLW wrote the paper.

References:

Abignano G, Del Galdo F (2014) Quantitating skin fibrosis: innovative strategies and their clinical implications. *Curr Rheumatol Rep* 16:404.

Artlett CM (2010) Animal models of scleroderma: fresh insights. *Current opinion in rheumatology* 22:677-82.

Asano Y, Stawski L, Hant F, *et al.* (2010) Endothelial Fli1 deficiency impairs vascular homeostasis: a role in scleroderma vasculopathy. *Am J Pathol* 176:1983-98.

Barisic-Dujmovic T, Boban I, Clark SH (2008) Regulation of collagen gene expression in the Tsk2 mouse. *J Cell Physiol* 215:464-71.

Bruckner P, Bachinger HP, Timpl R, *et al.* (1978) Three conformationally distinct domains in the amino-terminal segment of type III procollagen and its rapid triple helix leads to and comes from coil transition. *European journal of biochemistry / FEBS* 90:595-603.

Bunce M, O'Neill CM, Barnardo MC, *et al.* (1995) Phototyping: comprehensive DNA typing for HLA-A, B, C, DRB1, DRB3, DRB4, DRB5 & DQB1 by PCR with 144 primer mixes utilizing sequence-specific primers (PCR-SSP). *Tissue antigens* 46:355-67.

Christner PJ, Hitraya EG, Peters J, *et al.* (1998) Transcriptional activation of the alpha1(I) procollagen gene and up-regulation of alpha1(I) and alpha1(III) procollagen messenger RNA in dermal fibroblasts from tight skin 2 mice. *Arthritis Rheum* 41:2132-42.

Christner PJ, Peters J, Hawkins D, *et al.* (1995) The tight skin 2 mouse. An animal model of scleroderma displaying cutaneous fibrosis and mononuclear cell infiltration. *Arthritis Rheum* 38:1791-8.

Christner PJ, Siracusa LD, Hawkins DF, *et al.* (1996) A high-resolution linkage map of the tight skin 2 (Tsk2) locus: a mouse model for scleroderma (SSc) and other cutaneous fibrotic diseases. *Mamm Genome* 7:610-2.

Cordes SP (2005) N-ethyl-N-nitrosourea mutagenesis: boarding the mouse mutant express. *Microbiol Mol Biol Rev* 69:426-39.

Del Galdo F, Matucci-Cerinic M (2014) The search for the perfect animal model discloses the importance of biological targets for the treatment of systemic sclerosis. *Ann Rheum Dis* 73:635-6.

Denton CP, Engelhart M, Tvede N, *et al.* (2009) An open-label pilot study of infliximab therapy in diffuse cutaneous systemic sclerosis. *Ann Rheum Dis* 68:1433-9.

Gentiletti J, McCloskey LJ, Artlett CM, *et al.* (2005) Demonstration of autoimmunity in the tight skin-2 mouse: a model for scleroderma. *Journal of immunology* 175:2418-26.

Hocher B, Schwarz A, Fagan KA, *et al.* (2000) Pulmonary fibrosis and chronic lung inflammation in ET-1 transgenic mice. *American journal of respiratory cell and molecular biology* 23:19-26.

Leistritz DF, Pepin MG, Schwarze U, *et al.* (2011) COL3A1 haploinsufficiency results in a variety of Ehlers-Danlos syndrome type IV with delayed onset of complications and longer life expectancy. *Genet Med* 13:717-22.

Leroy V, Monier F, Bottari S, *et al.* (2004) Circulating matrix metalloproteinases 1, 2, 9 and their inhibitors TIMP-1 and TIMP-2 as serum markers of liver fibrosis in patients with chronic hepatitis C: comparison with PIIINP and hyaluronic acid. *Am J Gastroenterol* 99:271-9.

Liu X, Wu H, Byrne M*, et al.* (1997) Type III collagen is crucial for collagen I fibrillogenesis and for normal cardiovascular development. *Proceedings of the National Academy of Sciences of the United States of America* 94:1852-6.

Long KB, Artlett CM, Blankenhorn EP (2014) Tight skin 2 mice exhibit a novel time line of events leading to increased extracellular matrix deposition and dermal fibrosis. *Matrix Biol*.

Majewski S, Wojas-Pelc A, Malejczyk M*, et al.* (1999) Serum levels of soluble TNF alpha receptor type I and the severity of systemic sclerosis. *Acta Derm Venereol* 79:207-10.

Maurer B, Busch N, Jungel A*, et al.* (2009) Transcription factor fos-related antigen-2 induces progressive peripheral vasculopathy in mice closely resembling human systemic sclerosis. *Circulation* 120:2367-76.

Nishiyama Y, Nejima J, Watanabe A*, et al.* (2001) Ehlers-Danlos syndrome type IV with a unique point mutation in COL3A1 and familial phenotype of myocardial infarction without organic coronary stenosis. *J Intern Med* 249:103-8.

Noveroske JK, Weber JS, Justice MJ (2000) The mutagenic action of N-ethyl-N-nitrosourea in the mouse. *Mamm Genome* 11:478-83.

Peters J, Ball ST (1986) Tight Skin 2 (Tsk2). *Mouse News Letters*:91-2.

Quillinan NP, McIntosh D, Vernes J*, et al.* (2014) Treatment of diffuse systemic sclerosis with hyperimmune caprine serum (AIMSPRO): a phase II double-blind placebo-controlled trial. *Ann Rheum Dis* 73:56-61.

Ramachandran GN, Kartha G (1955) Structure of collagen. *Nature* 176:593-5.

Richard V, Solans V, Favre J*, et al.* (2008) Role of endogenous endothelin in endothelial dysfunction in murine model of systemic sclerosis: tight skin mice 1. *Fundamental & clinical pharmacology* 22:649-55.

Rosenberg WM, Voelker M, Thiel R*, et al.* (2004) Serum markers detect the presence of liver fibrosis: a cohort study. *Gastroenterology* 127:1704-13.

Siracusa LD, McGrath R, Ma Q*, et al.* (1996) A tandem duplication within the fibrillin 1 gene is associated with the mouse tight skin mutation. *Genome Res* 6:300-13.

Sondergaard K, Heickendorff L, Risteli L*, et al.* (1997) Increased levels of type I and III collagen and hyaluronan in scleroderma skin. *Br J Dermatol* 136:47-53.

Strachan T, Read AP (1999) *Human Molecular Genetics.*, 2nd edn. Wiley-Liss, New York.

Yamamoto T, Takagawa S, Katayama I*, et al.* (1999) Animal model of sclerotic skin. I: Local injections of bleomycin induce sclerotic skin mimicking scleroderma. *J Invest Dermatol* 112:456-62.

Tables

Nucleotide position on chr 1 (mm9)	Genotype of Tsk2/+	Genotype of B6	Genotype of 101/H	Present in Other Strains?	Potential candidate for *Tsk2*?	Protein or mRNA containing substitution
SNP found by RNA-Seq						
44,675,490	A	T	T	No	No, outside interval	*Gulp1* Intron
44,833,682*	C	T	T	No	YES	*Gulp1*Intron
45,378,353*	A	T	T	No	YES	COL3A1 Exon (C33S)
45,432,389	C	G	Nd	Yes	No	*Col5a2* 3'UTR
45,441,243	C	A	C	No	No, in 101/H	*Col5a2* Intron
45,860,529	G	A	G	Yes	No	*Wdr75* Intron
45,874,790	T	C	T	Yes	No	*Wdr75* Intron
45,875,728	C	T	C	Yes	No	*Wdr75* Exon
45,880,257	CG	AC	CG	No	No, in 101/H	WDR75 Exon
46,872,610	T	G	Nd	Yes	No	*Slc39a10* Intron
46,874,711	C	T	C	Yes	No	*Slc39a10* Intron
46,939,340	T	C	T	Yes	No	BC040767 Intron
46,939,624	A	G	Nd	Yes	No	BC040767 Intron
SNP found by 454 Sequencing						
44,833,682*	C	T	T	No	YES	*Gulp1*Intron
45,378,353*	A	T	T	No	YES	COL3A1 Exon (C33S)
45,465,923	A	T	T	No	YES	*Col5a2* Intron
46,124,856	A	G	A	Yes	No	*Dnahc76* Intron
46,124,857	A	C	T	Yes	No	*Dnahc76* Intron
46,268,651	C	T	T	No	No, outside interval	*Dnahc76* Intron

Table 1. Nucleotide changes between Tsk2/+ mice and 101/H or B6 mice

presence in other non-fibrotic strains (http://phenome.jax.org/) or individually verified by a All single-copy nucleotide changes found by RNA-Seq or 454 sequencing were checked for their phototyping assay (Bunce *et al.*, 1995) and/or resequencing to confirm the single nucleotide change. SNP that were ruled out by one of these assays are considered not to be potential candidates for *Tsk2*. When known, genotypes shown for 101/H are from RNA-Seq, 454 sequencing or phototyping. Nd = not determined. *, seen in both assays.

A.	Genotype and phenotype of progeny		
Parents	Tsk2/+ (Tight skin)	WT / WT (Normal skin)	Tsk2/Tsk2 (lethal)
Tsk2/+ x Tsk2/+	22	21	0
	$Col3a1^{+}/ Col3a1^{-}$	$Col3a1^{+}/ Col3a1^{+}$	$Col3a1^{-}/ Col3a1^{-}$
$Col3a1^{-/+}$ x $Col3a1^{-/+}$	16	13	3

B.	Genotype and phenotype of progeny			
Parents	$WT/Col3a1^{+}$ (Normal skin)	$Tsk2/Col3a1^{+}$ (Tight skin)	$WT/Col3a1^{-}$ (Normal skin)	$Tsk2/Col3a1^{-}$
Tsk2/+ x $Col3a1^{-/+}$	12	10	15	0

Table 2. Progeny born from *Col3a1*-deficient, *Col3a1*-sufficient, and Tsk2/+ mice.

All progeny were assessed for chromosome 1 markers (SNPS and microsatellites) that characterize the origin of the tested allele (*Tsk2* or *Col3a1*).

Table 2A (top) shows the number of mice born of each genotype and phenotype from Tsk2/+ x Tsk2/+ or $Col3a1^{-/+}$ x $Col3a1^{-/+}$ parents.

Table 2B (bottom) shows the number of mice born of each genotype and phenotype from Tsk2/+ x $Col3a1^{-/+}$ parents; note there are no compound heterozygotes (*Tsk2/Col3a1*-) born from this mating.

Figure Legends:

Figure 1. *Tsk2* lies between and not including 44.67 – 46.27Mb Mb on chromosome 1

(**A**) The *Tsk2* interval was narrowed by genotyping back-crossed mice on the B6 and B6.chr 1-A/J backgrounds. Grey bars (101/H) depict the original parental strain, bearing *Tsk2*. White bars depict the B6 genome. Indefinite areas between typed markers are grey. Recombinants A – G bear novel recombination sites. The phenotypes are tight (T – Tsk2/+) or loose (L – WT).

(**B**) With the use of new markers (arrows, see text), the current interval comprises *Col3a1, Col5a2, Wdr75, Slc40a1,* part of *Gulp1*, and part of *Dnahc7b*; the five latter genes do not have coding region mutations. The elements of the *Gulp1* gene above 44.67 Mb are excluded by the recombination in mouse F, and *Dnahc7b* below 46.27 is excluded by Mouse G.

Figure 2. *Col3a1* is the only interval gene expressed at high levels in the skin of Tsk2/+ mice.

(**A**) This graph shows gene expression for the seven *Tsk2* interval genes, as determined from the RNA-Seq abundance results.

(**B**) Heat map for seven *Tsk2* interval genes detected as transcripts in RNA-Seq.

(**C** + **D**) Distribution of nucleotide calls in heterozygous Tsk2/+ and homozygous WT mice for *Col3a1* and *Gulp1*.

Figure 3. Mouse Col3a1-KO fibroblasts transfected with mutant *Col3a1*^{Tsk2} express a more fibrotic protein profile than *Col3a1*^{WT} transfectants.

(A) Culture supernatants assayed by Western blot for COL1A1. *Col3a1*^{Tsk2} transfectants produced 34% more COL1A1 than *Col3a1*^{WT} ($p<0.001$) or mock transfectants ($p<0.0001$).

(B) *Col1a1* mRNA is more highly expressed in *Col3a1*-KO fibroblasts transfected with *Col3a1*^{Tsk2} than with *Col3a1*^{WT} ($p<0.0001$).

(C) There was no significant difference in efficiency of plasmid transfection between *Col3a1*^{Tsk2} and *Col3a1*^{WT} .

(D) *Col3a1*$^{-/-}$ fibroblasts transfected with *Col3a1*^{Tsk2} show a significant increase in Gene Ontology (GO) terms associated with fibrosis.

(E) Expression of the genes that contributed most to the ECM enrichment results in in *Col3a1*^{Tsk2} *vs. Col3a1*^{WT} transfected mice fibroblasts or in 4-week old female Tsk2/+ *vs.* WT mice.

(F) Expression of genes that contributed to integrin binding term.

(G) Expression of genes that contributed to transmembrane receptor protein kinase activity term.

Figure 4. Tsk2/+ mice have increased reticular fiber accumulation and COL3A1 in skin compared WT littermates.

(A) Reticular fiber staining was performed on mice of the indicated ages (2-23 weeks). Stars mark the location of the epidermis. COL3A1 fibers (black staining) are much thicker and more abundant at each life stage in Tsk2/+ than in WT. Fibers were found to be especially pronounced in the panniculus carnosus region of the tissue; increased staining of COL3A1 in the dermis was also noted. The dermal reticular fibers are composed entirely of COL3A1 protein as this protein is receptive to silver impregnation, and they are increased in Tsk2/+ mice. All images were taken at 200X magnification.

(B + C) Skin lysates were analyzed for COL3A1 content (both bands) relative to beta-actin (not shown) by western blot analysis. Tsk2/+ mouse skin has significantly more COL3A1 protein than WT mouse skin ($p=0.0025$, ANOVA).

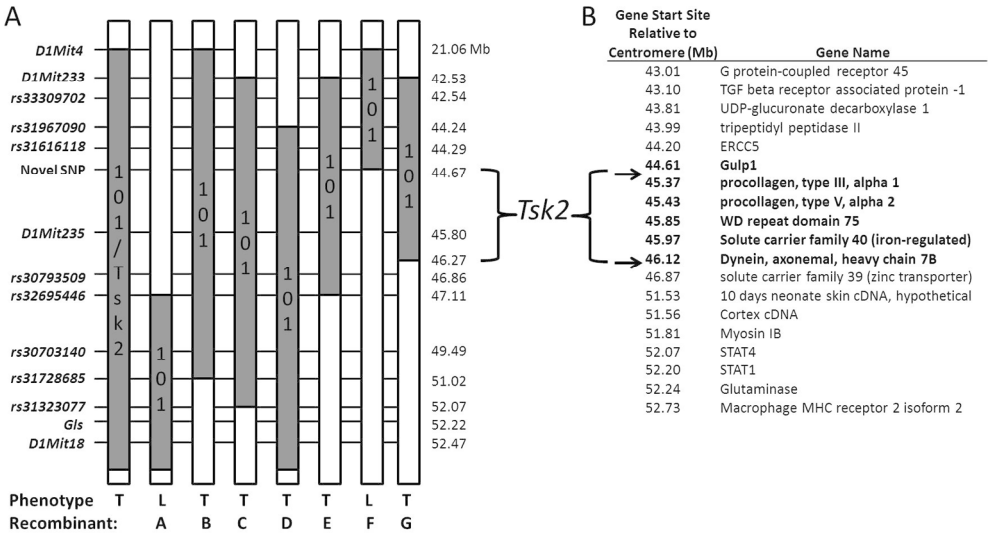

Figure 1
301x167mm (150 x 150 DPI)

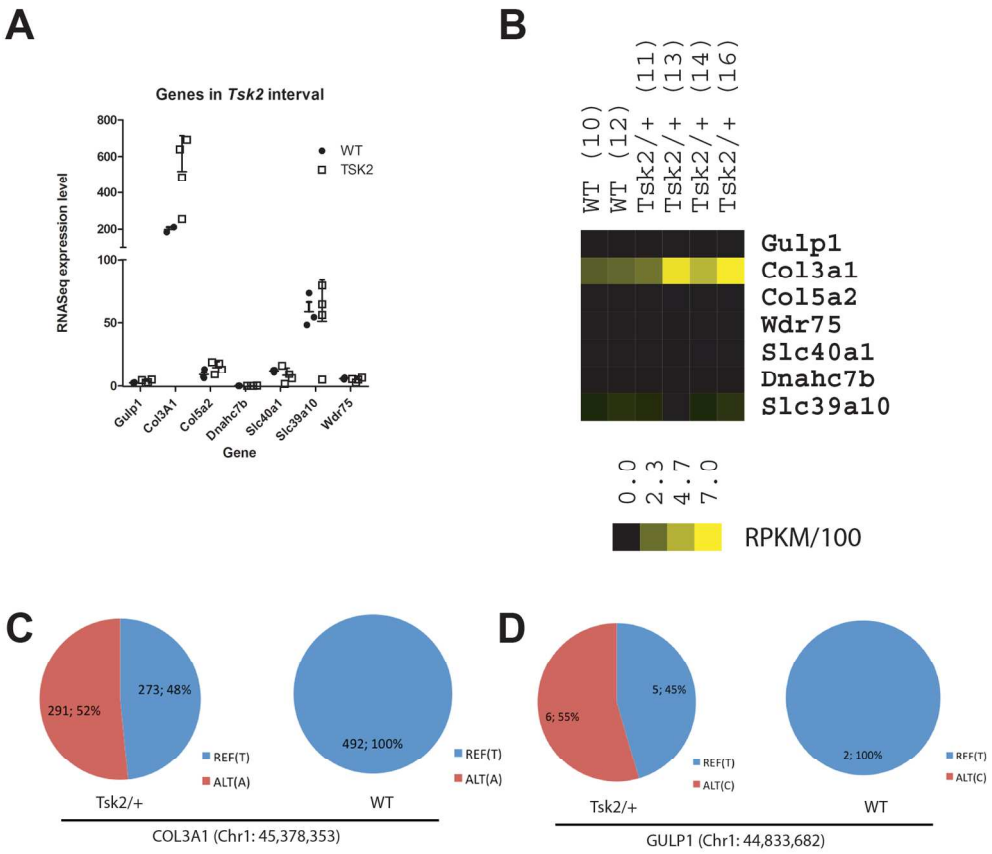

Figure 2
155x134mm (300 x 300 DPI)

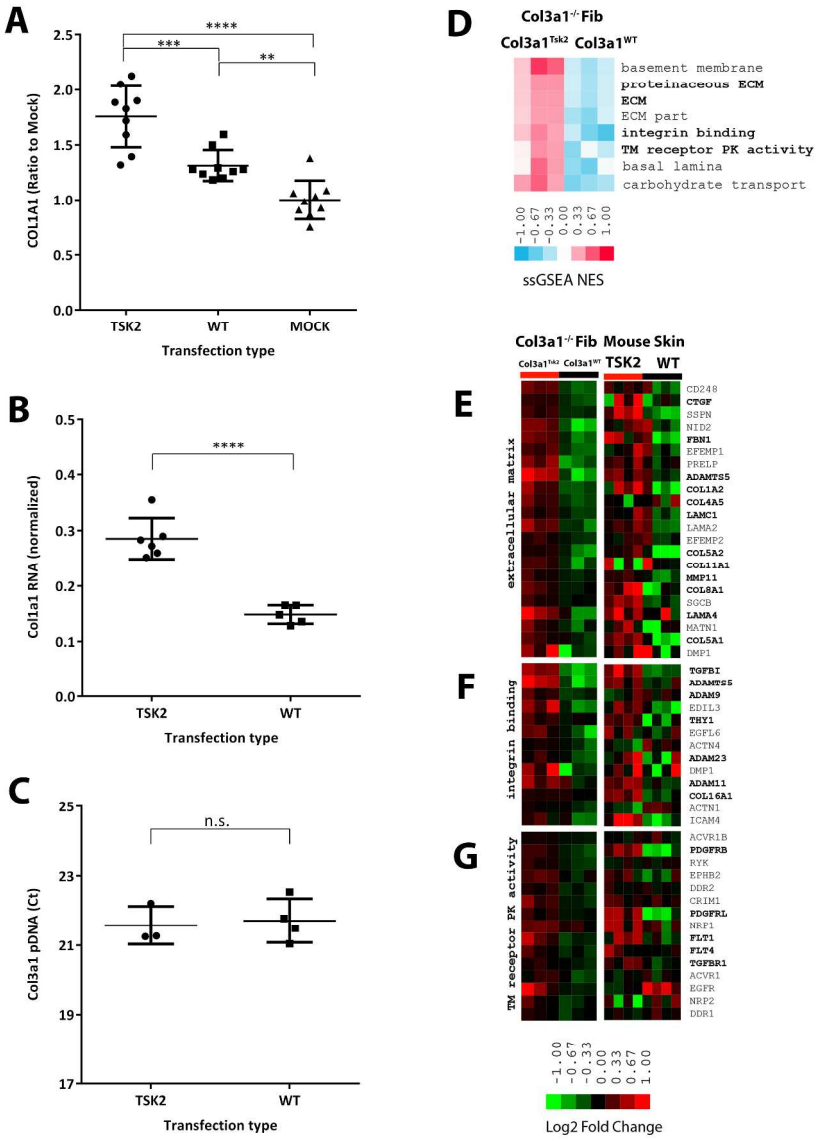

Figure 3. Mouse Col3a1-KO fibroblasts transfected with mutant Col3a1Tsk2 express a more fibrotic protein profile than Col3a1WT transfectants.

(A) Culture supernatants assayed by Western blot for COL1A1. Col3a1Tsk2 transfectants produced 34% more COL1A1 than Col3a1WT ($p<0.001$) or mock transfectants ($p<0.0001$).
(B) Col1a1 mRNA is more highly expressed in Col3a1-KO fibroblasts transfected with Col3a1Tsk2 than with Col3a1WT ($p<0.0001$).
(C) There was no significant difference in efficiency of plasmid transfection between Col3a1Tsk2 and Col3a1WT .
(D) Col3a1-/- fibroblasts transfected with Col3a1Tsk2 show a significant increase in Gene Ontology (GO) terms associated with fibrosis.
(E) Expression of the genes that contributed most to the ECM enrichment results in in Col3a1Tsk2 vs. Col3a1WT transfected mice fibroblasts or in 4-week old female Tsk2/+ vs. WT mice.

(F) Expression of genes that contributed to integrin binding difference.
(G) Expression of genes that contributed to transmembrane receptor protein kinase activity difference.

265x378mm (300 x 300 DPI)

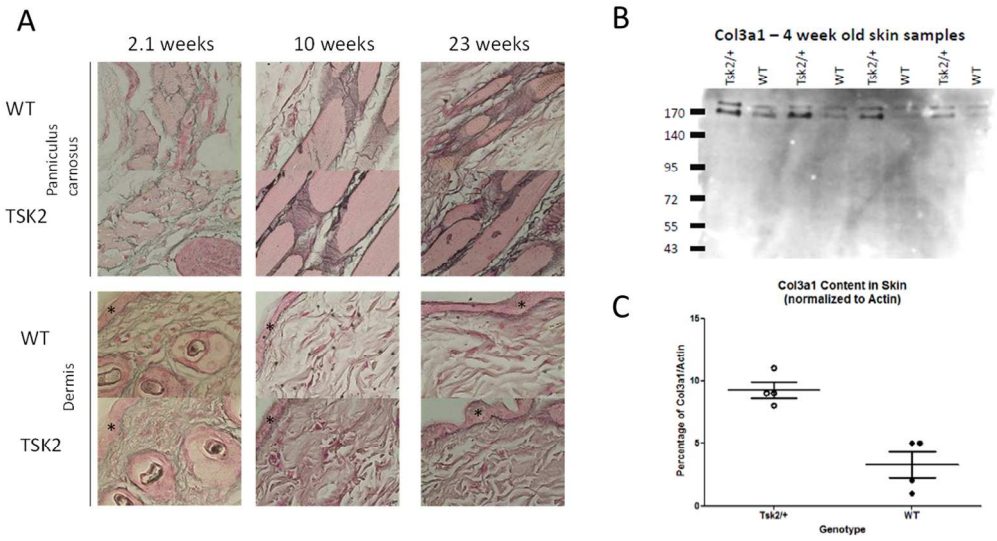

Figure 4. Tsk2/+ mice have increased reticular fiber accumulation and COL3A1 in skin compared WT littermates.

(A) Reticular fiber staining was performed on mice of the indicated ages (2-23 weeks). Stars mark the location of the epidermis. COL3A1 fibers (black staining) are much thicker and more abundant at each life stage in Tsk2/+ than in WT. Fibers were found to be especially pronounced in the panniculus carnosus region of the tissue; increased staining of COL3A1 in the dermis was also noted. The reticular fibers are composed entirely of COL3A1 protein as this protein is receptive to silver impregnation, and they are increased in Tsk2/+ mice. All images were taken at 200X magnification.
(B + C) Skin lysates were analyzed for COL3A1 content (both bands) relative to beta-actin (not shown) by western blot analysis. Tsk2/+ mouse skin has significantly more COL3A1 protein than WT mouse skin

Supplemental Materials and Methods

Animal husbandry: Breeding pairs of Tsk2/+ mice were obtained from Dr. Paul Christner at Jefferson University and housed at Drexel University College of Medicine. Tsk2/+ mice were serially backcrossed the C57Bl/6J (B6) background. Recombinant B6.Tsk2/+ mice were bred to B6.chr 1-A/J mice (Jackson Laboratory, Bar Harbor, ME) and the resulting B6.Tsk2/+ F1 mice were backcrossed to B6.chr 1-A/J mice. Wild-type littermates were used as controls.

DNA isolation: Tail snips were taken from weanlings, and DNA was isolated from the tissue using a GenElute Mammalian Genomic DNA Miniprep Kit (Sigma-Aldrich, St. Louis, MO), following the manufacturer's protocols. DNA was diluted to a working concentration of 40 ng/μl.

Microsatellite and SNP typing: 120 ng of DNA per reaction was used when amplifying microsatellites by polymerase chain reaction (PCR). PCR products were separated by electrophoresis on a 3% agarose gel. .100 ng of DNA per reaction was used for SNP typing, as previously described (Bunce *et al.*, 1995), to map the boundaries of the recombinations. Microsatellite *D1Mit233*, sequence forward 5'-TAGACCCATCACTTTCCAAG-3' and reverse 5'- ACTGGCTAAAGTA TCCTAGAAAGGG-3' was run at an annealing temperature of 49 ^{o}C. Microsatellites *D1Mit235* sequence forward 5'-CACCTGGCTAAGAGACCATACC-3' and reverse 5'-GCCTCCACTACCACCATCTC-3'; a microsatellite in the *Glutaminase* gene (*Gls*) sequence forward 5'-TGTGCACTT GAGAATTTTGCTT-3' and reverse 5'-CCCACATACTGGACCTACCC-3'; and *D1Mit18* sequence forward 5'-TCTGGTTCCAGGCTTGATTC-3'and reverse 5'-TCACAAGTGA GGCTCCAGG-3' were run at an annealing temperature of 50 ^{o}C.

SNP typing: Specific locations of polymorphisms between B6 (which is very similar to

101/H) and A/J were determined using Mouse Genome Informatics (www.informatics.jax.org), and primers for SNP typing were designed using Primer 3 online software (http://frodo.wi.mit.edu) and synthesized by Integrated DNA Technologies (www.idtdna.com). PCR products were separated by electrophoresis on a 1.5% agarose gel.

Complementation analysis with Col3a1$^{-/+}$ mice: Col3a1$^{-/+}$ mice (bearing one allele containing *Col3a1* and one allele where *Col3a1* has been knocked out) were received as a generous gift from Dr. Xianhua Piao at Harvard Medical School. Tsk2/+ mice were crossed to Col3a1$^{-/+}$ mice to verify that the SNP in *Col3a1* is *Tsk2*, as Tsk2/Tsk2 homozygous mice are not viable, and if *Tsk2* is located in *Col3a1*, then *Tsk2/Col3a1*$^{-}$ mice will not be viable. The resulting first generation of the cross was genotyped by PCR for Tsk2/+ using the microsatellites listed above and primers specific to *Col3a1* or the inserted neomycin cassette (see supplemental material). ***In vitro* assessment of fibrogenesis by *Col3a1*^{Tsk2}:** We constructed a plasmid harboring the Col3a1^{Tsk2} allele by introducing the Tsk2 T→ A mutation into a wild-type Col3a1 clone (pCMV6-Kan/Neo; Origene). Skin explants of newborn mice from [Col3a1KO/+ x Col3a1KO/+] litters were harvested and cultured *in vitro* and genotyped for KO/KO homozygosity One *Col3a1*-KO line was transfected with plasmid containing 5 μg of either the *Col3a1*^{Tsk2} or *Col3a1*^{WT} gene, using the calcium-phosphate co-precipitation method for 3 h and then treated with 10% glycerol/PBS for 2 min, washed and cultured for 48 h as previously described (Artlett *et al.*, 1998). Supernatants were retained and cell lysates were harvested directly from the dish at 48 hours.

RNA isolation and real-time PCR. RNA was isolated from fibroblasts using a RNA isolation kit from Clontech (Mountain View, CA) following manufacturer's instructions. cDNAs were synthesized from 2.0 μg of total RNA using an High Capacity cDNA Reverse Transcription

kit (Applied Biosystems, Foster City, CA). Primers for quantitative real-time PCR (qRT-PCR) were designed and synthesized as described for SNP typing. Relative quantification of all products was measured using SYBR Green chemistry (Applied Biosystems, Foster City, CA). Expression was normalized to the geometric mean of the expression of house-keeping genes actin and β2-microglobulin, and relative expression of each gene was calculated using the ΔCt formula. The fold increase or decrease in *Col3a1*^{Tsk2} or *Col3a1*^{WT} transfected cells was calculated as a ratio over the expression in mock transfected controls (ΔΔCt). For primer sequences, see supplemental material.

RNA-Seq – Sample RNA preparation: Total RNA was prepared from three WT and four Tsk2/+ mice skin biopsies using Qiagen RNeasy Fibrous Tissue Mini Kit. The RNA integrity (RIN) was determined by Agilent Bioanalyzer Nano chip. All samples used for this study had RIN scores of 7 or greater (Erik Garrison, 2012).

RNA-Seq: RNA-seq sequencing libraries were prepared for the seven samples using NuGEN Ovation RNA-Seq System (NuGen, San Carlos, CA). Libraries were multiplexed and sequenced on an Illumina HiSeq 2000 platform to obtain 16.7-50.9 million 50 bp paired-end reads per sample. The raw reads were aligned to the reference mouse genome (MM9 assembly) using Tophat software with default parameters (Trapnell *et al.*, 2012a; Trapnell *et al.*, 2012b). Supplemental Figure 1 shows RNA-Seq read coverage for three interval genes.

Variant calling and SNP identification: In order to identify coding region and intronic genetic variation we analyzed the data using Freebayes software (Erik Garrison, 2012). The following parameters were used: "freebayes –r 1:44200000..47100000 –f MM9.fai –b <tophat_aligned_bamfile> -v <output_SNP.vcf>" We compared the WT and Tsk2/+ mice to the MM9 reference genome strain (B6).

454 Sequencing: Samples were captured and amplified as described in the Roche Nimblegen sequence capture manual (Version 1.0). Based on qPCR analysis, control capture regions showed an enrichment range of 14 to 50 fold for the samples tested. Titanium general libraries were prepared from the captured DNAs from two 101/H mice and two Tsk2/+ mice using 5000 ng of DNA as described in the GS FLX Titanium, General Library Preparation Method Manual, October, 2008 (Roche Molecular Systems, Nutley, NJ). Enriched captured fragments binding to beads, titration, emulsion PCR, emulsion breaking, bead enrichment, and pico-titer plate-based pyrosequencing were performed as described in GS FLX Titanium emPCR and Sequencing Protocols, October, 2008. Sequence capture array probes were designed by Roche Nimblegen using the mouse genome sequence between 44,241,286 and 47,116,890 on chromosome 1 of mouse genome (mm9). Probes were designed corresponding to 56.3% of the linkage region, however in practice a larger area was captured due to the overhang of the larger fragments (~600bp) being used. Probes could not be designed to the remaining 43.7% due to it being composed of repetitive sequence.

Multiplexed 454 sequenced reads were assembled using Newbler v2.6 with scaffolding against the same chromosome region that the probes were derived from. Separate assemblies were created for each of the four mice by MID number, and lists of variants for each mouse were obtained from the assembler output. Variants were filtered by quality (phred scores >30), depth of coverage (>13 reads), and heterozygosity (>20% of reads differed from the reference). Variants were mapped to exons, introns, and intergenic regions within the linkage region and set analysis between the 204 and 101 lineages were performed using custom perl scripts. Sets were examined for variants between the 204 and 101 line, and between all samples and the reference to identify heterozygous SNPs uniquely present in the tsk2 line.

Complementation analysis with Col3a1$^{-/+}$ mice: WT forward (common) primer 5'-CTTCTCACCCTTCTTCATCCC-3', WT reverse primer 5'-AGCCTGTTCAATCGGTACC-3', and neomycin reverse primer 5'- GCTATCAGGACATAGCGTTGG-3'. A second primer set was used to verify the knock out, WT forward (common) primer 5'-AGGGCCTTCAGAGGATTTTC-3', WT reverse primer 5'-CCATCCCCTCAGCAGTAAA-3', and the neomycin reverse 5'-GFCCAGAGGCCACTTGTGTAG-3'. Reactions were run at an annealing temperature of 63 ^{o}C and PCR products were separated by electrophoresis on a 2% agarose gel.

Real-time PCR. For primer sequences, the following were used: Col1a1 F: ACTGGTACATCAGCCCGAAC; COL1A1 R: CTACGCTGTTCTTGCAGTGATAG; COL3A1 F: CTGCTCGGAACTGCAGAGAC; COL3A1 R: CCACCAGTGCTTACGT; ACTIN F: CAGCTTCTTTGCAGCTCCTT; ACTIN R:CACGATGGAGGGGAATACAG; B2MG F: TCGCTCGGTGACCCTAGTCTTT; and B2MG R: ATGTTCGGCTTCCCATTCTCC. The fold increase or decrease in *Col3a1*^{Tsk2} or *Col3a1*^{WT} transfected cells was calculated as a ratio over the expression in mock transfected controls (ΔΔCt). Transfection efficiency of plasmids into the *Col3a1*-KO fibroblasts was determined from samples of plasmid-derived DNA taken from the cell lysates (5 µl) amplified with the Col3a1 primers.

DNA microarray hybridization and data analysis: RNA was isolated as above and used to create cDNA for the microarray analyses. Samples were amplified and labeled using the Agilent Low Input Linear Amplification kit (Agilent Technologies, Santa Clara, CA) and were hybridized against Universal Mouse Reference (UMR) (Strategene, La Jolla, CA) to Agilent Whole Mouse Genome arrays (G4122F) (Agilent Technologies, Santa Clara, CA) in a common reference based design. Microarrays were hybridized and washed in accordance with

manufacturer's protocols and scanned using a dual laser GenePix 4000B scanner (Axon Instruments, Foster City, CA). The pixel intensities of the acquired images were then quantified using GenePix Pro 5.1 software (Axon Instruments, Foster City, CA). All microarrays were visually inspected for defects or technical artifacts, and poor quality spots were manually flagged and excluded from further analysis.

The data were loaded to the UNC Microarray Database (UMD). Raw data is available from NCBI GEO at accession number GSEXXXX (submission in process).

Pre-processing based on GenePattern [1] modules was run with default parameters unless noted otherwise. Non-centered expression data for relevant samples were pulled down. Missing values were imputed via ImputeMissingValuesKNN module with k=5. Expression values for probes were collapsed to unique gene symbols via CollapseDataset module using Agilent mouse genome annotation file from GSEA FTP site. Expression data were median-centered by genes in Cluster 3.0 [2] and used to create a class label file to define phenotype classes (e.g. Tsk2 vs. WT) via ClsFileCreator module.

Pre-processed expression data were used to identify differentially expressed functional terms between 2 classes of samples. This was done via Gene Set Enrichment Analysis (GSEA) [3, 4] module using permutations by gene set. GSEA was run vs. the entire Gene Ontology (GO) [5] database of gene sets. In order to visualize differentially expressed GO gene sets on a single sample basis, single sample GSEA (ssGSEA) [6] was run via ssGSEAProjection module vs. GO database of gene sets. Raw ssGSEA enrichment scores were normalized by dividing by the absolute maximum ssGSEA enrichment score and median-centering rows in Cluster 3.0 thus generating ssGSEA normalized enrichment scores (NES). ssGSEA NES for significant GO gene

sets (GSEA FDR<5% between 2 classes of samples) were pulled down and visualized in TreeView [7].

Western blot analysis of *in vitro* COL3A1 and COL1A1 expression and *in vivo* COL3A1 expression: Collagen content was determined by western blot analysis. *In vitro:* culture supernatant was collected. *In vivo*: skin was homogenized in RIPA buffer (Sigma-Aldrich, St Louis MO) using a glass homogenizer and centrifuged at 8,000 x g for 10 minutes at 4 ^{o}C to pellet debris. Total protein was measured with a Bradford assay (Sigma-Aldrich, St Louis MO). Approximately 20 ul of culture supernatant or 75 µg of protein from skin lysate was added to reducing buffer, boiled, and then loaded onto an 8% SDS gel. After separation, proteins were transferred to a polyvinylidene fluoride membrane. The membrane was blocked in 5% nonfat milk in Tris buffered saline and then probed with goat anti-COL3A1 (#sc-8781) or goat anti-COL1A1 (#sc-28657) from Santa Cruz Biotechnology, Inc, Santa Cruz, CA, or rabbit anti-β-Actin (#4967, Cell Signaling Technologies, Boston, MA) and then probed with a secondary antibody, donkey anti-goat (#705-035-003, Jackson ImmunoResearch Laboratories, West Grove, PA) or goat anti-rabbit (#111-035-003, Jackson ImmunoResearch) respectively, and developed using SuperSignal West Dura ECL reagent (Thermo Scientific Inc, Rockford, IL). Band intensities were measured using ImageQuant TL Software (GE Healthcare Life Sciences).

Reticular fiber staining: Reticular fibers were stained using the Chandler's Precision Reticular Fiber Stain kit (American Master*Tech, Lodi CA) according to the manufacturer's protocol.

Statistics: A two-tailed student's t-test or a one-way ANOVA was used to determine statistical significance of collagen protein expression, as noted.

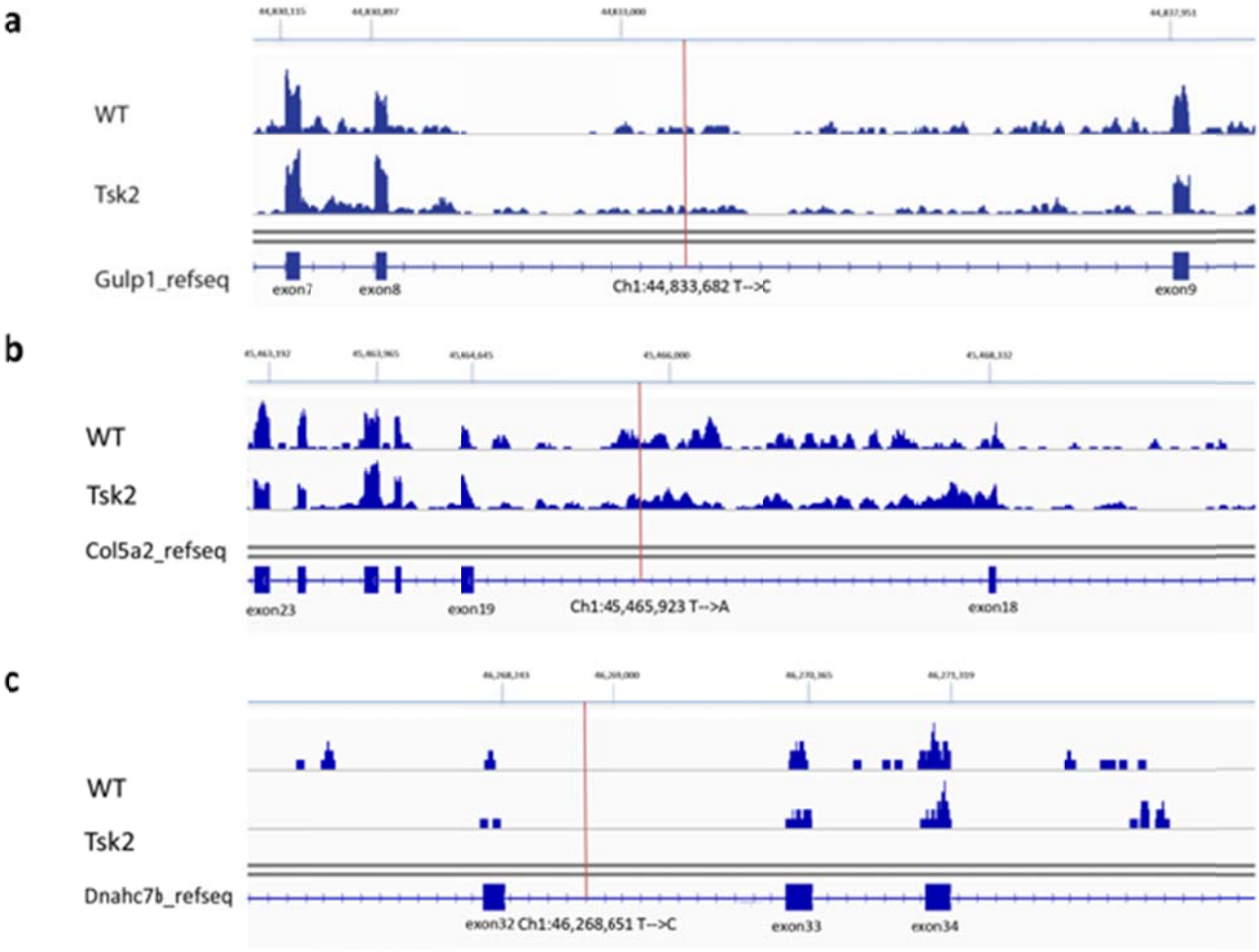

Supplemental Figure 1. RNA-Seq read coverage for *Gulp1, Col5a2* and *Dnahc7b* exons flanking the intronic *Tsk2*-specific SNPs.

Exonic coverage is similar between WT and Tsk2/+ animals and CuffDiff analysis for differentially spliced messages did not detect differential splicing. The coverage graphs are

generated by BEDTools and visualized in Integrative Genomics Viewer. Numbers are the chromosome 1 location in nucleotides. The red bars indicate the locations of the SNPs. (**A**) Reads coverage near the *Gulp1* SNP. (**B**) Reads coverage near the *Col5a2* SNP. (**C**) Reads coverage near the *Dnahc7b* SNP.

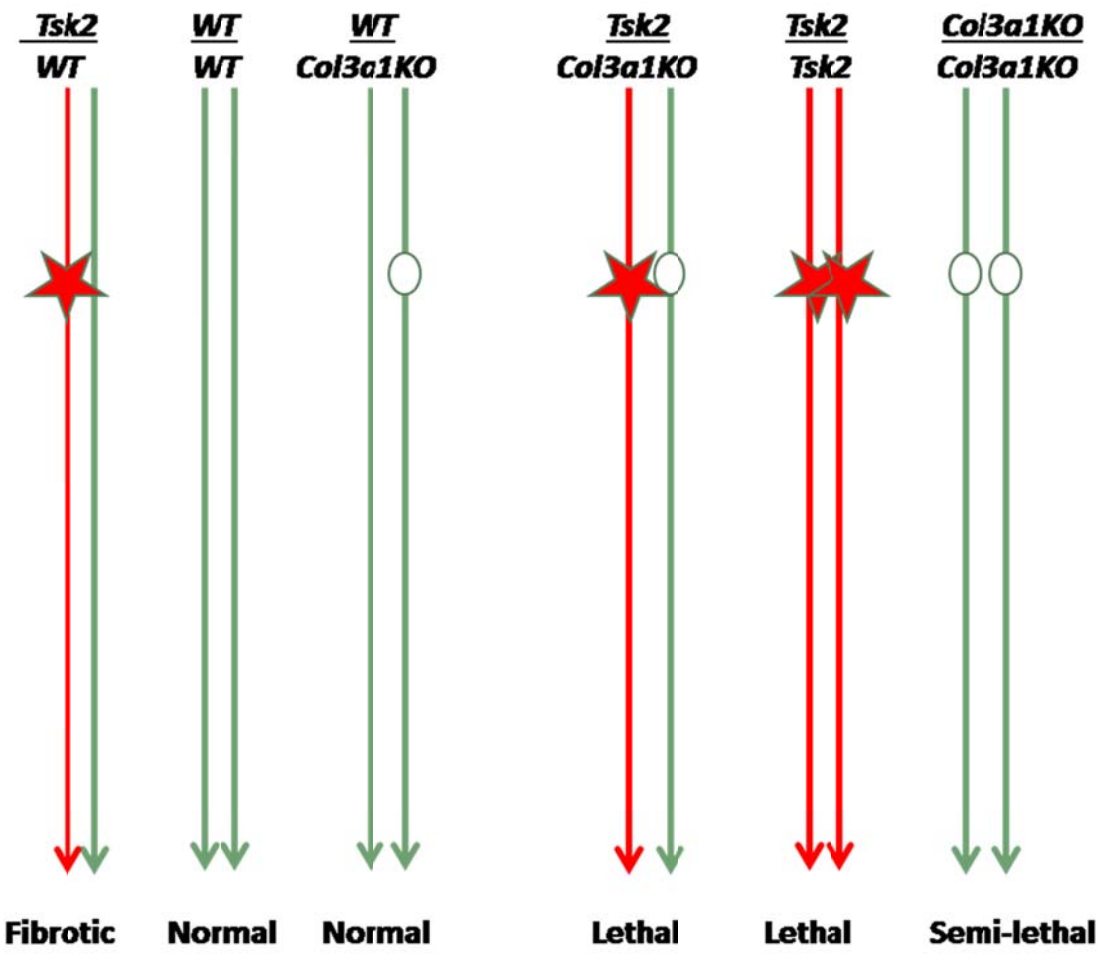

Supplementary Figure 2. Complementation analysis for *Col3a1* and *Tsk2*.

The six possible genotypes generated by intercrossing (Tsk2/+ x *Col3a1*-KO/+) F1 mice are shown, with the three definitive genotypes shown on the right. If the *Tsk2* gene is identical to the *Col3a1* gene, no viable progeny will result bearing both *Tsk2* and the null allele of *Col3a1*, and this is what we observed ("lethal"). Most of the viable progeny bearing the null allele of *Col3a1* will be WT at the *Tsk2/Col3a1* locus, because approximately 90% of homozygous *Col3a1*-KO mice die before birth ("semi-lethal"), and the *Tsk2* chromosome does not rescue ("complement") the *Col3a1*-KO. The *Col3a1*-KO is indicated by the "hole" in the chromosome; the *Tsk2* gene by a star.

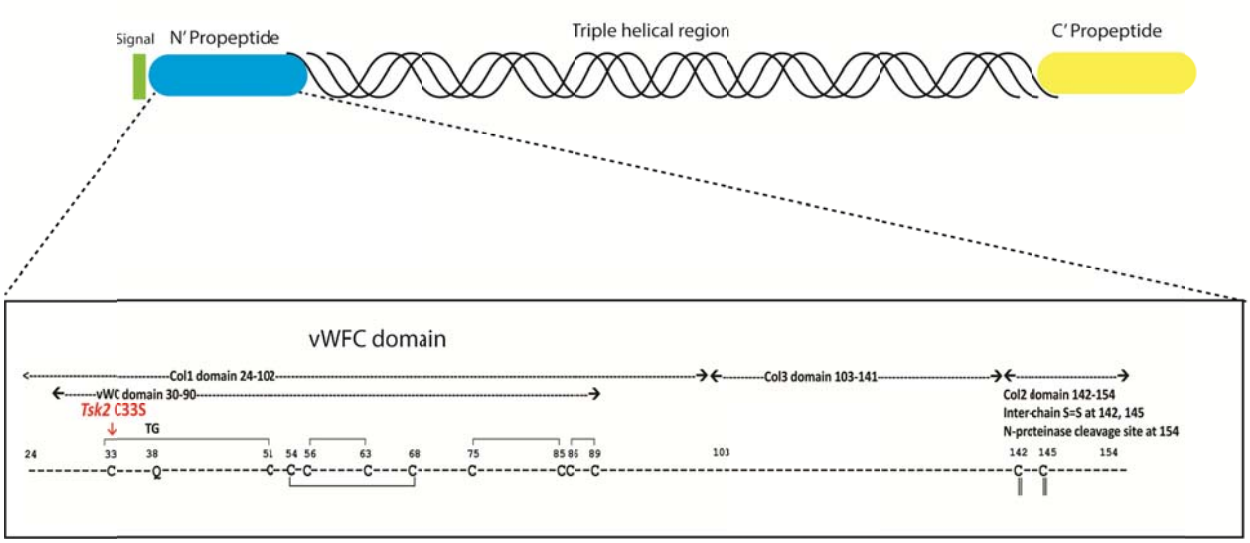

Supplementary Figure 3. Schematic representation of the mouse COL3A1 protein, with an expanded view of PIIINP.

A red arrow indicates the mutation in Cys33 in Tsk2/+ mice. The signal peptide extends from residue 1 to 23, and the Col I domain begins at amino acid 24 and extends to amino acid 102. A von Willebrand factor type c domain (VWC) is predicted between amino acids 30 and 90; the predicted transglutamination site, based on homology with human, cow, and pig Col3A1 molecules sites (Bowness *et al.*, 1987), is shown at amino acid 38 (TG). Intrachain disulphide bonds (C:C) are depicted, based on homology with other Type 3 collagens (Bruckner *et al.*, 1978). The Col3 and Col2 domains at the carboxyl terminal of the PIIINP peptide are indicated at amino acids 103-141 and 142-154, respectively.

Title: Interspecies Comparative Genomics Identifies Optimal Mouse Models of Scleroderma

Authors: Jennifer L. Sargent[1], Zhenghui Li[1], Antonios O. Aliprantis[2], Matthew Greenblatt[3], Raphael Lemaire[4], Ming-hua Wu[5], Jun Wei[5], Adam Harris[6], Kristen Long[7], Chelsea Burgwin[7], Carol M. Artlett[7], Elizabeth P. Blankenhorn[7], Robert Lafyatis[4], John Varga[5], Stephen H. Clark[6], Michael L. Whitfield[1,§]

Affiliations:

[1] Department of Genetics
Geisel School of Medicine at Dartmouth
Hanover, NH 03755 USA

[2] Department of Medicine, Division of Rheumatology, Allergy and Immunology
[3] Department of Pathology
Brigham and Women's Hospital
Smith Building Rm 650A
1 Jimmy Fund Way
Boston, MA 02115

[4] Rheumatology Section
Boston University School of Medicine
Boston, MA, 02115, USA

[5] Feinberg School of Medicine
Northwestern University
Division of Rheumatology
Chicago, IL, 60611, USA

[6] Department of Genetics
University of Connecticut Health Center
Farmington, CT, 06030, USA

[7] Department of Microbiology and Immunology
Drexel University College of Medicine
Philadelphia, PA, 19129, USA

Running Title: Animal models of SSc molecular subsets

[§]To whom correspondence should be addressed:
Michael L. Whitfield, Ph.D.
Department of Genetics
Dartmouth Medical School
7400 Remsen
Hanover, NH 03755
michael.whitfield@dartmouth.edu
phone 603.650.1109, fax 603.650.1188

Abstract: (limit 250 words)

Scleroderma (Systemic sclerosis; SSc) is a devastating autoimmune disease with considerable heterogeneity. Immune dysfunction, fibrosis and vasculopathy are major features of the disease, however the interplay between these components is poorly understood. The highly heterogeneous clinical presentation of SSc has hindered understanding the mechanisms that drive pathogenesis. Development of appropriate animal models of SSc has proven extremely challenging, and their relevance to human disease is difficult to assess. Here we use interspecies comparative analysis techniques on genomic data from mouse models and patients, to determine which animal models of SSc best reflect the SSc intrinsic subsets on a molecular level, providing models for pre-clinical testing. We show that gene expression in skin of sclGVHD and bleomycin mouse models best reflects that of the human SSc *inflammatory* subset. We report that skin of Tsk2/+ mice at 4 weeks of age shares gene expression features, including enrichment of a TGFβ-responsive signature and proliferating cells, with the *fibroproliferative* SSc subset. A TGFβ target implicated in fibrosis, *Tnfrsf12a* (the *Tweak-Receptor* / *Fn14*) is found at increased levels in both the human fibroproliferative subset and in the skin of Tsk2/+ mice compared to relevant controls. These findings provide important insight that will serve to guide mechanistic and translational pre-clinical studies in SSc, and provides mouse models for each of the SSc subsets. We have conclusively demonstrated that gene expression patterns in skin of mouse models can be used to quantitatively assess the relevance of models to subsets of human disease on a molecular level.

One Sentence Summary: Genome-wide mapping shows that gene expression patterns in molecularly distinct animal models of fibrosis quantitatively map to different subsets of human scleroderma providing distinct models for target identification and preclinical testing.

Keywords: systemic sclerosis; skin; human intrinsic gene expression subsets; murine models; Tsk2/+; Tsk/+; sclGVHD; Bleomycin; fibrosis; DNA microrrays; interspecies comparison; TGF-beta; IL13; Tnfrsf12a (Tweak-Receptor)

Main Text:

Introduction

A lack of clear genetic associations and the spectrum of heterogeneity in the clinical presentation of scleroderma (systemic sclerosis; SSc) have limited the development of a single agreed-upon animal model of the disease. We have demonstrated that molecular subsets of SSc exist (*1-3*) and that different signaling pathways underlie each of these molecular subsets of SSc (*4, 5*). We postulate that the SSc subsets might arise through different mechanisms, or alternatively, the subsets might represent different stages of disease progression. Given the distinct molecular features of SSc subsets it is possible that each of the subsets might be most accurately represented by one or more mouse models. Identification of appropriate models for each subset is necessary to effectively develop therapeutics that specifically target each of these groups of patients. We conducted an integrated interspecies analysis of gene expression in skin of four commonly used mouse models of SSc to identify those models in which skin gene expression and deregulated pathways most accurately reflects that of the molecular subsets of SSc.

TGFβ signaling has been demonstrated to in part underlie the *fibroproliferative* subset of patients (*4*), whereas IL4 and IL13 signaling is predominantly enriched in the *inflammatory* subset of patients (*5*). Multiple mouse models have been used to study disease mechanisms in SSc (*6*) but no single model has been widely accepted as adequately reflecting all aspects of the human condition. Here we have directly compared the similarities and differences in the molecular events underlying pathogenesis of SSc, and in models of the disease. To our knowledge this is the first

integrative and comparative analysis of genome-wide expression in animal models for a heterogeneous human autoimmune disease.

Results

To our knowledge no direct comparisons have been made between the bleomycin-induced SSc mouse model or the Tsk2/+ model with human SSc; although both mouse models share features with human SSc such as immune cell filtration, ECM deposition, and skin fibrosis (*7-10*). The datasets and analysis for human SSc skin and the sclGVHD mouse model gene expression have been previously published (*1, 5*). We used distance weighted discrimination (DWD) analysis methods (*11*) to remove platform and species biases, and to integrate the human SSc biopsy and the mouse model gene expression datasets (Figure 1). Groupings in the human and mouse tissue datasets were specified based on either their intrinsic subset classification (*1*) or by model. In all, eleven groups were specified for intrinsic gene selection. 1217 genes were selected from the merged dataset by our algorithm (see methods), and the samples and genes organized by hierarchical clustering (Table 1).

As expected, after hierarchical clustering of the combined dataset, SSc skin biopsy samples clustered into the same groupings of the original molecular subsets (*1*). We were specifically interested in understanding how gene expression in different mouse models resemble specific subsets of human SSc. The sclGVHD samples clustered adjacent to the *inflammatory* patient samples, consistent with the findings of Greenblatt *et al*. [5], and the Tsk2/+ mice at 4 weeks of age shared a dendrogram branch with the *fibroproliferative* subset, suggesting that the skin of these mice share gene expression

features with the skin from patients in this subset (Figure 2). Bleomycin-injected mice at 7 days and at 21 days clustered together, and shared a branch with the *inflammatory* subset. Samples from Tsk1/+ mice and the Tsk2/+ mice at 16 weeks clustered on a branch with the *limited* subset of patients.

We have previously demonstrated enrichment of IL13-driven gene expression patterns in both the *inflammatory* subset and in sclGVHD mice (*5*). As previously demonstrated, membrane-associated IL13-specific receptor subunit *IL13RA1* has coordinately high relative expression in both groups along with *AIF1* and *CCL2*, both of which are IL13-regulated; all show high expression again in this multiple model, interspecies comparison (Figure 3B) (*12*). Expression of many of these genes is similarly increased in the bleomycin-induced fibrotic model, consistent with the characterized role of IL13 signaling in fibrosis in these mice (*13, 14*).

Despite similarities between sclGVHD and bleomycin-induced fibrosis, a prominent cluster of genes distinguishes these two models. This group of genes is not induced by bleomycin, but is highly upregulated in early sclGVHD. Many of the genes in this cluster are expressed at intermediate levels in SSc inflammatory skin and are targets associated with interferon signaling, such as *STAT1, IRF1, CCL5, IFI30*, and *JAK3* (Figures 3B).

A large number of the genes found coordinately regulated in the *fibroproliferative* subset and in Tsk2/+ mice at one month are associated with cell proliferation, including *KI67, CENPE, KIF20A, MCM7*, and *POLE2* (Figure 3A) (*15*). Skin samples from Tsk2/+ mice and their wild-type littermates were stained for the key signature molecule of the proliferative subset, *KI67*. The results (shown in Figure 6) confirmed the microarray

findings that showed up-regulated *KI67* mRNA transcripts, which are expressed in significantly more cells, especially in hair follicle locations, in male Tsk2/+ mice. Interestingly, gene expression in skin samples from Tsk1/+ at 6 weeks of age and Tsk2/+ mice at 16 weeks did not show a strong resemblance to the genes differentially expressed in diffuse SSc, however, they do show some resemblance to limited SSc. In our detailed mechanistic studies of sclGVHD and Tsk2/+, we have found a strong correlation between age of the mice, the gene expression in the model and their resemblance of the human SSc subsets.

To examine the shared features of gene expression in the molecular subsets and in the mouse models on a global scale, we created a module map of enriched GO terms in the integrated human SSc and mouse model gene expression dataset (Figure 4). Many GO terms associated with proliferation and mitosis such as *mitotic checkpoint, cell division, regulation of mitosis and DNA replication initiation* were similarly positively enriched in the Tsk2/+ mice at one month and in the *fibroproliferative* biopsies, consistent with the increased expression of genes involved in cell cycle progression. Other GO terms coordinately regulated in this subset and in Tsk2/+ 4 week mice include those associated with RNA metabolism (*RNA splicing, mRNA processing* and *RNA binding*), translation (*protein-RNA complex assembly, ribosome* and *eukaryotic 43S initiation complex*) and DNA repair (*DNA-dependent DNA replication* and *DNA repair*). Proteins involved in these processes such as topoisomerase I and RNA polymerase I are frequent antigenic targets for autoantibodies in SSc (*16-20*). GO terms associated with lipid biogenesis such as *fatty acid metabolic process*, *lipid metabolic process* and *sterol biosynthetic process*, are enriched and downregulated in a portion of *fibroproliferative*

biopsies and similarly downregulated in the Tsk2/+ mouse skin biopsies. Loss of subcutaneous fat is a characteristic feature of both diffuse SSc (*21*) and Tsk2/+ model (*10*). Additionally, it has been demonstrated that lipid biogenesis and fibrotic processes in fibroblasts are mutually antagonistic signaling systems. Activation TGFβ-signaling inhibits lipid biogenesis via PPARγ pathways and vice versa (*22, 23*). PPARγ ligands have also been shown to suppress bleomycin-induced fibrosis in lungs (*24*).

Modules shared in skin from sclGVHD mice at two weeks and the *inflammatory* subset were mostly associated with inflammatory and immune system processes, such as *immune system process, inflammatory response, chemokine activity,* and *response to biotic stimulus*. Increased expression of ECM-associated pathways is also evident in the *inflammatory* and *limited* subsets, as well as in the bleomycin-induced fibrosis and Tsk1/+ models, suggesting that pathways underlying fibrosis in these patients and these models may also be conserved.

Having established that skin from Tsk2/+ mice at 4 weeks shares gene expression features with the *fibroproliferative* subset, we specifically examined a role for TGFβ-signaling associated gene expression in this model. An *in vivo* TGFβ-responsive signature in mouse skin was generated and expression of these genes examined in skin from Tsk2/+ animals. Total RNA was prepared from skin samples of C57Bl/6 mice that had been surgically implanted with subcutaneous pumps containing 50, 250 or 1250ng of TGFβ, or phosphate-buffered saline (PBS) as a control, for 7 days. Gene expression data relative to the PBS treatment control is shown. We have termed the 719 probes that showed a 2-fold or more change in gene expression the mouse TGFβ-responsive signature (Figure 5). Canonical TGFβ targets found induced in this signature include

TIMP1, *PAI1*, COL1A1, *SPP1*, *LOX*, *THBS* and *SPARC*, demonstrating that this signature is representative of a response to TGFβ in the skin of these animals. The data for the mouse TGFβ-responsive signature was extracted from the compendium of gene expression in skin of the models. Expression of TGFβ-responsive signature genes is enriched in skin from Tsk2/+ animals at 4 weeks (Figure 5B) suggesting that TGFβ-signaling is active in the skin of these mice.

To confirm the molecular similarities between the patients in the *fibroproliferative* subset and Tsk2/+ mice we analyzed the expression of the TGFβ-regulated gene tumor necrosis factor receptor superfamily, member 12a (*Tnfrsf12a*; also designated *Tweak-R*, *fibroblast growth factor-inducible-14*). *Tweak-R* is highly expressed in the *fibroproliferative* subset and was among a set of genes highly correlated to worse skin disease (*1*). *Tweak-R* mRNA levels were also found increased in the fibroproliferative subsets of Milano *et al*. (Figure 6A; $p < 0.00001$); gene expression differences for *Tweak-R* (*Tnfrsf12a*) were confirmed by qRT-PCR (*1*). We performed IHC on sections of skin taken from Tsk2/+ and their wild-type littermates to detect the levels of TWEAK-R. The *Tweak-R* gene is induced by TGFβ (*25*) and there is an ~1.5-fold increase in numbers of TWEAK-R positive cells at in skin of 4-week-old Tsk2/+ mice compared to their littermates (Figure 6B; $p = 0.013$). Taken together with the findings of enrichment of TGFβ-signaling in *fibroproliferative* skin biopsies (*4*), it seems that Tsk2/+ skin at 4 weeks reflects the biology of this subset of SSc.

Discussion

The identification of mouse models that share gene expression patterns with the *fibroproliferative* and *inflammatory* subsets of SSc provides the research community with valuable tools in which to closely examine the molecular mechanisms underlying disease in these subsets. The data presented here are consistent with our earlier findings that sclGVHD mice share underlying mechanistic pathways with the *inflammatory* subset of SSc (*5*). Here we have extended those findings by identifying Tsk2/+ mice at 4 weeks of age as a promising model of disease for the *fibroproliferative* subset. We have used multiple approaches to demonstrate parallels in gene expression in this mouse and *fibroproliferative* skin biopsies, including analysis of individual genes and clusters, examination of global similarities based on co-expression of GO terms, and specifically testing for enrichment of TGFβ-responsive gene expression in both species.

The role of TGFβ signaling in fibrosis and as a driver of disease in SSc is well established. An important new finding is the demonstration that Tsk2/+ mice have activation of TGFβ responsive gene expression. We have shown that Tsk2/+ results from an ENU induced point mutation in the PIIINP fragment of the *Col3a1* gene (Long et al. *submitted*). We show that the TGFβ target, *Tnfrsf12a* (*Tweak-R* or *Fn14*) is highly expressed both in SSc patients of this subset and in Tsk2/+ mice at 4 weeks of age. Interestingly, mice deficient for *Tweak-R* have significantly reduced liver progenitor cell proliferation in response to chemical liver injury (*26*). Its ligand, *Tweak* / *Tnfsf12,* has been implicated as a driver of inflammation and proliferation of fibroblasts / epithelial cells and can contribute to kidney fibrosis (*27, 28*). The kidneys of *Tweak* KO mice show a decreased number of myofibroblasts with lower proliferation, and reduced ECM accumulation; mice over-expressing TWEAK have increased kidney fibrosis (*27*). We

propose that a common mechanism underlying the fibroproliferative subset of SSc and the Tsk2/+ model is due in part to TGFβ signaling leading to activation of the *Tweak / Fn14* signaling axis.

The deregulation of TGFβ signaling in the bleomycin model has been previously demonstrated (*29, 30*). The bleomycin-induced fibrosis model has also been used to advance knowledge of the roles for both TGFβ and IL13 in fibrosis and has been particularly informative for revealing the interactions between these signaling pathways in fibrotic processes (*13, 14*). These results are confirmed here.

The resemblance of the Tsk1/+ mouse to the SSc subsets is not clear or consistent with prior findings (*31*). We found no significant parallels of gene expression in skin of these animals at 6 weeks of age with the molecular subsets of SSc. Detailed analysis of Tsk1/+ at other time points might show stronger similarities to gene expression in SSc skin. The Genomica module map analysis did not demonstrate any contribution to gene expression patterns by B-lymphocytes in Tsk1/+ as has been previously reported. It is possible that the reported reliance of the phenotype in these mice on functional IL4 signaling (*32*) is relevant to the *inflammatory* or *limited* subsets, however the GO term analysis implemented in these studies is not sensitive enough to draw definitive conclusions from these data.

With few tools available for studying disease mechanisms in this poorly understood disease, the benefits of the results of this study are clear. First, by using gene expression as a readily quantifiable phenotype in skin, we have shown that the Tsk/2+ mouse, the sclGVHD and bleomycin-induced fibrosis mouse models are similar to their respective human subsets not by gross morphology approximations, but by robust

molecular measures. Additionally, identification of the pathways similarly deregulated in human SSc subsets and in mouse models, provides new, urgently needed tools for optimizing development of therapeutics that specifically target each of the intrinsic subsets of scleroderma. The mechanisms in these mouse models can be used to identify drugs for SSc patients in the clinic and target their molecular subsets. The development of a routine diagnostic for SSc patients as well as drugs that target each subset will greatly facilitate treatment of this disease.

Materials and Methods

Study Design:

Mouse skin samples were obtained from experts in the field (Table 1). Microarray data from human SSc samples were obtained from prior published studies. SSc patients met the ACR criteria for systemic sclerosis and included both diffuse and limited systemic sclerosis patients as well as a subset of patients with morphea. We performed biological rather than technical replicates for the different mouse samples. The study was designed to identify the best mouse models to study each of the human SSc subsets. This is a major unmet need since heterogeneity in the disease has confounded basic science studies as well as clinical trials. Our data show that different mouse models represent different subsets of SSc disease.

Mouse models of SSc:

All animal protocols were institutionally approved by the Animal Care and Use Committee at University of Connecticut Health Center, Brigham and Women's hospital, Boston University School of Medicine, Northwestern Feinberg School of Medicine and Drexel University College of Medicine. The sclGVHD model and data have been described previously (*5*). Depilated Tsk2/+ (*33*) mouse back skin samples were stored in RNAlater. These mice are heterozygous for the Tsk2 mutation on chromosome 1 and were maintained in an inbred line developed by backcrossing onto C57BL/6J (>N10). Tsk1/+ back skin samples were obtained from six week old mice (*34*). C57BL/6-^{Fbn}Tsk+/+Pldn^{pa} mice were obtained from Jackson Laboratories and maintained by breeding with C57BL/6 mice. Tsk1/+ and Tsk2/+ heterozygous mice were identified by assessment of skin tightness over the back and by genotyping as described (*34*). In

bleomycin-induced fibrosis, six- to eight-week-old female BALB/cJ mice (Jackson Laboratory) were given daily subcutaneous injections of bleomycin (1 mg/kg) and sacrificed at either 7 days or 21 days. Skin at the site of injection was biopsied. All skin tissue was stored in RNAlater (Ambion) for shipping and storage.

***In vivo* TGFβ-responsive gene signature:**

Total RNA samples from the back skins of mice treated with subcutaneous pumps containing TGFβ were generated at Boston University Medical Center. Prior to surgery, mice were injected with buprenorphine. For pump insertion, C57BL/6 mice were placed under general anesthesia using isoflourane by inhalation. After complete anesthesia was achieved, the mice were placed on a warm towel, their backs shaved, the surgical area sterilized with betadine and a 1 cm incision made through the skin over the interscapular region. The sterile pumps containing 50, 250 or 1250ng of TGFβ or PBS were inserted into a subcutaneous pocket made by gently teasing apart the fascia layer. Skin was closed with 1-2 staples. Mice were sacrificed 7 days after surgery and the skin from around the pump insertion site harvested for total RNA preparation.

RNA isolation and microarray hybridization:

Total RNA was isolated from skin samples using standard Trizol (Invitrogen, Carlsbad, CA) procedures. Samples were manually minced, suspended in 1mL Trizol reagent and mechanically disrupted with a PowerGen 125 homogenizer (Fisher Scientific, Pittsburgh, PA). Samples were spun to remove any particulate matter and total RNA isolated by chloroform phase separation and isopropanol precipitation according to the manufacturer's instructions. Samples were further purified using the RNA cleanup procedure and RNeasy mini-columns (Qiagen, Valencia, CA). Total RNA was quantified

on a NanoDrop ND-1000 Spectrophotometer (Agilent Technologies, Santa Clara, CA) and quality of the total RNA was assessed on 1.5% agarose gels.

Samples were amplified and labeled using the Agilent Low Input Linear Amplification kit (Agilent Technologies, Santa Clara, CA) and were hybridized against Universal Mouse Reference (UMR) (Strategene, La Jolla, CA) to Agilent Whole Mouse Genome arrays (G4122F) (Agilent Technologies, Santa Clara, CA) in a common reference based design. Microarrays were hybridized and washed in accordance with manufacturer's protocols and scanned using a dual laser GenePix 4000B scanner (Axon Instruments, Foster City, CA). The pixel intensities of the acquired images were then quantified using GenePix Pro 5.1 software (Axon Instruments, Foster City, CA). All microarrays were visually inspected for defects or technical artifacts, and poor quality spots were manually flagged and excluded from further analysis. The data were loaded to the UNC Microarray Database (UMD).

Microarray data processing and analysis:

The data were downloaded from the UMD as lowess-normalized $\log_2$ Cy5/Cy3 ratios. Only probes that passed a filter of intensity/background ratio ≥1.5 in one or both channels and for which at least 80% of the data was of sufficient quality were used. Each data table was multiplied by negative one, thereby converting the $\log_2$ Cy5/Cy3 ratios to $\log_2$ Cy3/Cy5 ratios for all analyses. For interspecies comparisons mouse genes were matched to their human orthologs using the Mouse Genome Database (MGD) Database at Jackson Laboratories (*35*). All human and mouse data were median centered and clustered using Cluster 3.0 (*36*) and all heat maps generated and visualized in TreeView version 1.0.13 (*36*).

Gene expression data for probes in the human SSc and mouse datasets were collapsed by human and mouse gene symbols respectively. Mouse genes were then matched to their human orthologs as described. Only genes for which at least 80% of the data, in both the human and mouse datasets, was available were selected for the integrated analysis, resulting in selection of 6000 genes. Missing data values were imputed using the KNN-nearest neighbors function in the bioinformatics toolbox in Matlab R2008b (10 nearest neighbors). Systematic biases in the data were corrected by implementation of distance weighted discrimination (DWD) in Matlab (*11*).

Groups for intrinsic gene selection in the integrated interspecies dataset are specified in Table 4.1. Intrinsic genes were selected using an intrinsic gene identifier algorithm (*37*) and are defined as those genes that demonstrate greatest consistency within a group but highest variability across all samples analyzed. The intrinsic gene identifier computes a weight score for each gene that is inversely proportional to its intrinsic nature. 1217 genes that demonstrated a weight intrinsic score threshold below 0.30 were selected for further analysis (*37*).

Module map analysis was performed in Genomica (*38*). Gene expression data for the merged datasets was matched to the appropriate Entrez Gene Identifier corresponding to the human gene annotation. Statistically significantly enriched GO terms were selected ($p < 0.05$; FDR 0.05; hypergeometric distribution) and clustered according to their enrichment scores. Samples were organized as per the sample clustering of the 1217 intrinsic genes (Figure 4).

Gene expression data from this study are available from NCBI GEO at the following accession numbers: GSE9285 (human SSc data (*1*)), GSE24410 (SclGVHD

mouse model (*5*). Submission of GSEXXXX* (Tsk2/+) and GSEXXXX* (Bleomycin-induced fibrosis) are currently in process and will be made freely available upon publication.

Immunohistochemistry:

To visualize TWEAK-R positive and Ki-67 positive cells, paraffin-embedded sections were deparaffinized with two washes of xylene and two washes of ethanol. Antigens were unmasked with 10 mM citrate buffer at 100 ^{o}C for 25 min, then blocked with 5% goat serum. Rabbit anti-TWEAK-R monoclonal antibody at 1:100 (ab109365,Abcam, Cambridge, MA) , or rabbit anti-Ki67 polyclonal antibody at 1:250 (ab9260, Millipore, Darmstadt, Germany) in blocking buffer was applied to the sections overnight at 4˚C. Slides were washed three times with PBS to remove unbound antibody and incubated with Cy3-conjugated goat anti-rabbit IgG at 1:200 (for TWEAK-R) or at 1:500 (for Ki-67, JacksonImmuno-111-165-006, Jackson ImmunoResearch Laboratories, West Grove, for 40 min at room temperature. DAPI (Life Technologies, Carlsbad CA) was used as a counterstain and to visualize the nuclei.

Statistical Analysis:

Pearson correlations were calculated and plotted in Microsoft Office Excel 2007. Positive cells in the sections were counted at 40X magnification from at least 6 fields of view per sample, and four different mice per genotype. The numbers per field were compared for statistical significance by 1-way ANOVA using GraphPad Prism software.

References:

1. A. Milano *et al*., Molecular subsets in the gene expression signatures of scleroderma skin. *PLoS ONE* **3**, e2696 (2008).
2. S. A. Pendergrass *et al*., Intrinsic gene expression subsets of diffuse cutaneous systemic sclerosis are stable in serial skin biopsies. *J Invest Dermatol* **132**, 1363 (May, 2012).
3. M. E. Hinchcliff *et al*., Molecular Signatures in Skin Associated with Clinical Improvement During Mycophenolate Treatment in Systemic Sclerosis. *J Invest Dermatol* **In Press**, (2013).
4. J. L. Sargent *et al*., A TGFbeta-responsive gene signature is associated with a subset of diffuse scleroderma with increased disease severity. *J Invest Dermatol* **130**, 694 (Mar, 2009).
5. M. B. Greenblatt *et al*., Interspecies Comparison of Human and Murine Scleroderma Reveals IL-13 and CCL2 as Disease Subset-Specific Targets. *Am J Pathol*, (Jan 11, 2012).
6. P. J. Christner, S. A. Jimenez, Animal models of systemic sclerosis: insights into systemic sclerosis pathogenesis and potential therapeutic approaches. *Curr Opin Rheumatol* **16**, 746 (Nov, 2004).
7. I. Y. Adamson, D. H. Bowden, The pathogenesis of bloemycin-induced pulmonary fibrosis in mice. *Am J Pathol* **77**, 185 (Nov, 1974).
8. J. Zhao *et al*., Smad3 deficiency attenuates bleomycin-induced pulmonary fibrosis in mice. *Am J Physiol Lung Cell Mol Physiol* **282**, L585 (Mar, 2002).
9. P. J. Christner *et al*., A high-resolution linkage map of the tight skin 2 (Tsk2) locus: a mouse model for scleroderma (SSc) and other cutaneous fibrotic diseases. *Mammalian genome : official journal of the International Mammalian Genome Society* **7**, 610 (Aug, 1996).
10. P. J. Christner, J. Peters, D. Hawkins, L. D. Siracusa, S. A. Jimenez, The tight skin 2 mouse. An animal model of scleroderma displaying cutaneous fibrosis and mononuclear cell infiltration. *Arthritis Rheum* **38**, 1791 (Dec, 1995).
11. M. Benito *et al*., Adjustment of systematic microarray data biases. *Bioinformatics* **20**, 105 (Jan 1, 2004).
12. P. C. Fulkerson, C. A. Fischetti, L. M. Hassman, N. M. Nikolaidis, M. E. Rothenberg, Persistent effects induced by IL-13 in the lung. *Am J Respir Cell Mol Biol* **35**, 337 (Sep, 2006).
13. M. Matsushita, T. Yamamoto, K. Nishioka, Upregulation of interleukin-13 and its receptor in a murine model of bleomycin-induced scleroderma. *Int Arch Allergy Immunol* **135**, 348 (Dec, 2004).
14. A. O. Aliprantis *et al*., Transcription factor T-bet regulates skin sclerosis through its function in innate immunity and via IL-13. *Proc Natl Acad Sci U S A* **104**, 2827 (Feb 20, 2007).
15. M. L. Whitfield, L. K. George, G. D. Grant, C. M. Perou, Common markers of proliferation. *Nat Rev Cancer* **6**, 99 (Feb, 2006).
16. E. L. Greidinger *et al*., African-American race and antibodies to topoisomerase I are associated with increased severity of scleroderma lung disease. *Chest* **114**, 801 (Sep, 1998).

17. P. Q. Hu, N. Fertig, T. A. Medsger, Jr., T. M. Wright, Correlation of serum anti-DNA topoisomerase I antibody levels with disease severity and activity in systemic sclerosis. *Arthritis Rheum* **48**, 1363 (May, 2003).
18. V. D. Steen, Autoantibodies in systemic sclerosis. *Semin Arthritis Rheum* **35**, 35 (Aug, 2005).
19. K. Hanke *et al*., Diagnostic value of anti-topoisomerase I antibodies in a large monocentric cohort. *Arthritis Res Ther* **11**, R28 (Feb 21, 2009).
20. G. Reimer, K. M. Rose, U. Scheer, E. M. Tan, Autoantibody to RNA polymerase I in scleroderma sera. *J Clin Invest* **79**, 65 (Jan, 1987).
21. R. Fleischmajer, V. Damiano, A. Nedwich, Alteration of subcutaneous tissue in systemic scleroderma. *Arch Dermatol* **105**, 59 (Jan, 1972).
22. A. K. Ghosh *et al*., Disruption of transforming growth factor beta signaling and profibrotic responses in normal skin fibroblasts by peroxisome proliferator-activated receptor gamma. *Arthritis Rheum* **50**, 1305 (Apr, 2004).
23. M. Wu *et al*., Rosiglitazone abrogates bleomycin-induced scleroderma and blocks profibrotic responses through peroxisome proliferator-activated receptor-gamma. *Am J Pathol* **174**, 519 (Feb, 2009).
24. Y. Aoki *et al*., Pioglitazone, a peroxisome proliferator-activated receptor gamma ligand, suppresses bleomycin-induced acute lung injury and fibrosis. *Respiration* **77**, 311 (2009).
25. M. W. Milks *et al*., The role of Ifng in alterations in liver gene expression in a mouse model of fulminant autoimmune hepatitis. *Liver Int* **29**, 1307 (Oct, 2009).
26. A. Jakubowski *et al*., TWEAK induces liver progenitor cell proliferation. *J Clin Invest* **115**, 2330 (Sep, 2005).
27. A. C. Ucero *et al*., TNF-related weak inducer of apoptosis (TWEAK) promotes kidney fibrosis and Ras-dependent proliferation of cultured renal fibroblast. *Biochim Biophys Acta* **1832**, 1744 (Oct, 2013).
28. L. X. Zhu, H. H. Zhang, Y. F. Mei, Y. P. Zhao, Z. Y. Zhang, Role of tumor necrosis factor-like weak inducer of apoptosis (TWEAK)/fibroblast growth factor-inducible 14 (Fn14) axis in rheumatic diseases. *Chinese medical journal* **125**, 3898 (Nov, 2012).
29. G. Lakos *et al*., Targeted disruption of TGF-beta/Smad3 signaling modulates skin fibrosis in a mouse model of scleroderma. *Am J Pathol* **165**, 203 (Jul, 2004).
30. B. Santiago *et al*., Topical application of a peptide inhibitor of transforming growth factor-beta1 ameliorates bleomycin-induced skin fibrosis. *J Invest Dermatol* **125**, 450 (Sep, 2005).
31. R. M. Baxter, T. P. Crowell, M. E. McCrann, E. M. Frew, H. Gardner, Analysis of the tight skin (Tsk1/+) mouse as a model for testing antifibrotic agents. *Lab Invest* **85**, 1199 (Oct, 2005).
32. C. J. Ong *et al*., A role for T helper 2 cells in mediating skin fibrosis in tight-skin mice. *Cell Immunol* **196**, 60 (Aug 25, 1999).
33. T. Barisic-Dujmovic, I. Boban, S. H. Clark, Regulation of collagen gene expression in the Tsk2 mouse. *J Cell Physiol* **215**, 464 (May, 2008).
34. J. Bayle *et al*., Increased expression of Wnt2 and SFRP4 in Tsk mouse skin: role of Wnt signaling in altered dermal fibrillin deposition and systemic sclerosis. *J Invest Dermatol* **128**, 871 (Apr, 2008).

35. C. J. Bult, J. T. Eppig, J. A. Kadin, J. E. Richardson, J. A. Blake, The Mouse Genome Database (MGD): mouse biology and model systems. *Nucleic Acids Res* **36**, D724 (Jan, 2008).
36. M. B. Eisen, P. T. Spellman, P. O. Brown, D. Botstein, Cluster analysis and display of genome-wide expression patterns. *Proc Natl Acad Sci U S A* **95**, 14863 (Dec 8, 1998).
37. C. M. Perou *et al*., Molecular portraits of human breast tumours. *Nature* **406**, 747 (Aug 17, 2000).
38. E. Segal *et al*., Module networks: identifying regulatory modules and their condition-specific regulators from gene expression data. *Nat Genet* **34**, 166 (Jun, 2003).
39. J. I. Herschkowitz *et al*., Identification of conserved gene expression features between murine mammary carcinoma models and human breast tumors. *Genome Biol* **8**, R76 (2007).

Figure legends

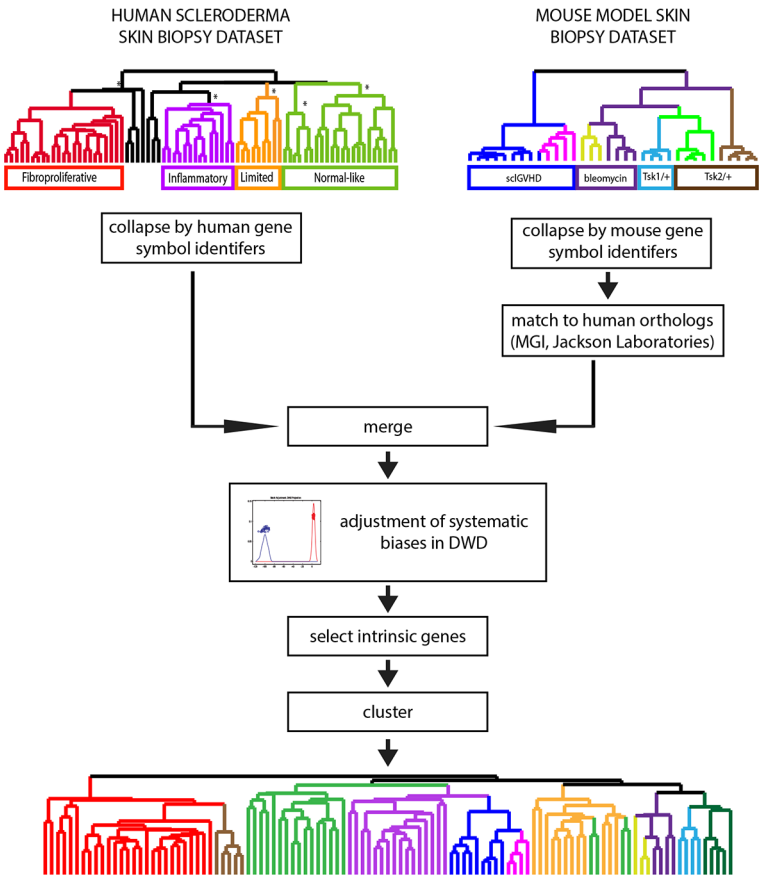

Fig. 1. Implementation of integrated interspecies analysis for systemic sclerosis. The schematic of the analysis strategy based on that of Herschkowitz *et al*. (*39*) is shown. Human and mouse datasets were merged as described in the text, the biases removed using DWD, and the intrinsic genes selected and clustered for further analysis.

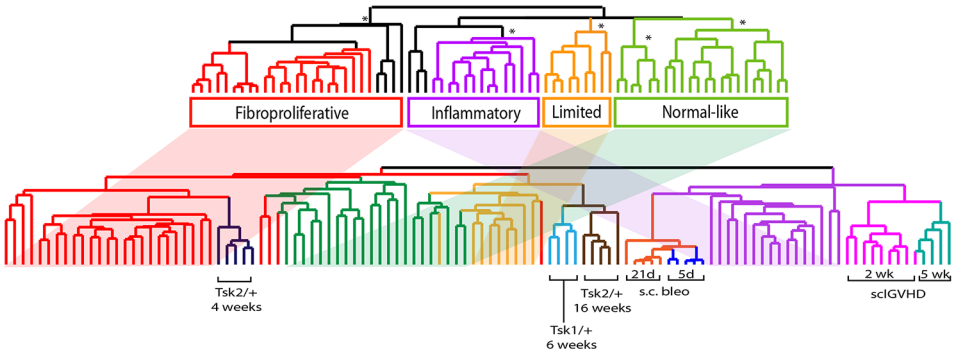

Fig. 2. Integrated human mouse expression data clustering. The upper dendrogram shows the organization of the molecular subsets of SSc. The shading indicates the placement of these subsets in the integrated dataset cluster analysis. Microarrays from the mouse models are interspersed among the human subsets. Notably, Tsk2/+ 1 month samples cluster on the same branch as the *fibroproliferative* subset and sclGVHD mice at 2 weeks and at 5 weeks are found clustered with the *inflammatory* subset. Samples from the bleomycin mouse model show are most closely associated with inflammatory subset but show aspects of inflammatory and fibroproliferative gene expression.

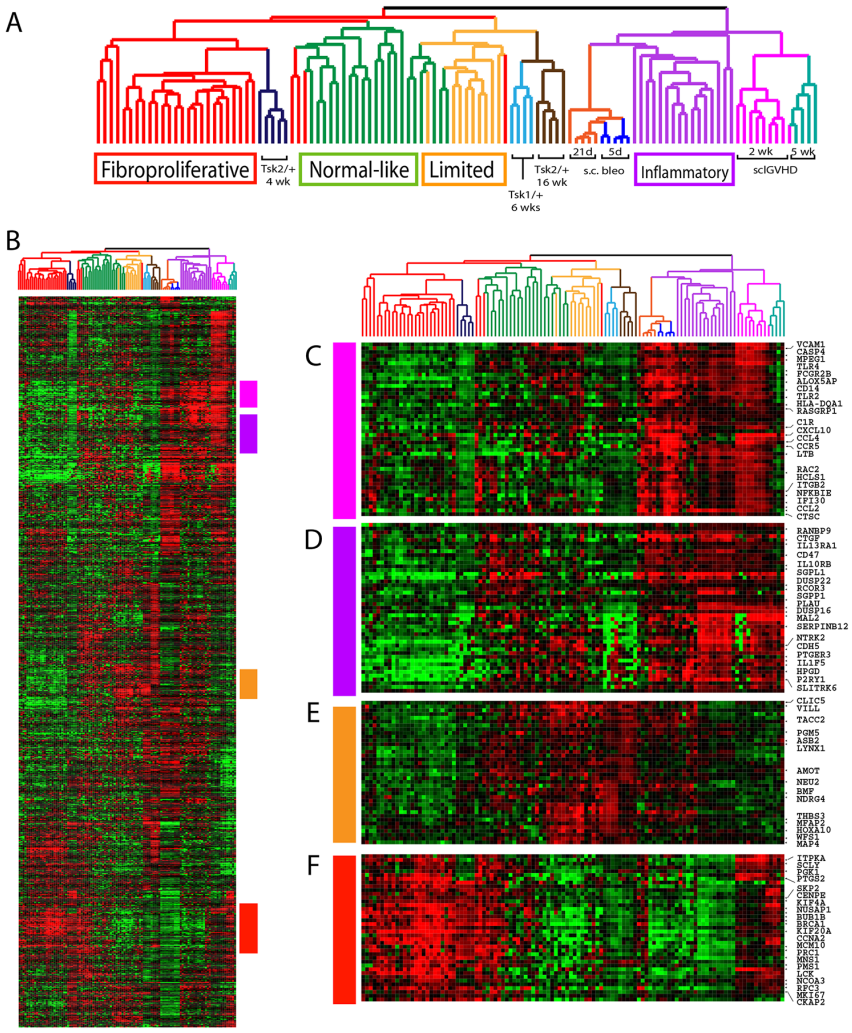

Fig. 3. Clusters of gene expression patterns are shared in human SSc skin and in the mouse models. **(A)** 1217 intrinsic genes were clustered in the gene and array dimensions. The sample dendrogram is that from Figure 1. Selected clusters of interest are shown. Gene expression features shared by the sclGVHD mice and the *inflammatory* subset include those induced by IL13 **(B)** and IFN-signaling **(C-E)**. Genes associated with proliferation were up-regulated in Tsk2/+ mice at 1 month and in the *fibroproliferative* subset **(F)**. A cluster of genes was found up-regulated in the *inflammatory* and *limited* subsets as well as the sclGVHD and other models **(G)**.

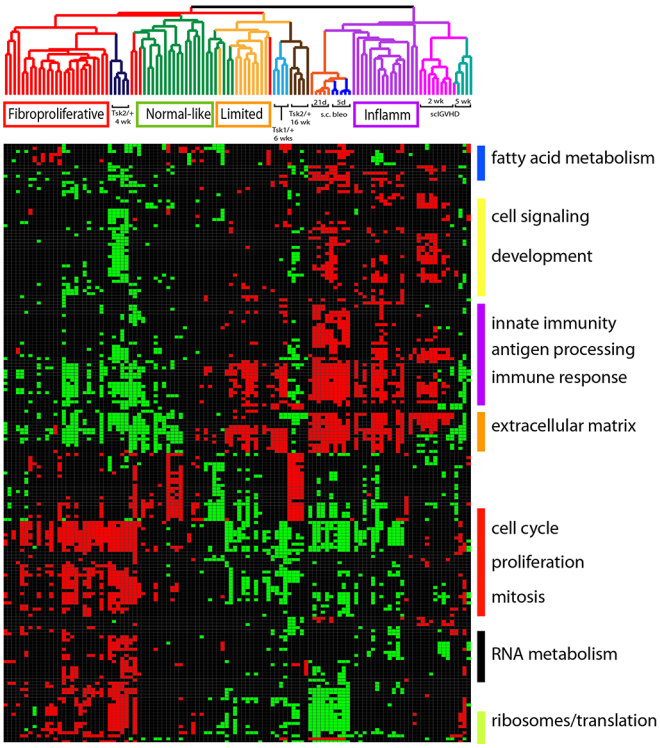

Fig. 4. Module map of coordinately regulated GO terms in human SSc and in mouse models. A module map of enriched GO terms was created using gene expression from the integrated interspecies microarray dataset. Modules significantly enriched ($p < 0.05$, FDR 0.05, hypergeometric distribution) in at least 15 of the 109 arrays were selected and are displayed. Clusters of select GO terms are shown to the right of the module map. Each column represents a microarray and each row is a GO term. The arrays have been ordered as per the intrinsic clustering shown in Figure 1. Positively enriched and negatively enriched modules are shown by red and green squares respectively.

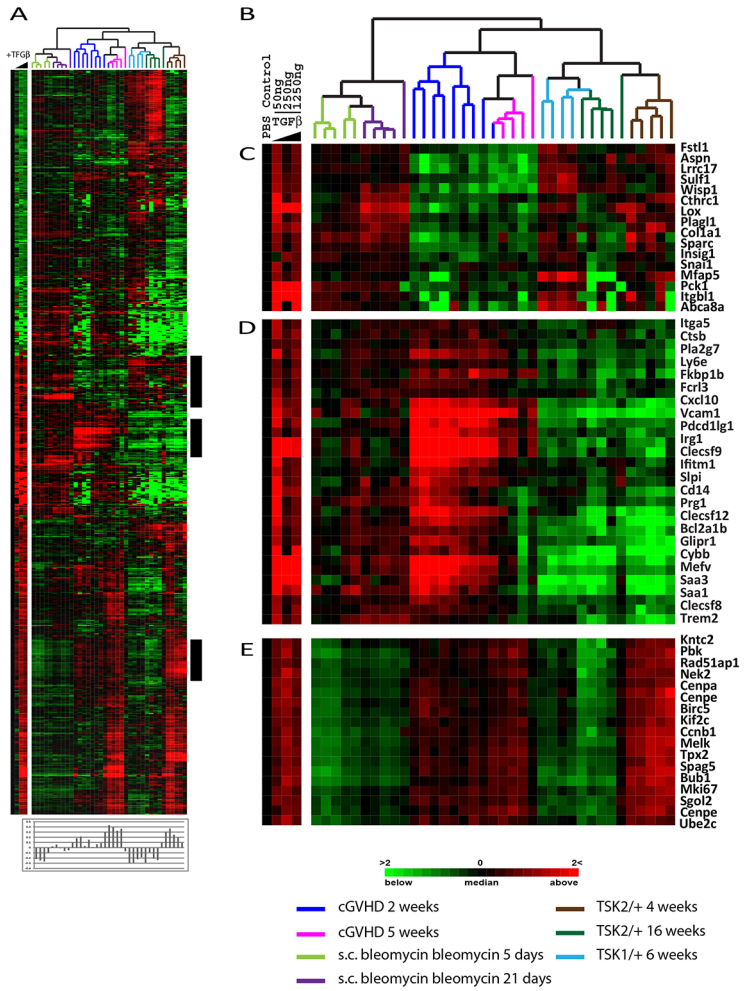

Fig. 5. TGFβ-responsive signature gene expression in SSc mouse models. ***A.*** Pumps containing PBS or 50, 250 or 1250ng of TGFβ were surgically inserted subcutaneously in B57/B6 mice for 7 days and skin analyzed by DNA microarray. 719 genes changed in expression >2-fold from the PBS control in at two doses of TGFβ. Data were T0 transformed against the PBS control and the blue wedge is indicative of increasing TGFβ concentrations. Data for the 719 TGFβ-responsive genes were extracted from the SSc mouse models and clustered in the array and gene dimensions. Pearson correlations of the 1250ng TGFβ dose and each microarray were calculated and are plotted directly beneath the heatmap. The TGFβ dose response is shown to the left of the heatmap. The highest

TGFβ gene expression is observed in 5 week samples from the sclGVHD mouse and 4 week old Tsk2/+ mice. **B.** Dendrogram of mouse samples analyzed colored-coded by model. **C.** Canonical TGFβ targets COL1A1, WISP1, SPARC, and TIMP1 were found TGFβ-responsive. **D.** TGFβ-induced genes highly expressed in the sclGVHD model. **E.** Proliferation genes induced by the TGFβ treatment.

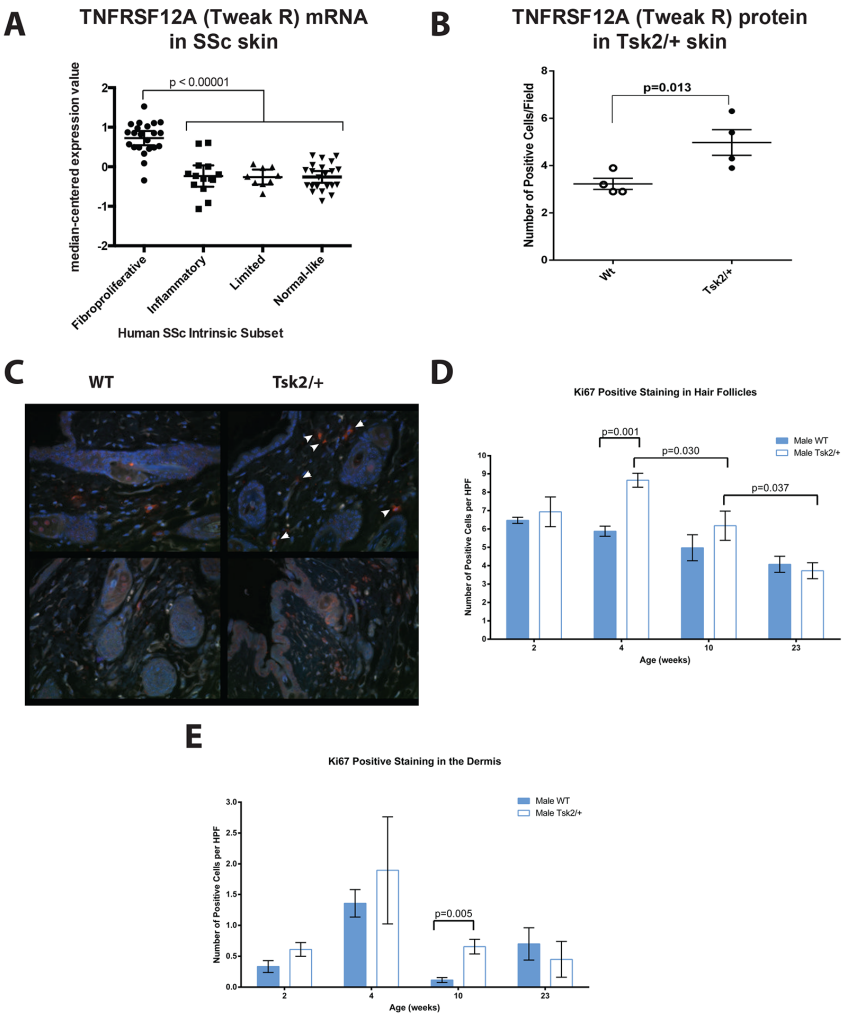

Fig. 6. Tweak R (TNFRSF12A) is highly differentially expressed in both the fibroproliferative SSc patients and the Tsk2/+ mouse model. (A) SSc patients in the fibroproliferative subset express significant more *tnfrsf12a* (*Tweak-R*) than normal controls or patients in the inflammatory, proliferative or normal-like subsets ($p < 0.00001$). (B) Tsk2/+ mice expressed 1.6-fold more TNFRSF12A (TWEAK-R) than wild type littermates ($p=0.013$). Four-week-old female mice were scored for the number of TWEAK-R (Fn14)+ cells per field of view (400X magnification). Significance was calculated with a paired t-test using at least 8 fields of view per mouse and 4 mice per genotype. (C) Representative immunofluorescent images of two wild type mice (Left)

and two Tsk2/+ mice (Right). Skin samples were obtained from the lower dorsal back, paraffin embedded, and evaluated by immunofluorescence for the presence of TWEAK-R(red) and DAPI(blue). (D) and (E), KI67 staining for proliferating cells in the hair follicles and dermis of Tsk2 mice at 2, 4, 10 and 23 weeks of age. We find a significant increase only in the 4 and 10 week samples.

Intrinsic Group	Description	Species	# of Microarrays
1	Fibroproliferative (previously *diffuse-proliferation*)	human	27
2	inflammatory	human	17
3	limited	human	9
4	normal-like	human	22
5	cGVHD 2 weeks	mouse	9
6	cGVHD 5 weeks	mouse	4
7	s.c. bleomycin 5 days	mouse	3
8	s.c bleomycin 27 days	mouse	4
9	Tsk2/+ 4 weeks	mouse	4
10	Tsk2/+ 16 weeks	mouse	5
11	Tsk1/+ 6 weeks	mouse	4

Table 1. Eleven groups were specified for intrinsic gene analysis.

Four goups of human samples were specified based on the intrinsic subsets of SSc (*1*) and seven groups of mouse models were defined based on the model type and different timepoints were specified. (s.c. subcutaneous).